Systems Level Cancer Disease Target Identification Using Tumor Microenvironment Dynamics

by

Funmilayo Lydia MAKINDE

Thesis presented in partial fulfilment of the requirements for the degree of Master of Science in Mathematics in the Faculty of Science at Stellenbosch University

UNIVERSITEIT
iYUNIVESITHI
STELLENBOSCH
UNIVERSITY

1918 · 2018

Department of Mathematical Sciences,
University of Stellenbosch,
Private Bag X1, Matieland 7602, South Africa.

Supervisor: Dr. Gaston Kuzamunu Mazandu

December 2018

Declaration

By submitting this thesis electronically, I declare that the entirety of the work contained therein is my own, original work, that I am the sole author thereof (save to the extent explicitly otherwise stated), that reproduction and publication thereof by Stellenbosch University will not infringe any third party rights and that I have not previously in its entirety or in part submitted it for obtaining any qualification.

Date: December 2018 .....

Abstract

Systems Level Cancer Disease Target Identification Using Tumor Microenvironment Dynamics

Funmilayo Lydia MAKINDE

Department of Mathematical Sciences,
University of Stellenbosch,
Private Bag X1, Matieland 7602, South Africa.

Thesis: MSc. (Mathematics)

December 2018

Cancer is the second driving reasons for death around the world. It is an abnormal growth of cells which can migrate and recreate cellular microenvironment and can also be caused by successive alterations that occur in a set of specific genes in the cell. As dangerous and deadly as cancer is, there is still a gap in our understanding of the mechanism of its establishment, its recurrence cycle and its elimination. It was observed that cancer stem cells are regulated by the complex interaction component that makes up the tumor microenvironment (TME), through a network of growth factors and cytokines.

Therefore, focusing on and understanding the role of these components and the level of concentration of modulating factors present in the TME can play a significant role in battling cancer. Many research projects have investigated the dynamics of these cytokines in the context of cancer in order to understand the evolution of cancer for improving diagnostic, prognostic and therapeutic strategies. However, these research are mostly restricted to cells that directly perform cytotoxic effect on cancer cells, such as the natural killer (NK) and cytotoxic T lymphocytes (CTLs or CD8 + T) cells. They do not explicitly integrate cytokine-mediated innate-adaptive immunity in the tumor dynamics. Moreover, none of those research has combined cellular-level mathematical models with protein-protein interaction network analysis, to predict essential proteins, biological processes and enriched pathways associated with cancer disease.

Hence, in this study, we present a new mathematical model to investigate the dynamics between tumor cell and host immune system component (i.e., innate and adaptive immune cells and cytokines) in the TME . Results from the numerical solution of our model indicate the capacity of a tumor to escape from immunologic surveillance due to low cytotoxic immune cells (i.e. NK cells and CD8 + T cells) at the tumor site while more of these cytotoxic immune cells at the tumor site results in tumor regression. Our model, therefore, supports strengthening the cytotoxic immune cells in the TME which we see as a significant way of contributing to tumor regression. Also, from the analysis of our model, cytokines such as IL-10, IL-23, TNF-α, TGB-β and IFN-γ has been shown to make contributions significantly to the dynamics of tumor development based on the observed dynamics in the level of concentrations in the TME.

Finally, switching of an immune (effector) cell from resting to active states, is triggered by some proteins working in a complex protein-protein interaction (PPI) network. We identified proteins which likely regulate immune cells and cytokines contributing to breast cancer disease outcome and infer essential proteins based on Protein-proteins interaction network, as well as significant pathways and enriched biological processes associated with breast cancer. These biological processes and pathways and essential proteins identified can be further assessed to check for their suitability as targets for the breast cancer disease for the improvement of effective therapeutic strategies.

Keywords: Immune cells, Tumor cells, Cytokines, TME, Mathematical modelling, Proteins.

Opsomming

Stelsel Vlak Kanker Siektes Teiken Identifikasie met behulp van Tumor Mikro Omgewing Dinamika

("Systems Level Cancer Disease Target Identification Using Tumor Microenvironment Dynamics ")

Funmilayo Lydia MAKINDE

Departement Wiskundige Wetenskappe,
Universiteit van Stellenbosch,
Privaatsak X1, Matieland 7602, Suid Afrika.

Tesis: MSc. (Wiskunde)

Desember 2018

Kanker is die tweede oorsaak van dood ter wêreld. Dit is 'n abnormale groei van selle wat kan migreer en herskep sellulêre mikro-omgewing en kan ook veroorsaak word deur opeenvolgende veranderinge wat voorkom in 'n stel spesifieke gene in die sel. So gevaarlik en dodelik soos kanker vir ons samelewing is, is daar steeds 'n gaping in ons begrip van die meganisme van sy vestiging, sy herhalingsiklus en die uitskakeling daarvan. Dit is opgemerk uit navorsing dat kanker stamselle gereguleer word deur die komplekse interaksie komponent wat die tumor mikro-omgewing (TME), deur middel van 'n netwerk van groeifaktore en sitokiene.

Daarom fokus op en verstaan die rol van hierdie komponente en die vlak van konsentrasie van moduleringfaktore wat in die TME teenwoordig is, kan 'n belangrike rol speel in die stryd teen kanker. Baie navorsingsprojekte het die dinamika van hierdie sitokiene ondersoek in die konteks van kanker om die evolusie van kanker te verstaan vir die verbetering van diagnostiese, prognostiese en terapeutiese strategieë. Hierdie navorsing word egter meestal beperk tot selle wat direk sitotoksiese effek op kankerselle, soos die natuurlike moordenaar (NK) en sitotoksiese T limfosiete (CTLs of CD8 + T) selle. Hulle integreer eksplisiet sitokien-gemedieerde aangebore-adaptiewe immuniteit in die tumor dinamika. Daarbenewens het geen van hierdie navorsing op wiskundige

modelle op sellulêre vlak met proteïen interaksie netwerk analise ondersoek om noodsaaklike proteïene, biologiese prosesse en verrykde paaie wat met kanker geassosieer word te voorspel nie.

Daarom bied ons in hierdie studie 'n nuwe wiskundige model wat saamgestel is uit gewone differensiaalvergelykings om die dinamika tussen tumorselle en gasheer immuunstelsel komponent (dws aangebore en adaptiewe immuunselle en sitokiene) in die TME. Resultate van die numeriese oplossing van ons model dui aan die kapasiteit van 'n tumor om te ontsnap uit immunologiese toesig is as gevolg van lae sitotoksiese immuun selle (dws NK-selle en CD8 + T selle) by die tumor terwyl meer van hierdie sitotoksiese immuun selle op die tumor site in tumor lei regressie. Ons model ondersteun dus die versterking van die sitotoksiese immuun selle in die TME wat dien as 'n duidelike manier om by te dra tot tumorregressie. Ook, uit die analise van ons model, sitokiene soos IL-10, IL-23, TNF-α, TGB-β en IFN-γ is getoon dat dit 'n bydrae lewer tot die dinamika van die tumor ontwikkeling gebaseer op die waargenome dinamika in die vlak van konsentrasies in die tumor mikro-omgewing.

Laastens, die omskakeling van 'n immuun (effektor) sel van rus na aktiewe toestande word gereguleer deur sommige proteïenwerk in 'n komplekse proteïen-proteïen interaksie (PPI) netwerk. Ons het proteïene geïdentifiseer wat waarskynlik immuun selle en sitokiene reguleer wat bydra tot die uitkoms van borskanker siektes en essensiële proteïene gebaseer op proteïen-proteïen interaksie netwerk, asook belangrike paaie en verrykde biologiese prosesse wat met borskanker geassosieer word, aflei. Hierdie biologiese prosesse en paaie en noodsaaklik proteïene geïdentifiseer kan verder geassesseer word om na te gaan of hulle geskik is vir teikens vir die borskanker siekte vir die verbetering van effektiewe terapeutiese strategieë.

Keywords: Immuun selle, Tumor selle, sitokiene, TME, wiskundige modellering, proteïene.

Acknowledgements

I want to give God all the glory for good health and grace given unto me for the successful completion of my research masters. My sincere appreciation goes to my supervisor in person of Dr. Gaston Kuzamunu Mazandu for his guidance and availing me with all the necessary information needed throughout the phase of this essay.

My profound gratitude also goes to Dr. Milaine, all staff of the African Institute for Mathematical Sciences (AIMS) South Africa, both academic and non academic, my colleagues, who has in one way or the other made my stay at AIMS memorable and worthwhile.

Finally, I must express my very profound gratitude to my family: my parents; Elder and Mrs Makinde, my lovely Aunt; Ronke Abiodun Makinde, my siblings; Ayodeji, Anna, Olusola and Damilola Makinde, and my love, Adetayo Ibijola, for their unfailing support, love, and continuous encouragement throughout my study. May God continue to be with you all.

Dedications

I dedicate this project to my family.

Contents

List of Figures

List of Tables

Chapter 1

Introduction

1.1 Background

1.1.1 Evolution of cancer in the tumor microenvironment (TME)

Cancer can be characterized as a group of disease formed as a result of uncontrolled development and spread of abnormal cells which occurs in different parts of the body or organs. According to the World Health Organisation (WHO), cancer is the second driving reason for morbidity and mortality [116]. As shown in Figure 1.1, about 16% of people died from cancer in 2016. Likewise, 30% of most cancer deaths are due to the five leading behavioural and dietary risks, namely: high body mass index, low fruit and vegetable intake, lack of physical activity, alcohol use and tobacco use. Tobacco use is the most salient risk factor for cancer. It causes 22% of global cancer mortalities and 71% of global lung cancer mortalities [115]. Cancer can also be caused by viral infections such as hepatitis B virus (HBV), hepatitis C virus (HCV) and human papillomavirus (HPV). They have been seen to cause up to 70% of all cancer deaths in low- and middle-income countries in 2008 [115]. Furthermore, there are some non-modifiable risk factors which cause cancer, of which are, inherited genetic mutation, hormones and immune conditions [16]. It has been observed that some types of cancer are more common in men and women. The five most common types of cancer recognised in 2012 affecting men are: lung (with 16.7% of the total death), prostate (15%), colorectum (10%), stomach (8.5%) and liver (7.5%) cancer while, among women, are breast (25.2%), colorectum (9.2%), lung (8.7%), cervix (7.9%) and stomach (4.8%) cancer. Globally, cancer deaths are anticipated to keep increasing with an expected 13.1 million deaths in 2030 [115].

Cancer originates from the abnormal growth of cells that serve no purpose, and referred to as *tumor*. It develops from benign growth with minor genetic alteration which

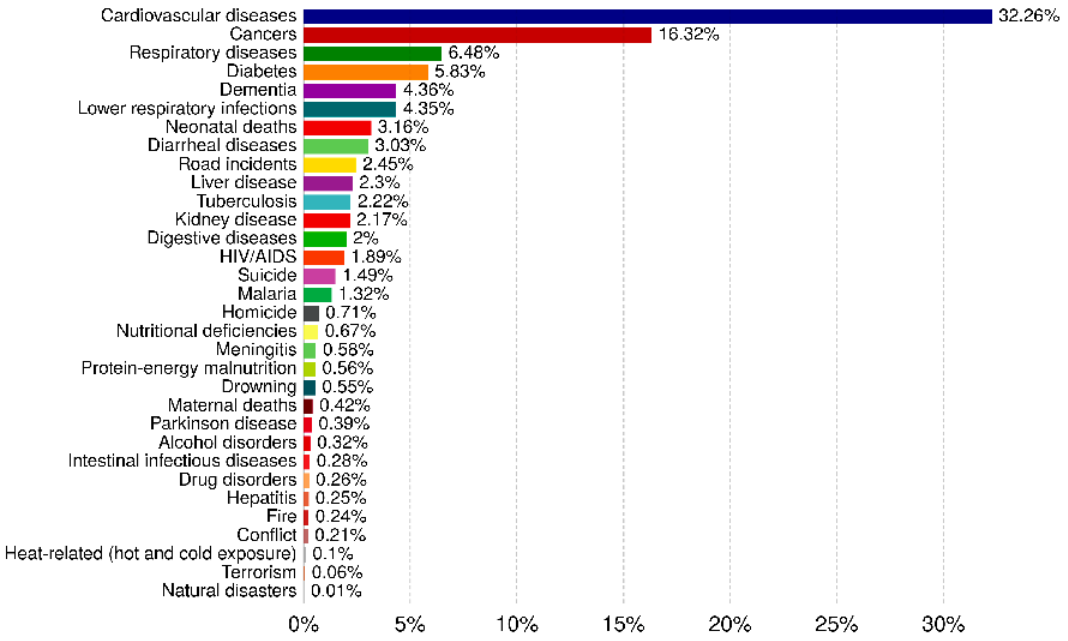

Figure 1.1: Data refers to the specific cause of death, which is distinguished from risk factors for death, such as air pollution, diet and other lifestyle factors. This is shown by cause of death as the percentage of total deaths [94].

advance, as a result of mutations that have been accumulated over time, to more aggressive cancer: pre-malignant (pre-cancerous) and malignant (cancerous) tumor. In certain scenarios, *metastasis* occurs. That is cancerous cells spread from the original tumor and attack different organs and tissue. The development of cancer within an individual takes an evolutionary process similar to the evolution of species. In the evolution of species, individuals in a population tend to evolve by *mutation* and *selection*. By mutation, we mean the change in the gene of a cell that can be passed to the offspring, while a selection is simply an increase in the diversity of life. Similarly, tumor evolves by mutation and selection. However, these processes acting on cells in a tissue are caused by *carcinogens* (a substance likely to cause cancer in living tissue) [18]. The concept that explains the reproducibility of the evolutionary process of tumor is known as *tumorigenesis*. In tumorigenesis, despite the presence of confounding factors (e.g. genetic background, micro-environment), each tumor of the same type or subtype can be seen as an independent realisation of the same evolutionary process.

Evidence has shown that the *tumor microenvironment* (TME), that is, a well defined environment composed of many components (the immune cells and growth factors) where tumor cells can compete, have great influence on the behaviour of tumorigenic

cells, as its components assume a major role in the development of tumor which includes tumor initiation and metastasis [7]. Furthermore, signalling molecules, such as *cytokines* are also seen to play a vital role in the tumor microenvironment. They are proteins secreted by many cell types of the immune system which mediate and regulate immune and inflammatory reactions in the TME. Cytokines can be grouped into two types: the *pro-inflammatory* and *anti-inflammatory* cytokines. On one hand, the pro-inflammatory cytokine enhances inflammation at the tumor site thereby recruiting the immune cells for cytotoxic activity in order to eliminate or inhibits tumor growth. It, therefore, contributes to tumor regression. On the other hand, the anti-inflammatory cytokine reduces inflammation at the tumor site which in turn recruits immune cells in favour of the tumor cells. It, therefore, enhances tumor progression.

1.1.2 Protein-Protein Functional Interaction (PPFI) Networks

In life science research, the interaction of biological entities, such as metabolites, proteins, and genes, have emerged to be of great interest and very important. Biological networks, such as metabolic, protein interaction and gene regulatory networks, are often used to represent interplay between different interactions [57]. Moreover, several biological studies found that a protein does not accomplish its function alone but collaborate with different proteins to carry out its function. Thus, it makes processes to be fulfilled via protein-protein functional interaction networks in living cells. These interactions are biologically divided into two categories: *physical* and *genetic* interactions. Physical contact among proteins is called physical interactions, while genetic interactions between proteins consist of the mechanism through which a given protein performs its functions [75].

In this thesis, we denote by *protein-protein functional interactions* those acquired from knowledge about shared evolutionary history, cooexpression, pathway, physical and genetic interactions. Interactions between proteins can either be direct or indirect via some intermediates proteins thus generating a *protein-protein functional interaction network* [75]. In this network, *nodes/vertices* are proteins while *edges/links* are functional interaction or connection amidst proteins of an organism. Mathematically, protein-protein functional interaction networks are visualized as an undirected graph $\mathcal{N}(\mathcal{P}, \mathcal{I})$, where $\mathcal{P}$ is the set of proteins and $\mathcal{I}$ is the set of functional relationships depicting the paths of communication and metabolism of an organism. Understanding protein-protein functional interaction networks might deepen our knowledge of biological systems, including molecular pathways. Also, it help explain functions of diverse proteins in disease outcome and elucidate essential interactions contributing to the system stability and integrity [75].

1.2 Problem Statement

As dangerous and deadly as cancer is, there is still a gap in our understanding of the mechanism of its establishment, recurrence cycle and elimination [37]. Many research studies have suggested approaches which may improve treatments of cancer. Existing treatments like surgery, chemotherapies and radiotherapies have performed key roles in the elimination of cancer. However, these treatments do not generally guarantee a cure, as later metastasis can occur in the patient. Over time, efforts have been made in developing *immunotherapy*. This is a treatment that entails strengthening a cancer patient immune system by enhancing its ability to recognise and fight cancer. It prevents cancer recurrence, and its development can be controlled for a long term through a process known as *Immunosurveillance*, by which the immune system search for and recognises foreign pathogens, for example, bacteria, viruses, pre-malignant and malignant cells in the body [37].

It has been shown that cancer stem cells are regulated by the complex interaction components that make up the tumor microenvironment, through a network of growth factors and cytokines [56]. Therefore, focusing on and understanding the role of this component and the level of concentration of modulating factors present in the TME can play a significant role in battling cancer. Many research projects have investigated the dynamics of these cytokines about cancer in order to understand its evolution for improving diagnostic, prognostic and therapeutic strategies. However, these research are mostly restricted to cells that directly perform cytotoxic effect on cancer cells, such as the natural killer (NK) and cytotoxic T lymphocytes (CTLs or $CD8^+$ T) cells, and they do not explicitly integrate cytokine-mediated innate-adaptive immunity in a tumor dynamics [26, 69]. Moreover, emerging abundance availability of large protein sequence and public gene databases had been proven to have the capability to provide new insights into the biology of organisms and can give rise to the enhancement of drug target selection process by identifying genes that are extremely important to cancer growth [75, 76]. Moreover, none of those research has combined cellular-level mathematical models with protein-protein functional interaction network analysis, to predict essential proteins, biological processes and enriched pathways associated with cancer disease.

1.3 Objectives of the Project

This project is aimed at identifying breast cancer disease target using mathematical modelling and computational simulations of tumor microenvironment dynamics. In order

to achieve it, the objectives are:

- Describing the tumor-immune system interaction through the network of cytokines in the presence of cancer in the tumor microenvironment,
- Formulating and analysing the mathematical model that describes the dynamics of tumor growth and the host immune system components in the tumor microenvironment,
- Identifying cytokines that play a significant role in the inhibition and activation of immune responses leading to tumor progression and regression, respectively and
- Identifying proteins that can trigger key cytokines in the model, analysing their interactions with other proteins in human, and possibly elucidate essential proteins as a biomarker for effective treatment to eliminate breast cancer.

1.4 Outline of the Project

This project is arranged into five chapters. In Chapter 2, we explore some of the related works to this thesis by first reviewing relevant biological literature on immune response associated to tumor growth in the tumor microenvironment, some of the proposed mathematical models on the dynamics of tumor-immune interaction in the tumor microenvironment, and key measures important for understanding protein-protein functional interaction network analysis. In Chapter 3, we develop a new mathematical model to investigate the dynamics of cancer growth and host immune system components through a network of cytokines in the tumor microenvironment. We also perform both analytical and numerical analysis of the model. In Chapter 4, we identify proteins and breast cancer genes that regulate key cytokines in our model by first characterising a unified human protein-protein functional interaction network using human protein sequences database gotten from different biological data sources. Also, we suggest essential proteins as a new development for an effective treatment to eliminate breast cancer. Chapter 5 summarises the thesis and formulate some recommendations.

Chapter 2

Literature Review

In this chapter, we review related works to this thesis by first reviewing the relevant biological literature on immune response associated to tumor growth in the tumor microenvironment, review some of the proposed mathematical models on the dynamics of tumor-immune interaction, and also present some useful measures that will be used in the analysis of protein-protein interaction network.

2.1 The immune system

The human *immune system* is the system of cells, tissues and organs that work together to defend the body against infection and toxins. There are two types of immune system: *innate* and *adaptive* immune system.

2.1.1 The innate immune system

The innate immune system also known as *non-specific immune system* is regarded as the first line of defence in our body's immune system. It gives the initial defence against pathogenic infections once a pathogen (bacterium or virus) attacks the body. It is activated by the presence of molecules called *antigens* and the chemical properties presented by the pathogens. As shown in Figure 2.1, the innate immune cells are granulocytes (neutrophils, eosinophil, and basophil), mast cells, complement protein, $\gamma\delta$T cell, natural killer T cell, macrophage, dendritic cells (DCs) and natural killer cells (NK cells). The latter three are essential in tumor recognition and shall, therefore, be used in the analysis of the tumor microenvironment [47, 71, 100, 104].

Macrophages are derived from the process of *hematopoiesis* in the bone marrow. Once they sense the presence of invaders, they are being activated and are the first type of

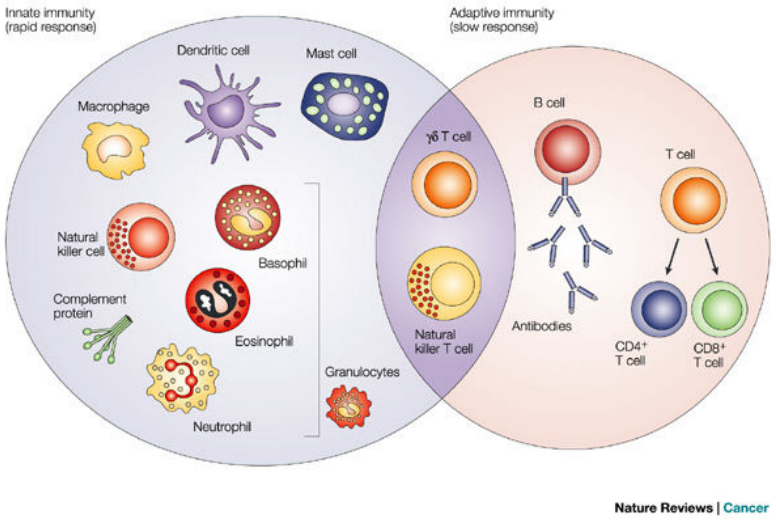

Figure 2.1: An illustration of the immune system (https://www.nature.com/nrc/).

cells which arrive at the infection site and then undergo a process known as *phagocytosis* whereby the macrophages engulf the invader and destroy it [100].

Unlike macrophages, natural killer cells do not attack pathogens directly. Instead, once they receive a signal from the infected host cell, through the expression of specific receptors, they are being activated and then destroy such infected host cells to stop the spread of the infection [100]. On the other hand, dendritic cells function as the brain of the immune system and have been seen to act as a link between the innate and the adaptive immune system [100]. They are therefore crucial for the activation of the adaptive immune system.

2.1.2 The adaptive immune system

The adaptive immune system, also known as *specific immune system*, is a defence system that is made up of relatively specialised cells and processes that eliminate or prevent the development of abnormal conditions. It can recognise the antigens as it produces memory cells and in the case where the antigen is already known, adaptive immune cells might be more efficient than those of the innate immune [100]. Unlike the innate immune system, the adaptive immune system depends on fewer cells, such as the B cells and T cells, as depicted in Figure 2.1, to carry out its task.

B cells are also derived from the process of hematopoiesis in the bone marrow. They are associated with the antibody-mediated immune response by displaying unique proteins known as *antibodies* on their surface to recognise pathogens and tag them for de-

struction.

However, T cells are derived from the thymus and are associated with the cell-mediated immune response. They can recognise infected cells with the help *major histocompatibility complex* (MHC) class I and II molecules, whose primary role is to attach itself to antigens gotten from pathogens and display them on the cell surface for acknowledgement by the appropriate T-cells [100]. T cells then use their receptor, i.e., *T cell receptor* (TCR) to view the presented antigens. They are categorized into three main types: cytotoxic T lymphocytes (CTLs), helper T cells (Th cells) and the regulatory T cells (Treg).

- *Cytotoxic T lymphocytes (CTLs)* also known as *$CD8^+$ T cell* primary job is to destroys virus-infected cells. When a cell is being infected by a virus, peptides will be loaded on MHC class I molecule which will then be transported on the surface of the infected cells. CTLs will use their receptor to identify the infected cells and destroy them. They need a cytokine called *interleukin-2* (IL-2) for continued proliferation, and activated Th cells are the major supplier of this cytokine [100].
- *Helper T cells (Th cell)* also known as *$CD4^+$ T cell* secretes chemical messengers (cytokines) that have dramatic effects on other immune system cells. They are basically cytokine factories. Th cells are activated by first recognising its cognate antigen displayed on MHC class II molecule [100]. Once activated, it then proliferates to build up clone composed of different types of Th cells namely: *type 1 helper T* (Th1) cells, *type 2 helper T* (Th2) cells, *type 17 helper T* (Th17) cells and *regulatory T cells* (Treg), whose receptors can recognise the same antigen. When these cells become matured, they can produce cytokines needed to control and direct activities of the immune system. By doing this, Th cells help control the strength of the CTLs response and made it capable of killing many target cells or invaders by secreting cytokines such as *tumor necrosis factor alpha* (TNF-α) and *interferon gamma* (IFN-γ) because they have anti-tumor and antimicrobial effects [100].
- *regulatory T cells(Treg)* keeps the immune system from over reacting [100].

2.2 The role of immune response in cancer

Many research studies have proved the vital role of the immune system in the control of tumor development and progression [47, 71, 100, 104]. The immune cells coupled with some other components in the tumor microenvironment has been seen to be useful in fighting against tumor cells. Among the cells in the immune system, macrophages, NK

cells, DCs and T cells have been discovered to play critical roles in the immune response in cancer [17, 45, 46, 81, 97, 125].

2.2.1 The role of macrophages in the immune response in cancer

Macrophages are differentiated from a kind of white blood cell, called *monocyte*, in the bone marrow. The function of macrophages in immune response can be described as multifaceted. It performs the first line of defence against tumorigenesis acts by directly killing tumor cells and producing different antitumor mediators. However, they are capable of acquiring invasive and metastatic activities [97]. They can also be *immunosuppressive* by inhibiting inflammation or immune stimulatory at the outset of the inflammatory response.

They are classified into two main subsets: *classical M1 macrophages* and *alternative M2 macrophages*. M1 macrophages are produced in response to Th1 cytokine IFN-γ and they are known for producing pro-inflammatory cytokines such as *interleukin-2* (IL-2), *interleukin-6* (IL-6), *interleukin-12* (IL-12) and TNF-α. The role of M1 macrophages is to prompt an antitumor response by activating cytotoxic activities i.e killing of pathogens and tumor cells [46, 47, 97]. Contrarily to M1, M2 macrophages are known for pro-tumorigenic and anti-inflammatory activities in the tumor microenvironment. They are produced in response to Th2 cytokines *interleukin-4* (IL-4) [97] and express a wide array of anti-inflammatory cytokine *interleukin-10* (IL-10) and *tumor growth factor beta* (TGF-β) [47, 97].

The macrophages in a tumor are known as *tumor associated macrophages* (TAMs). Once activated by cancer cells, they enhance tumor metastasis through a diverse mechanism such as *tumor angiogenesis* (i.e. the development of new blood vessels promoting tumor growth), and tumor cell migration and invasion[89]. TAMs are similar to M2 macrophages as they contribute to pro-tumorigenic and anti-inflammatory activities in the tumor microenvironment. They inhibit Th1, activates Th2 thereby initiating the immune response to inhibit killing of tumor cells [97]. Due to poor clinical prognosis and resistance to cancer therapy caused by TAMs, nowadays, TAMs are attractive target for cancer therapeutic intervention. From previous research studies, it was gathered that TAM-targeting cancer therapy should include: prevention of macrophages recruitment, the transition of pro-tumorigenic M2 phenotype into antitumor M1 and restriction of TAM survival [97].

2.2.2 The role of NK cells in the immune response in cancer

NK cells have been seen to be a key player in the immune surveillance of cancer and also able to prevent tumour growth [71, 97]. They are also involved in eradicating virus-infected cells and tumor. They can identify targets directly via activating or inhibitory receptors expressed on the cell surface of target cells (i.e. tumor cells). The ligand on the surface of tumor cells which differentiated it from normal cells triggers the receptors of NK cells thereby activating its cytotoxicity. NK cells are generally activated by different stimuli, of which are made of contact to the DCs, direct involvement of NK receptor(NKR) by stress-induced tumor molecules, and secretion of various cytokines such as interleukin-1(IL-1), IL-2, IL-12, IL-15, IL-18, IL-21 and IFN-γ [81].

Evidence has shown that cytokines IL-2, IL-12, IL-15, IL-18, and costimulatory protein *CD40* found on antigen presenting cells, enhances the NK cells effector activities. That is, IFN-γ production, proliferation and its cytotoxicity against tumor cells [17, 97]. IFN-γ secreted by activated NK cells have powerful antitumor activities, including inducing MHC class I expression and sensitizing tumor cells to $CD8^+$ T cell killing [71]. The combination of IFN-γ and CD40 play a significant role in the stimulation of DCs thereby enhancing IL-12 production by DCs. From Singh studies, the interaction between NK cells and DCs is vital for the augmentation of innate response and the activation of potent adaptive immunity [98].

2.2.3 The role of DCs in the immune response in cancer

Over the years, research has highlighted that the DCs is more potent in presenting antigens to the T cells in order to orchestrate the antigen-specific T cells responses. Hence, it is broadly agreed that the primary immune responses can only be initiated by the DCs [100, 104]. That is, they can efficiently activate naive T cells, while, the B cells and macrophages act as antigen presenting cells (APCs) in the augmentation of pre-activated T cells and also in the activation of memory T cells.

DCs play significant roles in activating, directing and regulating adaptive immune response. They are also critically involved in tumor immunosurveillance [104]. Moreover, some evidence *in vivo* have shown that tumor-infiltrating DCs are capable of recognising tumor antigens which have grown to maturity in the tumor microenvironment. Thus, they act as an effective APCs inducing a specific anti-tumor immune response. Due to the presence of tumor cells in the microenvironment, immature DCs are activated (or become matured) through the production of pro-inflammatory cytokine IL-12 made by activated macrophages. Matured DCs then present tumor antigens onto MHC class I

and II molecules displayed on its surface. Following the uptake, mature DCs then locate and activates cognate naive and central memory T cells in the draining lymph nodes. Licensing of mature DCs (i.e., the interaction of mature DCs with activated $CD4^+$ T cells or NKT cells through CD40 on the surface of DCs, and costimulatory protein *CD40L* on the surface of $CD4^+$ T cells) is firmly believed to be able to activates naive $CD8^+$ T cells efficiently. Otherwise, the $CD8^+$ T cells may function as an effector cell just for little lifespan [104].

2.2.4 The role of T cells in the immune response in cancer

The adaptive immune system performs a crucial role with regards to the host ability to produce an effective antigen-specific immune response against tumors [90]. The helper T cells ($CD4^+$ T cells) assume a vital role at the onset of adaptive immune response. They usually recognise peptides bound to MHC class II molecules on APCs which include dendritic cells, macrophages and B cells [45, 125]. From studies, it has been demonstrated that when tumors exhibit antigens which differentiated them from normal cells, they can be recognised by effector T cells of the adaptive immune system and prompt antitumor immune response in both human system and experimental mice [31]. As mentioned earlier, the *naive helper T* (Th0) cells develop into clone of effector subsets, namely: the type 1 helper T cells (Th1 cells), type 2 helper T cells (Th2 cells), type 17 helper T cells (Th17 cells) and regulatory T cells (Treg) upon activation. Each subset can be characterized on the source of cytokines they secrete. For example, Th1 cells secrete IFN-γ, Th2 cells secrete IL-4, Th17 cells secretes IL-17, and Treg secretes IL-10 which can modulate the function of other T cells [125].

Among the activated helper T cell subsets, Th1 cells have been seen to be one of the most promising in producing an antitumor immune response. Upon antigen encounter, Th1 cells produce a large amount of IFN-γ and also secrete pro-inflammatory cytokines including IL-2, TNF-α, and IFN-γ. On the other hand, Th2 cells are well-known for producing anti-inflammatory cytokines, such as IL-4, IL-5 and IL-13, and are in charge of coordinating humoral immunity responses. However, cytokines such as IL-6, TGF-β, IL-17, IL-21, and IL-23 are associated with Th17 cells, and they contribute to tumor progression and carcinogenesis in the context of chronic inflammation and infection [31].

From several studies, it has been gathered that positive clinical outcome can be allotted to Th1 effector cell infiltrating within tumors of patients with various cancer, in the sense that Th1 cells can control tumors through the secretion of IFN-γ which directly or indirectly affected immune activation and modulation. IFN-γ can also induce priming and maturation of cytotoxic activity of CTLs through the activation of DCs in the tumor

microenvironment and further prompt the elimination of tumor through activation of NK cells and M1 macrophages [86].

Universally, cytotoxic T lymphocytes (CTLs) also known as $CD8^+$ T cells is known to be the primary executor of effective anti-tumor T cell responses in the adaptive immune system due to its cytotoxic activity in the tumor microenvironment. It has been observed that tumors which evade $CD8^+$ T cells attack might have down-regulated the expression of MHC class I antigen. Moreover, $CD8^+$ T cell was shown to still maintain their anti-tumor effect in the absence of $CD4^+$ T cells, it can only last for limited time because the role of $CD4^+$ T cells is to improve the efficiency of $CD8^+$ T cells, thereby creating and sustaining long-term $CD8^+$ memory T cells response [45].

Also, $CD4^+$ T cells help in the activation and influence the differentiation and expansion of antigen-specific CTLs. Some evidence has suggested a direct role of effector $CD4^+$ T cell subsets in inhibiting tumor growth and production through the secretion of pro-inflammatory cytokines TNF-α and IFN-γ or direct cytolytic activity. This activity occurs by de-granulation of cytotoxic granule that contains toxic effector molecules, such as perforin and granzymes [107] or ligation of Fas Ligand(FasL) apoptotic killing pathway. This shows that $CD4^+$ T cells can eliminate tumor cells in the absence of $CD8^+$ T cells.

2.2.5 The role of cytokines secreted by innate immune cells in the TME

In the tumor microenvironment, the resting macrophages can differentiate the tumor cells from the normal cells due to the antigen presented on them. They are activated with the aid of pro-inflammatory cytokines IFN-γ [46]. The activated macrophage reacts by undergoing a process known as *phagocytosis* thereby eliminating the tumor cells.

Activated macrophages as already mentioned, are classified into two subtypes: M1 macrophages and M2 macrophages. M2 macrophages secrete anti-inflammatory cytokines, such as IL-10, TGF-β, IL-4 and IL-13, which are responsible for tumor progression and metastasis. Also, these cytokines facilitate the transition of M1 macrophages to M2 macrophages. Expression of IL-10 by M2 macrophages can help promote the production of IL-4 and IL-13 in Th2 cells [47]. On the contrary, M1 macrophages role is to cause an antitumor response by triggering cytotoxic activities and secreting pro-inflammatory cytokine IL-12 and IFN-γ. They also secrete IL-23 which develops and causes expansion of Th17 cells secreting IL-17, thereby contributing to inflammatory autoimmune pathologies[47].

The production of IL-12 by M1 macrophages in the tumor microenvironment activates the *immature dendritic cells* (iDCs). Following the uptake of tumor antigen pre-

sented onto the MHC class I and MHC class II molecules on themselves, they go through maturation and becomes *mature DCs* (mDCs). Through the secretion of IL-12 and also through pattern recognition receptor exhibited by the naive T cells upon identifying peptides produced by DCs, the cognate naive and central memory T cells composed of the $CD4^+$ T cells and $CD8^+$ T cells become activated [31, 104].

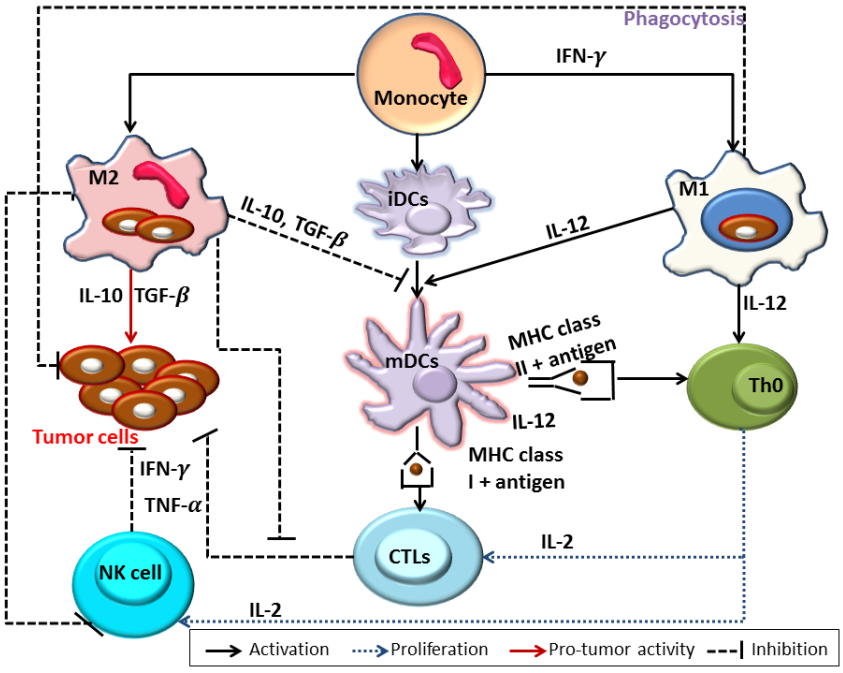

Figure 2.2: Activities of immune cells in the tumor microenvironment.

2.2.6 The role of cytokines secreted by adaptive immune cells in the TME

As illustrated in the schematic diagram Figure 2.2, naive $CD4^+$ T cells (Th0) are activated as a result of signals received from APCs such as dendritic cells or M1 macrophages upon encounter with antigen. After activation, $CD4^+$ T cells differentiate into a clone of its subsets namely: Th1, Th2, Th17, and T_{reg}, with each type having distinct cytokines secretion for a specific function in the tumor microenvironment [53] as shown in Figure 2.3.

Th1 cells development pathway is typically driven by IL-12, while Th2 cells arise as a result of an environment rich in IL-4 [13]. Th1 cells secrete IL-2 which acts as growth factor thereby enhancing the continued proliferation of Th1, NK and $CD8^+$ T cells in the TME. IL-2 secretion also stimulates the generation of IFN-γ by Th1 and prevent

activated cells from regressing to an inactive state. Furthermore, Th1 cells secrete IFN-γ and TNF-α, thereby enhancing cytotoxic capabilities of immune cells including M1 macrophages, NK cells and $CD8^+$ T cells to cancerous cells [13, 53]. Synergistically with TNF-α, the secretion of IFN-γ mediates cytotoxicity of tumor cells by inducing reactive oxygen species and inhibiting angiogenesis [125]. As already mentioned, Th2 cells are known for producing anti-inflammatory cytokines, such as IL-4, IL-5, and IL-13. All these cytokines promote M2 macrophages phenotype. In particular, IL-4 is as an autocrine growth factor for Th2 cells [120].

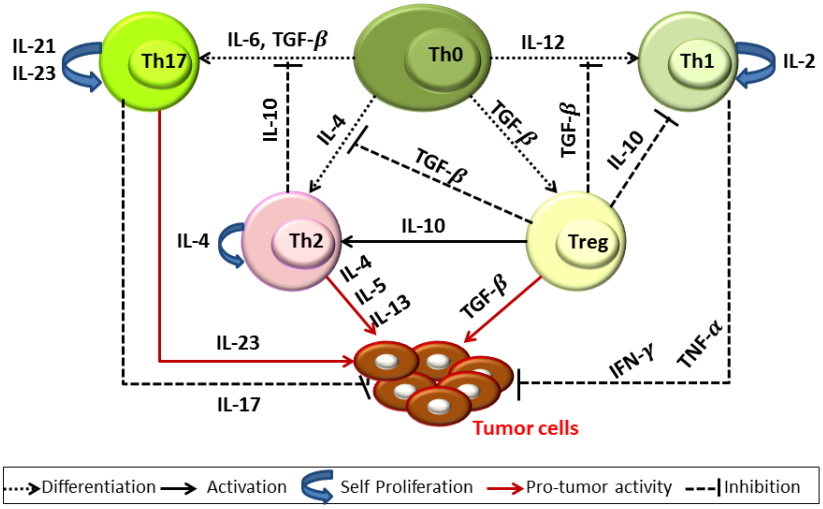

Figure 2.3: Th0 cells differentiation into clone of effector subsets.

Cytokine TGF-β and IL-6 enhances the differentiation of Th0 cells into Th17 cells. Th17 cells also proliferate by secreting IL-21 which further increase Th17 generation in an autocrine manner. IL-23, secreted by Th17 cells, also promotes the proliferation and inflammatory activity of Th17. Also, Th17 cells secrete IL-17 which promotes maturation of DCs family and induce IL-12 production from macrophages, thereby promoting CTLs activation [31].

However, regulatory T cells (Treg) depend on TGF-β for their differentiation. After differentiation, they secrete TGF-β which inhibits the Th1 and Th2 cells differentiation and also secrete IL-10 which promotes the proliferation of Th2-cytokines and inhibits

the proliferation of Th1-cytokines [2]. Several studies indicate IL-10 as a negative mediator in the cross-talk among the innate and adaptive anti-tumor immune response. They are known to hold APCs by inhibiting MHC molecules, down-regulating IL-12 production and inhibiting DCs maturation and differentiation as shown in Figure 2.2. They can potentially limit the protumor/antitumor effects of Th17 mediated inflammation, specifically by interacting with IL-10 receptors of Th17 cells [31]. IL-10 can also reduce the ability of $CD8^+$ T cells in eliminating cancer cells [67].

$CD8^+$ T cells secrete cytokine TNF-α and IFN-γ which enhance and strengthen its cytotoxic function against tumor cells. The combination of the two cytokines drives tumor cell into deterioration. Likewise, the natural killer cells induce direct killing of the tumor cells once they have been activated either through the secretion of IL-2 or its activated receptor as a result of recognition of tumor antigen presented on the tumor cells. They also secrete cytokine TNF-α and IFN-γ, thereby enhancing the cytotoxic effect made on the tumor cell leading to tumor regression [17]. NK cells also help at a later stage of tumor growth by acting as an aide in the priming process of Th1 and $CD8^+$ T cells through IFN-γ production [2].

2.2.7 The role of cytokines in cancer cells growth

Cancer cells inhibit IFN-γ production and paralyze antitumor effector cells (NK cells, $CD8^+$ T cells and M1 macrophages) through the secretion of immuno-suppressive factors, including IL-10, IL-6, VEGF (Vascular endothelial growth factor) and TGF-β [7]. Cytokines, secreted by M2 macrophages and Th2 cells, also contributes to tumor initiation, progression and metastasis. As the population of tumor grows very large in the microenvironment, tumor cells tend to lack oxygen. They, therefore, produce TGF-β, thereby encouraging angiogenesis and avoid the immune response which leads to tumor escape [50]. Interestingly, cytokine IL-23 is produced not only by DCs and macrophages, but also by cancer cells. As IL-12 acts on naive $CD4^+$ T cells, IL-23 also acts on memory $CD4^+$ T cells [38]. IL-23 has been shown to effectively suppress innate antitumor response and acts as an important molecular driver of Th17 cells [105]. Besides, IL-23 induces immunosuppression through down-regulation of $CD4^+$ and $CD8^+$ T cells infiltrating in tumor tissues [80].

2.3 Modelling tumors and the immune system

Over many years of research on anticancer immunotherapy, several mathematical models have been developed and analysed [26, 50, 54, 69]. Here, we explore some of the

important papers in the mathematical modelling of tumor-immune interaction. We concentrate on these papers because some of their ideas were used in formulating our model.

Kirschner and Panetta (1998) in their paper on modelling immunotherapy of the tumor-immune interaction, presented a mathematical model representing the dynamics between tumor cells, immune-immune-effector cells coupled with IL-2 dynamics. The result from their model shows that tumor cells elimination can only be done by combining both adoptive cellular immunotherapy (ACI) and administration of the cytokine IL-2. It, therefore, emphasizes the crucial role of cytokine-enhanced immune function in cancer treatment [54]. Furthermore, Baloni and Us (2013) built on the existing model and developed a mathematical model of tumor and immune-effector cells with scheduled chemotherapy. They concluded that the effect of scheduled IL-2 dose with chemotherapy and adoptive cellular immunotherapy reduces tumor growth [8].

De Pillis and Radunskaya (2003) in their paper formulated a mathematical model of tumor growth with the aim of addressing some arising questions concerning the mechanisms implicated in the immune response to a tumor challenge. The model is in the form of a system of ordinary differential equations (ODEs) focusing on the interaction between NK cells and $CD8^+$ T cells with tumor cells. It explores the dynamics of tumor escape as well as describes the development of immunity to upcoming tumor challenges [26].

Arciero et al. (2004) presented a mathematical model of a nonlinear system of ODEs describing the growth, immune escape and siRNA treatment of tumors. In their paper, they pointed out the vital role of pro-inflammatory and anti-inflammatory cytokines in cancer research. They used pro-inflammatory cytokine IL-2 and anti-inflammatory cytokine TGF-β as a case study. The interactions among immune cells, tumor cells and cytokine IL-2 and TGF-β were described. The results depict the pro-tumor activity of TGF-β. It weakens the immune system by reducing tumor antigen expression, thereby hindering the activation of immune effector cells. This results in the stimulation of tumor growth by promoting angiogenesis and its ability to escape host detection. The inclusion of siRNA treatment reduces TGF-β production by targeting the miRNA that codes for TGF-β. It thereby reduces the presence and the effect of TGF-β in the tumor cells, which, in turn, suppress the tumor cell [50].

Later on, de Pillis et al. (2006) advance by developing a mathematical model of a system of ODEs governing tumor development on a cell population level coupled with the combination of chemotherapy, vaccine and immunotherapy treatments. The situation whereby neither chemotherapy nor immunotherapy alone can be enough to

control tumor growth was established. They concluded that a combination of these therapies could lead to the eradication of tumors [27].

On the other hand, Robertson-Tessi et al. (2012) in their paper proposed a mathematical model of the interaction between tumor growth and immune system (including the main cell populations implicated in effector T-cell mediated tumor killing, i.e., the regulatory T cells (Tregs), helper T cells and dendritic cells). Multiple mechanisms of immunosuppression, such as cytokines and growth factors, which regulates the interaction between the cell population, were incorporated. Their report demonstrated the effect of Tregs and TGF-β on different classes of tumors. Access to fully grown tumor size by factors, such as TGF-β, induced immunosuppression, the transformation of helper T cells to Tregs, and limitation of the immune cell was shown to lead to tumor escape [91].

Moreover, Awang and Maan (2016) proposed a new mathematical model focusing on the function of NK cells and $CD8^+$ T cells in tumor-immune interaction. They included a subdivision of the tumor population into interphase and mitosis. Like others, they also discovered that immune suppression made by NK cells and $CD8^+$ T cells in the model greatly helps to stabilize the system and further inhibits the growth of tumor cells [6].

Mahasa et al. (2016) in their paper presented a mathematical model which involves different tumor cell and immune cell population. Their model depicts the progression and survival of tumor cells upon encounter with the immune system. This process is mediated by the activated $CD8^+$ T cells and natural killer cells. They came up with predictions showing that recruitment of NK-cells from an external source might perform a vital role in strengthening NK-cell immune surveillance. They also predicted that inhibition of tumor cells progression could not be efficiently carried out alone by the host immune system, but with addition of some external factors [69].

Most of the research studies that have been carried out of which few are reviewed above, only focus on modelling tumor-immune dynamics by considering the interaction in some specific host immune system, which was shown by Mahasa et al. (2016) to be ineffective against tumor cell progression. It is because there are some hidden factors that have not been considered while performing the analysis. These factors are complex interaction components found in the tumor microenvironment. They regulate cancer stem cells through network of cytokines and growth factors. Therefore in this research, key components, such as various immune cells and cytokines which made up the tumor microenvironment and in one way or the other contributes to tumor formation including tumor initiation and metastasis, will be incorporated in the formation of our new mathematical model to further investigate the dynamics of tumor-immune interaction.

2.4 Centrality Analysis Methods for Biological Networks

For a better understanding of the biological organization of humans from its protein functional network and probably use it as a means to establish effective treatment strategies for diseases, it is required to fully have an understanding of the network structure and how each protein contributes to the system biological processes [75]. For this reason, network centrality measures are used to identify proteins which are likely significant to the functioning of the system thereby contributing to the survival of humans and organisms. Different measures have been employed from other fields of science in order to understand the influences of nodes in a network. Of these measures are the centrality analysis measures of networks. In biology, centrality analysis is essential in analysing biological networks, and it is mainly used to identify key players in biological processes [57]

In the analysis of network, in particular biological network, it is essential to identify the most central node that influences the topology of the network based on the question at hand. In the course of this research, proteins are *nodes* while functional interaction or connection between proteins are *edges*. As stated earlier, among the centrality measure available, the following measures will be needed in our study.

We denote $\mathcal{P}(\mathcal{P},\mathcal{I})$ the functional network of proteins of an organism with $\mathcal{P}$ the set of nodes (i.e., interacting proteins) and $\mathcal{I}$ the set of links (i.e., functional interaction between proteins).

1. The **degree centrality** measure, $C_d(i)$, of a protein i is the number of edges incident to protein i. It is considered as a measure of a protein influence in the functional network. In other words, the more the degree of a protein is the greater the number of processes it might be involved in. In 2001 Jeong et al. used degree centrality to correlate the degree of a protein in a network of which if removed from the protein-protein interaction (PPI) network can lead to lethality [57]. Mathematically, degree centrality $C_d(i)$ of a node i is given [75] by

$$C_d(i) = deg(i) = \sum_{j\in\mathcal{P}} \zeta(i,j), \tag{2.4.1}$$

where

$$\zeta(i,j) = \begin{cases} 1 \text{ if } (i,j) \in \mathcal{I}, \\ 0 \text{ else.} \end{cases}$$

2. The **closeness centrality** measure of a protein i, $C_{clo}(i)$, is a centrality measure which indicates how important a protein is by how quickly it communicate with

every nodes of the network, or how close the node is to its neighbours. It uses average distance of a protein to all other proteins and it is defined as the reciprocal of this sum. In other words, closeness centrality measure $C_{clo}(i)$ of a node i is given by

$$C_{clo}(i) = \frac{n_c - 1}{\sum_{j \in \mathcal{P}} dist(i,j)} \tag{2.4.2}$$

where $dist(i,j)$ is the distance or shortest path between the nodes i and j and n_c is the number of node in the connected component containing i. The normalized closeness centrality is given by

$$\frac{(l_c - 1)}{(n_c - 1)C_{clo}(i)}$$

where l_c is the number of link in the connected component containing i [75].

3. The **betweenness centrality** measure, $C_b(w)$, of a protein w is the proportion of of shortest paths that passes through it. It measures the influence of w with regards to other proteins in the functional network. That is, it shows the value of the given protein in the communication between proteins. Mathematically, betweenness centrality of a node w is given by

$$C_b(w) = \sum_{i,j \in \mathcal{P}_w} \frac{\sigma_{ij}(w)}{\sigma_{ij}} \tag{2.4.3}$$

where σ_{ij} is the total number of shortest paths between i and j, $\sigma_{ij}(w)$ is the number of shortest paths from i to j that passes through w, and $\mathcal{P}_w = \{(i,j) \in \mathcal{P} \times \mathcal{P} : w \neq i \neq j\}$ [75] .

Chapter 3

Modelling TME Components Dynamics

Mathematical modelling of biological processes is often used to deepen our understanding of dynamics that is essential for an immune response. In this chapter, we focused on the most important immune cells and cytokines that have been identified to play a crucial role in cancer. The innate and adaptive immune cells under consideration are: the resting macrophages or monocytes (M0), M1 macrophages, M2 macrophages, natural killer (NK) cells, dendritic cells (DCs), helper T cells ($CD4^+$ T cells) and its subsets, effector T cells ($CD8^+$ T cells) and tumor cells [26, 50, 54, 69]. The cytokines and growth factors used are IL-2, IL-4, IL-5, IL-6, IL-4, IL-10, IL-12, IL-13, IL-17, IL-21, IL-23, TNF-α, TGF-β, and IFN-γ. We developed a new mathematical model describing the dynamics of cancer growth and the host immune system components in the tumor microenvironment. In addition to this, we performed the analytical and numerical analysis of the model.

3.1 Model Description and Assumptions

The formulation of our model is presented using nonlinear ordinary differential equations (ODEs) by considering the dynamics of the population of immune cells, tumor cells, and cytokines with respect to time t in the tumor microenvironment. Figure 3.1 depicts a schematic diagram describing the cytokine-mediated innate-adaptive immunity in a tumor dynamics. Below, we explain the stepwise formation of the model equation. The model variables and parameters used are summarised in Table 3.1 and Table 3.2, respectively.

Table 3.1: Description and units of variables used in the model

Variables	Description	Units
M_0	Density of resting macrophages	cells/ml
M_1	Density of pro-inflammatory tumor associated macrophages	cells/ml
M_2	Density of anti-inflammatory tumor associated macrophages	cells/ml
N	Density of natural killer cells	cells/ml
D	Density of dendritic cells	cells/ml
T_8	Density of $CD8^+$ cells	cells/ml
T_0	Density of the naive $CD4^+$ (helper) T cells (Th0)	cells/ml
T_1	Density of type-1-helper T cells (Th1)	cells/ml
T_2	Density of type-2-helper T cells (Th2)	cells/ml
T_{17}	Density of type-17-helper T cells (Th2)	cells/ml
C	Density of tumor cells	cells/ml
I_2	Concentration of interleukin-2 (IL-2)	pg/ml
I_4	Concentration of interleukin-4 (IL-4)	pg/ml
I_6	Concentration of interleukin-4 (IL-6)	pg/ml
I_{10}	Concentration of interleukin-10 (IL-10)	pg/ml
I_{12}	Concentration of interleukin-12 (IL-12)	pg/ml
I_{13}	Concentration of interleukin-13 (IL-13)	pg/ml
I_{17}	Concentration of interleukin-4 (IL-17)	pg/ml
I_{21}	Concentration of interleukin-10 (IL-21)	pg/ml
I_{23}	Concentration of interleukin-12 (IL-23)	pg/ml
I_γ	Concentration of interferon-gamma (IFN-γ)	pg/ml
T_α	Concentration of tumor necrosis factor-α (TNF-α)	pg/ml
T_β	Concentration of transforming growth factor-β (TGF-β)	pg/ml

3.1.1 Immune Cells Equations

Resting macrophages (M_0)

$$\frac{dM_0}{dt} = m - \alpha_1 I_\gamma M_0 - \alpha_2 M_0 C - \delta_0 M_0. \tag{3.1.1}$$

Equation (3.1.1) represents the dynamics of resting macrophages in the TME. Parameter m is the constant supply rate for macrophages which represents the fact that macrophages as one of the innate immune cells, are constantly present within the host body even in the absence of tumor. As mentioned earlier, once they are activated as a result of the presence of tumor cells in the TME, they polarized into two phenotypes: M1 macrophages and M2 macrophages. They respectively polarized at a rate α_1 and α_2 due to the presence of pro-inflammatory cytokine IFN-γ and tumor cells. The parameter δ_0 is the natural decay rate of the resting macrophages.

Table 3.2: Description and units of parameters used in the model

Parameter	Description	Units
d	External influx rate of DCs	cells/ml/day
m	External influx rate of macrophages	cells/ml/day
n	External influx rate of NK cells	cells/ml/day
σ_0	Constant supply of Th0 cells upon activation	cells/ml/day
σ_8	Constant supply of $CD8^+$ T cells upon activation	cells/ml/day
ρ_1	Proliferation rate of M1 Macrophages	day^{-1}
ρ_3	Proliferation rate of Th1 cell	day^{-1}
ρ_4	Proliferation rate of Th2 cell	day^{-1}
ρ_5	Proliferation rate of Th17 cell	day^{-1}
ρ_n	Proliferation rate of NK cells	day^{-1}
ρ_d	Proliferation rate of DCs	day^{-1}
ρ_t	Proliferation rate of $CD8^+$ T cells	day^{-1}
η	Half saturation constant of the immune response	
τ	Transition rate from M1 to M2 Macrophages by anti-inflammatory cytokines	day^{-1}
β_n	Inactivation rate of NK cells by tumor cells	day^{-1} $cell^{-1}$
β_1	Inactivation rate of Th1 cells by tumor cells	day^{-1} $cell^{-1}$
β_8	Inactivation rate of $CD8^+$ T cells by tumor cells	day^{-1} $cell^{-1}$
θ_1	Intrinsic growth rate of tumor cells	day^{-1}
θ_2	Maximum carrying capacity of tumor cells	$cell^{-1}$
α_m	Expansion rate of tumor cells by M2 macrophages	day^{-1}
γ_1	Expansion rate of NK and Th1 cells enhanced by IL-2	day^{-1}
γ_2	Expansion rate of dendritic cells enhanced by IL-12 and IL-17	day^{-1}
γ_3	Expansion rate of Th2 cells enhanced by IL-4 and IL-10	day^{-1}
γ_4	Expansion rate of Th17 cells enhanced by IL-21 and IL-23	day^{-1}
γ_5	Expansion rate of $CD8^+$ T cells by enhanced IL-2 and IL-17	day^{-1}
α_1	Polarization of resting macrophages into M1	cells/ml/day
α_2	Polarization of resting macrophages into M2	cells/ml/day
α_t	Activation rate of T cells	cells/ml/day
$\zeta_i's$	Th0 differentiation into it subsets	cells/ml/day
$\delta_i's$	Apoptosis rate of macrophage phenotypes	day^{-1}
δ_n	Apoptosis rate of NK cells	day^{-1}
δ_d	Apoptosis rate of DCs	day^{-1}
$\mu_i's$	Apoptosis rate of Th0 cell and its subsets	day^{-1}
μ_8	Apoptosis rate of $CD8^+$ T cells	day^{-1}
Φ	Elimination rate of tumor cells by immune effector cells	day^{-1}
μ_c	Apoptosis rate of tumor cells by TNF-α	day^{-1}
μ_e	Apoptosis rate of M2 macrophages by IFN-γ	day^{-1}
h_γ	Inhibition measure by IFN-γ	day^{-1}
h_β	Inhibition measure by TGF-β	day^{-1}
h_{10}	Inhibition measure by IL-10	day^{-1}
$\nu_i's$	Production rate of tumor suppressing cytokines by immune cells	pg/cell/day
$\nu_j's$	Production rate of tumor promoting cytokines by immune cells	pg/cell/day
$\nu_k's$	Production rate of tumor promoting cytokines by tumor cells	pg/cell/day
δ_s	Decay rate of tumor suppressing cytokines	day^{-1}
δ_p	Decay rate of tumor promoting cytokines	day^{-1}

M1 macrophages (M_1)

$$\frac{dM_1}{dt} = \alpha_1 I_\gamma M_0 + \frac{\rho_1 M_1 C}{\eta + C} - \tau(I_4 + I_{13} + I_6 + T_\beta)M_1 - \delta_1 M_1. \tag{3.1.2}$$

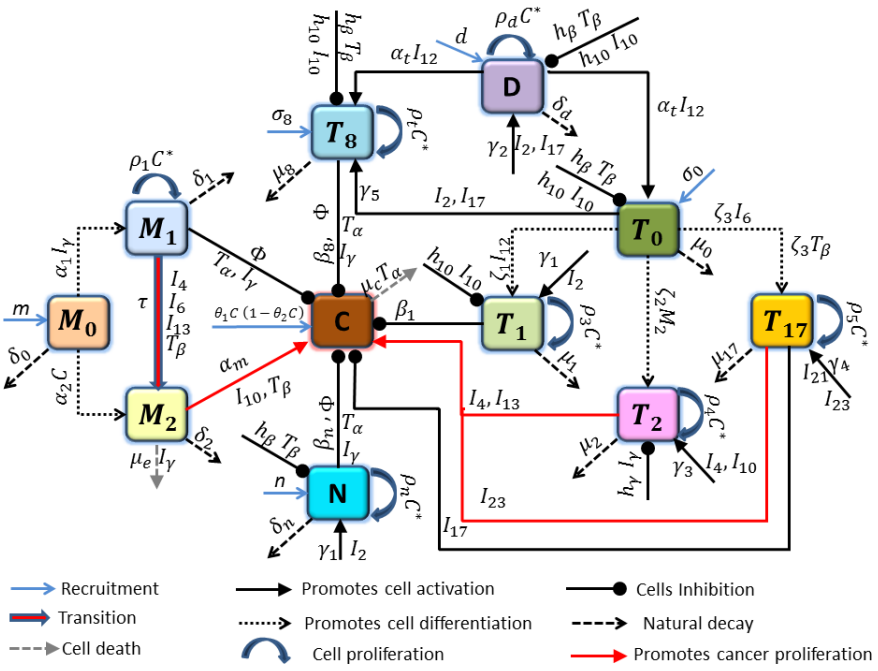

Figure 3.1: A schematic diagram of cytokine-mediated innate-adaptive immunity in a tumor dynamics. $C^* = \frac{C}{\eta+C}$. All variables and parameters shown in this figure are presented in Table 3.1 and 3.2. On most interaction arrows where the formula of the interaction is not given, we place on one side the variable(s) and on the other side the parameters(s) participating.

Equation (3.1.2) represents the dynamics of M1 macrophages in the TME. Parameter α_1 is the activation rate of M1 macrophages by IFN-γ. Once they are activated, they proliferate as represented in the second term in Michaelis-Menten form which describes the growth of immune cells in response to tumor cells. ρ_1 represents the proliferation rate of M1 macrophages due to stimulus and η the half saturation constant of the immune response. M1 macrophages undergo phagocytosis where they bind with the tumor cells by engulfing them and preparing them for death. The third term depicts the transition from M1 macrophages to M2 macrophages through anti-inflammatory cytokine IL-4, IL-13, IL-6 and TGF-β produced by Th2 cells and tumor cells respectively. Parameter τ is the transition rate from M1 to M2 [67] and δ_1 in the last term is the natural decay rate of M1 macrophages.

M2 macrophages (M_2)

$$\frac{dM_2}{dt} = \alpha_2 M_0 C + \tau(I_4 + I_{13} + I_6 + T_\beta)M_1 - \mu_e I_\gamma M_2 - \delta_2 M_2. \tag{3.1.3}$$

Equation (3.1.3) represents the dynamics of M2 macrophages also known as anti-inflammatory macrophages in the TME. Parameter α_2 is the activation rate of M2 macrophages by tumor cells. The second term as explained above is the transition from M1 to M2 macrophages thereby promoting the growth of tumor cells in the TME. The third term depicts the elimination of M2 macrophages by pro-inflammatory cytokine IFN-γ at a rate μ_e and δ_2 is the natural decay rate of M2 macrophages.

Natural killer cells (N)

$$\frac{dN}{dt} = n + \frac{\rho_n NC}{\eta + C} + \frac{\gamma_1 I_2 C}{1 + h_\beta T_\beta} - \beta_n NC - \delta_n N. \tag{3.1.4}$$

Nk cells are being supplied to the tumor site at a constant source n since they are normally present in the host body even in the absence of tumor cells in the TME. In the presence of tumor cells, NK cells are activated and proceed to proliferate in order to perform their cytotoxic activity. The proliferation made by NK cells in the TME due to stimulus is represented by the Michaelis-Menten form $\frac{\rho_n NC}{\eta + C}$. ρ_n stands for the proliferation rate of NK cells and η the half saturation constant of the immune response. This model makes sense because the proliferation of tumor-specific effector cells are triggered due to the presence of tumor cells but attains a saturation level at tumor population [6]. As depicted in the third term, IL-2 promotes NK cells proliferation at the tumor site with proliferation rate γ_1. This process is inhibited by TGF-β with inhibition measure h_β [7, 17]. The fourth term represents the local interaction or binding of NK cells to tumor cells with a binding rate β_n. This interaction can either result into programming tumor for lysis(i.e., death) or resulting to inactivation or killing of Nk cells [69]. δ_n is the natural decay rate of NK cells.

Dendritic cells (D)

$$\frac{dD}{dt} = d + \frac{\rho_d DC}{\eta + C} + \frac{\gamma_2 (I_{12} + I_{17}) C}{1 + h_\beta T_\beta + h_{10} I_{10}} - \delta_d D. \tag{3.1.5}$$

Parameter d in Equation (3.1.5) is assumed to be the constant supply rate of dendritic cells. The proliferation process is represented by the second term in Michaelis-Mentens form as explained in the previous equations where ρ_d represents the proliferation rate of DCs and η the half saturation constant of the immune response. Cytokine IL-12 and IL-17 promotes DCs activation with parameter γ_2 and this process is inhibited by anti-inflammatory cytokines IL-10 and TGF-β at rate h_{10} and h_β, respectively [31, 104]. δ_d in the last term is the decay rate of DCs.

CD4$^+$ T cells (T_0)

$$\frac{dT_0}{dt} = \alpha_t I_{12} D + \sigma_0 - \frac{\zeta_1 I_{12} T_0}{1 + h_\beta T_\beta} - \frac{\zeta_2 M_2 T_0}{1 + h_\beta T_\beta} - \frac{\zeta_3 (I_6 + T_\beta) T_0}{1 + h_{10} I_{10}} - \mu_0 T_0. \tag{3.1.6}$$

The DCs activate naive helper T cell(Th0) by secreting IL-12 at rate α_t[31, 104]. σ_0 in the second is the initial supply of CD4$^+$ T cells recruited to the tumor site. Parameter ζ_1, ζ_2 , and ζ_3 are the differentiation rates of Th0 into its subsets Th1,Th2 and Th17 upon encounter with IL-12, M2 macrophages, and IL-6 and TGF-β, respectively[13, 31]. h_β measures the inhibition rate of Th1 and Th2 by TGF-β while h_{10} measure inhibition of Th17 differentiation by IL-10 [2]. In order to simplify the model, we do not represent the assumption that Th0 differentiated into Treg. Hence, the last term depicts the natural decay of Th0 cells with rate μ_0.

Th1 cells (T_1)

$$\frac{dT_1}{dt} = \frac{\zeta_1 I_{12} T_0}{1 + h_\beta T_\beta} + \frac{\rho_3 T_1 C}{\eta + C} + \frac{\gamma_1 I_2 C}{1 + h_{10} I_{10}} - \beta_1 T_1 C - \mu_1 T_1 \tag{3.1.7}$$

Equation (3.1.7) represents the dynamics of Th1 cells with the first term representing Th0 differentiating into Th1 as explained in Equation (3.1.6). After differentiation, Th1 cells proliferate in order to secrete pro-inflammatory cytokines in the TME. This process is represented using Michaelis-Mentens form as previously explained in the equations above. Parameter ρ_3 represents the proliferation rate of Th1 cells, and the half saturation constant of the immune response is η. Moreover, in the third term, cytokine IL-2 enhances Th1 cells proliferation at the rate γ_1. This process is inhibited by IL-10 with inhibition measure h_{10} [2]. The fourth term stands for the inactivation of Th1 cells upon encounter with tumor cells with rate β_1 [53]. The last term is the decay of Th1 cells with rate μ_1.

Th2 cells (T_2)

$$\frac{dT_2}{dt} = \frac{\zeta_2 M_2 T_0}{1 + h_\beta T_\beta} + \frac{\rho_4 T_2 C}{\eta + C} + \frac{\gamma_3 (I_4 + I_{10}) C}{(1 + h_\gamma I_\gamma)} - \mu_2 T_2 \tag{3.1.8}$$

The first term in Equation (3.1.8) shows the differentiation of Th0 into Th2 as explained in Equation (3.1.6). Likewise, Th2 cells proliferation are represented using the Michaelis-Mentens form as previously explained where ρ_4 represents the proliferation rate of Th2 cells. The half-saturation constant of the immune response is η thereby secreting anti-inflammatory cytokines in the TME. Th2 cells proliferation is potentiated by IL-4 and promoted by IL-10 with rate γ_3 and this is inhibited by IFN-γ with parameter h_γ [13]. The last term is the decay of Th2 cells at a rate μ_2.

Th17 cells (T_{17})

$$\frac{dT_{17}}{dt} = \frac{\zeta_3(I_6 + T_\beta)T_0}{1 + h_{10}I_{10}} + \frac{\rho_5 T_{17}C}{\eta + C} + \gamma_4(I_{21} + I_{23})C - \mu_{17}T_{17} \tag{3.1.9}$$

Equation (3.1.9) represents the dynamics of Th17 cells. Its the first term represents Th0 differentiating into Th17 as explained in Equation (3.1.6). Th17 cells proliferation are modelled using the Michaelis-Mentens form as previously explained in the equations above. ρ_5 represents the proliferation rate of Th17 cells and η the half saturation constant of the immune response. Cytokine IL-23 and IL-21 promote th17 cells proliferation and expansion at the rate γ_4 [31]. Lastly, Th17 cells decay at a rate of μ_{17}.

CD8$^+$ T cells (T_8)

$$\frac{dT_8}{dt} = \alpha_t I_{12} D + \sigma_8 + \frac{\rho_t T_8 C}{\eta + C} + \frac{\gamma_5(I_2 + I_{17})C}{1 + h_\beta T_\beta + h_{10}I_{10}} - \beta_8 T_8 C - \mu_8 T_8 \tag{3.1.10}$$

The DCs activate CD8$^+$ T cells(CD8$^+$ T cells) by secreting IL-12 at rate α_t. After activation, CD8$^+$ T cells are recruited to the tumor site with initial supply σ_8. It then proliferates to carry out its cytotoxic activity on tumor cells. The third term, that is, the Michaelis-Menten form represents the proliferation of CD8$^+$ T cells in the TME with ρ_t representing the proliferation rate of CD8$^+$ T cells and η the half saturation constant of the immune response. This process is further enhanced and promoted by IL-2 and IL-17 with rate γ_5 which are further inhibited by IL-10 and TGF-β with inhibition measure h_{10} and h_β, respectively [2, 53, 67]. Likewise, the fourth term represents the local interaction or binding of CD8$^+$ T cells to tumor cells with a binding rate β_8. This interaction can either result into programming tumor for lysis or resulting to inactivation or killing of CD8$^+$ T cells [69]. Lastly, μ_8 is the decay rate of CD8$^+$ T cells.

3.1.2 Cancer Cell Equation (C)

$$\frac{dC}{dt} = \theta_1 C(1 - \theta_2 C) + \alpha_m M_2 - \Phi\left(M_1 + N + T_8\right)C - \mu_c T_\alpha C \tag{3.1.11}$$

The growth of tumor cells is modelled by the logistic term as depicted in the first term of Equation (3.1.11) which account for the deceleration in the growth of tumor cell as its size increases. Here θ_1 and θ_2 are the growth rate and carrying capacity of the tumor cells, respectively [34]. The second term depicts the fact that anti-inflammatory macrophages (M2) which function as the tumor associated macrophages (TAM) contributes to the growth of tumor cells pending their existence in the tumor microenvironment with parameter α_m. The third term is the local interaction between immune cells and tumor cells thereby bringing about their cytotoxic effect on the tumor cells at a rate

Φ. The last term shows that tumor cells are killed through the secretion of tumor suppressing cytokine TNF-α where μ_c is the elimination rate of tumor cells by TNF-α [34].

3.1.3 Cytokine Equation

$$\frac{dI_2}{dt} = \nu_2 T_1 - \delta_s I_2, \tag{3.1.12}$$
$$\frac{dI_4}{dt} = \nu_4 T_2 - \delta_p I_4, \tag{3.1.13}$$
$$\frac{dI_6}{dt} = \nu_6 C - \delta_c I_6, \tag{3.1.14}$$
$$\frac{dI_{10}}{dt} = \nu_{10} M_2 - \delta_p I_{10}, \tag{3.1.15}$$
$$\frac{dI_{12}}{dt} = \nu_{12} M_1 - \delta_s I_{12}, \tag{3.1.16}$$
$$\frac{dI_{13}}{dt} = \nu_{13} T_2 - \delta_p I_{13}, \tag{3.1.17}$$
$$\frac{dI_{17}}{dt} = \nu_{17} T_{17} - \delta_s I_{17}, \tag{3.1.18}$$
$$\frac{dI_{21}}{dt} = \nu_{21} T_{17} - \delta_s I_{21}, \tag{3.1.19}$$
$$\frac{dI_{23}}{dt} = \nu_c C + \nu_{23} T_{17} - \delta_p I_{23}, \tag{3.1.20}$$
$$\frac{dT_\alpha}{dt} = \nu_\alpha T_1 - \delta_s T_\alpha, \tag{3.1.21}$$
$$\frac{dT_\beta}{dt} = \nu_\beta C - \delta_c T_\beta, \tag{3.1.22}$$
$$\frac{dI_\gamma}{dt} = \nu_\gamma T_1 - \delta_s I_\gamma. \tag{3.1.23}$$

For simplicity, we assume that the cytokines are secreted by corresponding cells in TME at a constant rate. Here, IL-2, IFN-γ and TNF-α are produced by Th1 cells [13, 53], IL-12 is mainly produced by M1 macrophages [31, 47], IL-17 and IL-21 are produced by Th17 cells, IL-4, IL-5 and Il-13 are produced by Th2 cells [31, 120], IL-6 and TGF-β are produced by tumor cells [67], IL-10 is produced by M2 macrophages [47, 67] and IL-23 is produced by tumor cells and Th17 cells [31, 38, 47, 105]. All the ν_i's are the production rates of cytokines and δ_i's are their respective natural decay rates. Each parameter from Equation (3.1.1) to Equation (3.1.20) is assumed to be positive.

3.2 Model Reduction

From previous research, the growth of tumor cells involves numerous time scales which occurs roughly on weeks to months in *vitro* while in *vivo*, it takes a time interval of months to years. Recruitment of the immune cells under consideration occur on a time interval of days to weeks and secretion of inflammatory cytokines by these cells only occur on time interval of seconds to hours [67, 69]. In order to clearly understand the dynamics of tumor cells growth, we simplify the model using quasi steady state approximation (QSSA) for the concentration of the inflammatory cytokines by assuming that there is no change in concentration in time for all cytokines produced since they have a limited time of existence. Hence, from Equations (3.1.12)-(3.1.20) we have:

$$\begin{cases} I_2 &= \frac{\nu_2}{\delta_s} T_1, \\ I_4 &= \frac{\nu_4}{\delta_p} T_2, \\ I_6 &= \frac{\nu_6}{\delta_p} C, \\ I_{10} &= \frac{\nu_{10}}{\delta_p} M_2, \\ I_{12} &= \frac{\nu_{12}}{\delta_s} M_1, \\ I_{13} &= \frac{\nu_{13}}{\delta_p} T_2, \\ I_{17} &= \frac{\nu_{17}}{\delta_s} T_{17}, \\ I_{21} &= \frac{\nu_{21}}{\delta_s} T_{17}, \\ I_{23} &= \frac{\nu_c}{\delta_p} C + \frac{\nu_{23}}{\delta_p} T_{17}, \\ T_\alpha &= \frac{\nu_\alpha}{\delta_s} T_1, \\ T_\beta &= \frac{\nu_\beta}{\delta_p} C, \\ I_\gamma &= \frac{\nu_\gamma}{\delta_s} T_1. \end{cases}$$

We substituted these expressions into Equations (3.1.1)-(3.1.11) and assumed that the secretion of those cytokines produced by more than one immune cells varies. In order to further simplify the model, we neglected the cells with a lesser secretion of such cytokines. Hence, we obtain the following simplified model for cell dynamics in the tumor microenvironment.

$$
\begin{cases}
\frac{dM_0}{dt} = m - \kappa M_0 T_1 - \alpha_2 M_0 C - \delta_0 M_0, \\
\frac{dM_1}{dt} = \kappa M_0 T_1 + \frac{\rho_1 M_1 C}{\eta + C} - (\lambda T_2 + \varphi_1 C) M_1 - \delta_1 M_1, \\
\frac{dM_2}{dt} = \alpha_2 M_0 C + (\lambda T_2 + \varphi_1 C) M_1 - \xi_t T_1 M_2 - \delta_2 M_2, \\
\frac{dN}{dt} = n + \frac{\rho_n N C}{\eta + C} + \frac{\varepsilon_1 T_1 C}{1 + \xi_c C} - \beta_n N C - \delta_n N, \\
\frac{dD}{dt} = d + \frac{\rho_d D C}{\eta + C} + \frac{(\varepsilon_2 M_1 + \varepsilon_7 T_{17}) C}{1 + \xi_c C + \xi_2 M_2} - \delta_d D, \\
\frac{dT_0}{dt} = \omega M_1 D + \sigma_0 - \frac{\xi_d M_1 T_0}{1 + \xi_c C} - \frac{\zeta_2 M_2 T_0}{1 + \xi_c C} - \frac{\varphi_2 C T_0}{1 + \xi_2 M_2} - \mu_0 T_0, \\
\frac{dT_1}{dt} = \frac{\xi_d M_1 T_0}{1 + \xi_c C} + \frac{\rho_3 T_1 C}{\eta + C} + \frac{\varepsilon_1 T_1 C}{1 + \xi_2 M_2} - \beta_1 T_1 C - \mu_1 T_1, \\
\frac{dT_2}{dt} = \frac{\zeta_2 M_2 T_0}{1 + \xi_c C} + \frac{\rho_4 T_2 C}{\eta + C} + \frac{(\varepsilon_4 T_2 + \varepsilon_5 M_2) C}{1 + \xi_i T_1} - \mu_2 T_2, \\
\frac{dT_{17}}{dt} = \frac{\varphi_2 C T_0}{1 + \xi_2 M_2} + \frac{\rho_5 T_{17} C}{\eta + C} + (\epsilon_7 T_{17} + \epsilon_c C) C - \mu_{17} T_{17}, \\
\frac{dT_8}{dt} = \omega M_1 D + \sigma_8 + \frac{\rho_t T_8 C}{\eta + C} + \frac{(\varepsilon_8 T_1 + \varepsilon_9 T_{17}) C}{1 + \xi_c C + \xi_2 M_2} - \beta_8 T_8 C - \mu_8 T_8, \\
\frac{dC}{dt} = \theta_1 C(1 - \theta_2 C) + \alpha_m M_2 - \Phi\left(M_1 + N + T_8\right) C - \varepsilon_p T_1 C,
\end{cases}
\tag{3.2.1}
$$

where $\kappa = \frac{\alpha_1 \nu_\gamma}{\delta_s}$, $\lambda = \frac{\tau(\nu_4 + \nu_{13})}{\delta_p}$, $\varphi_1 = \frac{\tau(\nu_6 + \nu_\beta)}{\delta_p}$, $\xi_t = \frac{\mu_e \nu_\gamma}{\delta_s}$, $\varepsilon_1 = \frac{\gamma_1 \nu_2}{\delta_s}$, $\xi_c = \frac{h_\beta \nu_\beta}{\delta_p}$, $\varepsilon_2 = \frac{\gamma_2 \nu_{12}}{\delta_s}$, $\varepsilon_7 = \frac{\gamma_2 \nu_{17}}{\delta_s}$, $\xi_2 = \frac{h_{10} \nu_{10}}{\delta_p}$, $\omega = \frac{\alpha_t \nu_{12}}{\delta_s}$, $\xi_d = \frac{\zeta_1 \nu_{12}}{\delta_s}$, $\varphi_2 = \frac{\zeta_3(\nu_6 + \nu_\beta)}{\delta_p}$, $\varepsilon_4 = \frac{\gamma_3 \nu_4}{\delta_p}$, $\varepsilon_5 = \frac{\gamma_3 \nu_{10}}{\delta_p}$, $\xi_i = \frac{h_\gamma \nu_\gamma}{\delta_s}$, $\epsilon_7 = \frac{\gamma_4 \nu_{21}}{\delta_s} + \frac{\gamma_4 \nu_{23}}{\delta_p}$, $\epsilon_c = \frac{\gamma_4 \nu_c}{\delta_p}$, $\varepsilon_8 = \frac{\gamma_5 \nu_2}{\delta_s}$, $\varepsilon_9 = \frac{\gamma_5 \nu_{17}}{\delta_s}$, and $\varepsilon_p = \frac{\mu_c \nu_\alpha}{\delta_s}$ with general initial conditions $M_0(0) = M_0^0, M_1(0) = M_1^0, M_2(0) = 0, N(0) = N^0, D(0) = D^0, T_0(0) = T_0^0$, $T_1(0) = 0, T_2(0) = 0, T_{17}(0) = 0, T_8(0) = T_8^0$, and $C(0) = C^0$.

3.3 Model Analysis

In this section, we shall state some properties which guarantee the existence of non-negative solutions for our model as we are dealing with cell populations and only such solutions will be biologically meaningful.

Theorem 3.3.1 (Picard Lindelöf theorem)**.** *Consider the IVP,*

$$y'(t) = f(t, y(t)), \;\; y(t_0) = y_0, \;\; t \in [t_0 - \epsilon, t_0 + \epsilon]\,.$$

Suppose f is Lipschitz continuous in y and continuous in t. Then, for some value $\epsilon > 0$, there exist a unique solution $y(t)$ to the IVP within the range $[t_0 - \epsilon, t_0 + \epsilon]$ [93].

Theorem 3.3.2. *Let us denote* $y = (y_i)_{i=1,..,n}$ *and consider the function* $f : \mathbb{R}_+ \times \mathbb{R}^n_+ \to \mathbb{R}^n$ *continuous with respect to* (t, y) *and Lipschitz continuous with respect to* y*. If* $f_i(t, y) \geq 0$ *for* $(t, y) \in \mathbb{R}_+ \times \mathbb{R}^n$*, with* $y_i = 0$ *then for every* $y_0 \in \mathbb{R}^n_+$ *there exists* $T > 0$ *such that the solution to (3.2.1) exists on some interval* $[0, T)$*, is unique and positive. If* $T < \infty$*, then*

$$\limsup_{t \to T} \sum_{i=1}^{n} y_i = +\infty,$$

[93].

Theorem 3.3.3. *For the initial condition* $\left(M_0^0, M_1^0, M_2^0, N^0, D^0, T_0^0, T_1^0, T_2^0, T_{17}^0, T_8^0, C^0\right) \in \mathbb{R}^{11}_+$ *at* $t_0 = 0$ *the solution to (3.2.1) exists, is unique and non-negative on* $\mathbb{R}_+$*.*

Proof. Let us consider model (3.2.1) and denote

$$\begin{aligned}
f_1(X) &= m - \kappa M_0 T_1 - \alpha_2 M_0 C - \delta_0 M_0,\\
f_2(X) &= \kappa M_0 T_1 + \frac{\rho_1 M_1 C}{\eta + C} - (\lambda T_2 + \varphi_1 C) M_1 - \delta_1 M_1,\\
f_3(X) &= \alpha_2 M_0 C + (\lambda T_2 + \varphi_1 C) M_1 - \xi_t T_1 M_2 - \delta_2 M_2,\\
f_4(X) &= n + \frac{\rho_n N C}{\eta + C} + \frac{\varepsilon_1 T_1 C}{1 + \xi_c C} - \beta_n N C - \delta_n N,\\
f_5(X) &= d + \frac{\rho_d D C}{\eta + C} + \frac{(\varepsilon_2 M_1 + \varepsilon_7 T_{17}) C}{1 + \xi_c C + \xi_2 M_2} - \delta_d D,\\
f_6(X) &= \omega M_1 D + \sigma_0 - \frac{\xi_d M_1 T_0}{1 + \xi_c C} - \frac{\zeta_2 M_2 T_0}{1 + \xi_c C} - \frac{\varphi_2 C T_0}{1 + \xi_2 M_2} - \mu_0 T_0,\\
f_7(X) &= \frac{\xi_d M_1 T_0}{1 + \xi_c C} + \frac{\rho_3 T_1 C}{\eta + C} + \frac{\varepsilon_1 T_1 C}{1 + \xi_2 M_2} - \beta_1 T_1 C - \mu_1 T_1,\\
f_8(X) &= \frac{\zeta_2 M_2 T_0}{1 + \xi_c C} + \frac{\rho_4 T_2 C}{\eta + C} + \frac{(\varepsilon_4 T_2 + \varepsilon_5 M_2) C}{1 + \xi_i T_1} - \mu_2 T_2,\\
f_9(X) &= \frac{\varphi_2 C T_0}{1 + \xi_2 M_2} + \frac{\rho_5 T_{17} C}{\eta + C} + (\epsilon_7 T_{17} + \epsilon_c C) C - \mu_{17} T_{17},\\
f_{10}(X) &= \omega M_1 D + \sigma_8 + \frac{\rho_t T_8 C}{\eta + C} + \frac{(\varepsilon_8 T_1 + \varepsilon_9 T_{17}) C}{1 + \xi_c C + \xi_2 M_2} - \beta_8 T_8 C - \mu_8 T_8,\\
f_{11}(X) &= \theta_1 C(1 - \theta_2 C) + \alpha_m M_2 - \Phi\left(M_1 + N + T_8\right) C - \varepsilon_p T_1 C,
\end{aligned}$$

with $f = (f_1, f_2, f_3, f_4, f_5, f_6, f_7, f_8, f_9, f_{10}, f_{11})$, $X = (M_0, M_1, M_2, N, D, T_0, T_1, T_2, T_{17}, T_8, C)$, and $X_0 = \left(M_0^0, M_1^0, M_2^0, N^0, D^0, T_0^0, T_1^0, T_2^0, T_{17}^0, T_8^0, C^0\right)$.

Existence and uniqueness of the solution. It can be noticed that the function f is continuous and Lipschitz continuous with respect to X. According to the Picard theorem, Theorem 3.3.1, there exists $\tau_0 > 0$ such that the solution to (3.2.1) exists and is

defined locally at least on $[0, \tau_0]$. Again, let us consider the initial condition $X_1 = X(\tau_0)$ at $t_0 = \tau_0$. Using Theorem 3.3.1, it follows that there exist $\tau_0 \leq \tau_1 \in \mathbb{R}_+$ and a unique solution to (3.2.1) defined on $[\tau_0, \tau_1]$. By uniqueness of the solution of (3.2.1) with a given initial condition, it follows that the solutions of (3.2.1), obtained on $[0, \tau_0]$ and on $[\tau_0, \tau_1]$ form a unique solution of (3.2.1) on $[0, \tau_1]$ with the initial condition X_0 at $t_0 = 0$. Repeating this process infinitely many times, we obtain the maximal forward interval of a existence for the solutions of (3.2.1), $[0, +\infty)$.

Positivity of the solution. For $X \in \mathbb{R}^{11}_+$,

$$
\begin{aligned}
&f_1\left(0, M_1, M_2, N, D, T_0, T_1, T_2, T_{17}, T_8, C\right) \geq 0,\\
&f_2\left(M_0, 0, M_2, N, D, T_0, T_1, T_2, T_{17}, T_8, C\right) \geq 0,\\
&f_3\left(M_0, M_1, 0, N, D, T_0, T_1, T_2, T_{17}, T_8, C\right) \geq 0,\\
&f_4\left(M_0, M_1, M_2, 0, D, T_0, T_1, T_2, T_{17}, T_8, C\right) \geq 0,\\
&f_5\left(M_0, M_1, M_2, N, 0, T_0, T_1, T_2, T_{17}, T_8, C\right) \geq 0,\\
&f_6\left(M_0, M_1, M_2, N, D, 0, T_1, T_2, T_{17}, T_8, C\right) \geq 0,\\
&f_7\left(M_0, M_1, M_2, N, D, T_0, 0, T_2, T_{17}, T_8, C\right) \geq 0,\\
&f_8\left(M_0, M_1, M_2, N, D, T_0, T_1, 0, T_{17}, T_8, C\right) \geq 0,\\
&f_9\left(M_0, M_1, M_2, N, D, T_0, T_1, T_2, 0, T_8, C\right) \geq 0,\\
&f_{10}\left(M_0, M_1, M_2, N, D, T_0, T_1, T_2, T_{17}, 0, C\right) \geq 0,\\
&f_{11}\left(M_0, M_1, M_2, N, D, T_0, T_1, T_2, T_{17}, T_8, 0\right) \geq 0
\end{aligned}
$$

Therefore, according to Theorem 3.3.2, the unique solution of (3.2.1) is positive on $[0, +\infty)$. This suggests that, for any initial condition in $\mathbb{R}^{11}_+$, the problem (3.2.1) possesses a unique and positive solution in $\mathbb{R}^{11}_+$. □

3.3.1 Equilibrium Points and Basic Reproduction Number

Definition 3.3.4. *A point $v^* \in R$ is called an equilibrium point of $v' = f(v)$ if $f(v^*) = 0$.*

The equilibrium point of the system (3.2.1) is calculated by equating the time rate of

change of the equation to zero. Hence system (3.2.1) becomes,

$$\begin{cases} m - \kappa M_0^* T_1^* - \alpha_2 M_0^* C^* - \delta_0 M_0^* = 0 \\ \kappa M_0^* T_1^* + \dfrac{\rho_1 M_1^* C^*}{\eta + C^*} - (\lambda T_2^* + \varphi_1 C^*) M_1^* - \delta_1 M_1^* = 0 \\ \alpha_2 M_0^* C^* + (\lambda T_2^* + \varphi_1 C^*) M_1^* - \xi_t T_1^* M_2^* - \delta_2 M_2^* = 0 \\ n + \dfrac{\rho_n N^* C^*}{\eta + C^*} + \dfrac{\varepsilon_1 T_1^* C^*}{1 + \xi_c C^*} - \beta_n N^* C^* - \delta_n N^* = 0 \\ d + \dfrac{\rho_d D^* C^*}{\eta + C^*} + \dfrac{(\varepsilon_2 M_1^* + \varepsilon_7 T_{17}^*) C^*}{1 + \xi_c C^* + \xi_2 M_2^*} - \delta_d D^* = 0 \\ \omega M_1^* D^* + \sigma_0 - \dfrac{\xi_d M_1^* T_0^*}{1 + \xi_c C^*} - \dfrac{\zeta_2 M_2^* T_0^*}{1 + \xi_c C^*} - \dfrac{\varphi_2 C^* T_0^*}{1 + \xi_2 M_2^*} - \mu_0 T_0^* = 0 \\ \dfrac{\xi_d M_1^* T_0^*}{1 + \xi_c C^*} + \dfrac{\rho_3 T_1^* C^*}{\eta + C^*} + \dfrac{\varepsilon_1 T_1^* C^*}{1 + \xi_2 M_2^*} - \beta_1 T_1^* C^* - \mu_1 T_1^* = 0 \\ \dfrac{\zeta_2 M_2^* T_0^*}{1 + \xi_c C^*} + \dfrac{\rho_4 T_2^* C^*}{\eta + C^*} + \dfrac{(\varepsilon_4 T_2^* + \varepsilon_5 M_2^*) C^*}{1 + \xi_i T_1^*} - \mu_2 T_2^* = 0 \\ \dfrac{\varphi_2 C^* T_0^*}{1 + \xi_2 M_2^*} + \dfrac{\rho_5 T_{17}^* C^*}{\eta + C^*} + (\epsilon_7 T_{17}^* + \epsilon_c C^*) C^* - \mu_{17} T_{17}^* = 0 \\ \omega M_1^* D^* + \sigma_8 + \dfrac{\rho_t T_8^* C^*}{\eta + C^*} + \dfrac{(\varepsilon_8 T_1^* + \varepsilon_9 T_{17}^*) C^*}{1 + \xi_c C^* + \xi_2 M_2^*} - \beta_8 T_8^* C^* - \mu_8 T_8^* = 0 \\ \theta_1 C^* (1 - \theta_2 C^*) + \alpha_m M_2^* - \Phi \left(M_1^* + N^* + T_8^* \right) C^* - \varepsilon_p T_1^* C^* = 0 \end{cases} \tag{3.3.1}$$

We proceed by classifying and analysing the equilibrium points of system (3.3.1) as follows:

3.3.1.1 The tumor free equilibrium (TFE)

As the name implies, the tumor free equilibrium illustrates the equilibrium state whereby the system is free from the disease. In order to calculate the TFE, we set all the infectious compartment to zero. It follows that, in the case of our model, the compartment for tumor cells (C) and the anti-inflammatory macrophages (M_2) will be set to zero. That is, $C(t) = M_2(t) = 0$. Hence, solving system (3.3.1), the tumor free equilibrium point $E_0 = (M_0^*, M_1^*, M_2^*, N^*, D^*, T_0^*, T_1^*, T_2^*, T_{17}^*, T_8^*, C^*)$ is given by:

$$E_0 = \left(\frac{m}{\delta_0}, 0, 0, \frac{n}{\delta_n}, \frac{d}{\delta_d}, \frac{\sigma_0}{\mu_0}, 0, 0, 0, \frac{\sigma_8}{\mu_8}, 0 \right).$$

3.3.1.2 The endemic equilibrium

The endemic equilibrium point is the state where the tumor cells cannot be totally eradicated but remain in the population of the tumor microenvironment. The endemic equi-

librium point is solved using *Maple* software which confirms the existence of some positive cancer persistence equilibrium points. Due to the complexity of the results derived, we, therefore, do not state the solutions of the state variables. We shall, therefore, proceed to determine the threshold parameter. That is the basic reproductive number ($\mathcal{R}_0$) for our model which shall further be used for analysing the local and global stability of the tumor free equilibrium point of the model.

3.3.1.3 The basic reproduction number

The basic reproductive number $\mathcal{R}_0$ can be defined as the number of new infections produced by an infective individual (tumor cell) in a population at a disease free equilibrium [110]. In the case of this study, the basic reproductive number can be defined as the number of immune-cancerous cells caused by a tumor cell as a result of the local interaction between the immune cells and tumor cells in the tumor microenvironment at a tumor free equilibrium. Using next generation matrix, computing $\mathcal{R}_0$ requires us to first distinguish new infections from every other change in the cell population as explained below.

- Let $\mathcal{F}_i(x)$ be the rate at which a new infection appears in i^{th} compartment.
- $\mathcal{V}_i^+(x)$ be the rate at which individuals are transferred into compartment i by other means, and
- $\mathcal{V}_i^-(x)$ be the transfer rate of individuals out of the i^{th} compartment

We can therefore express the infectious compartment model in the form

$$\frac{dx_i}{dt} = \mathcal{F}_i(x) - \mathcal{V}_i(x),$$

where $\mathcal{V}_i(x) = \mathcal{V}_i^-(x) - \mathcal{V}_i^+(x)$, $x \in \mathbb{R}_+^{11}$, and $i = 1, 2, \ldots, m$ is the number of infectious compartment. Each function is assumed to be continuously differentiable at least twice in each variable [110]. Evaluating at the TFE E_0, we then have,

$$F = \left[\frac{\partial \mathcal{F}_i}{\partial x_j}(E_0)\right] \quad \text{and} \quad V = \left[\frac{\partial \mathcal{V}_i}{\partial x_j}(E_0)\right]$$

with $i \leq 1$ and $j \leq m$ such that $\mathcal{R}_0$ is the maximum eigenvalue of the matrix formed from FV^{-1}

In the case of our model, as stated earlier the disease compartments are the anti-inflammatory (M2) macrophages M_2 and tumor cells C, therefore the equation for the

infectious compartment model is given by

$$\frac{dM_2}{dt} = \alpha_2 M_0 C + (\lambda T_2 + \varphi_1 C) M_1 - \xi_t T_1 M_2 - \delta_2 M_2$$
$$\frac{dC}{dt} = \theta_1 C(1 - \theta_2 C) + \alpha_m M_2 - \Phi\left(M_1 + N + T_8\right) C - \varepsilon_p T_1 C$$

which implies that

$$\mathcal{F}_i = \begin{pmatrix} \mathcal{F}_1 \\ \\ \mathcal{F}_2 \end{pmatrix} = \begin{pmatrix} \alpha_2 M_0 C + \varphi_1 M_1 C \\ \\ 0 \end{pmatrix}.$$

and

$$\mathcal{V}_i = \begin{pmatrix} \mathcal{V}_1 \\ \\ \mathcal{V}_2 \end{pmatrix} = \begin{pmatrix} \xi_t T_1 M_2 + \delta_2 M_2 - \lambda T_2 M_1 \\ \\ \theta_1 \theta_2 C^2 + \Phi\left(M_1 + N + T_8\right) C + \varepsilon_p T_1 C - \alpha_m M_2 - \theta_1 C \end{pmatrix}.$$

Hence linearizing $\mathcal{F}_i$ and $\mathcal{V}_i$ at the tumor free equilibrium E_0 gives,

$$F = \begin{pmatrix} \frac{\partial \mathcal{F}_1(E_0)}{\partial M_2} & \frac{\partial \mathcal{F}_1(E_0)}{\partial C} \\ \\ \frac{\partial \mathcal{F}_2(E_0)}{\partial M_2} & \frac{\partial \mathcal{F}_2(E_0)}{\partial C} \end{pmatrix} = \begin{pmatrix} 0 & \frac{\alpha_2 m}{\delta_0} \\ 0 & 0 \end{pmatrix},$$

and

$$V = \begin{pmatrix} \frac{\partial \mathcal{V}_1(E_0)}{\partial M_2} & \frac{\partial \mathcal{V}_1(E_0)}{\partial C} \\ \\ \frac{\partial \mathcal{V}_2(E_0)}{\partial M_2} & \frac{\partial \mathcal{V}_2(E_0)}{\partial C} \end{pmatrix} = \begin{pmatrix} \delta_2 & 0 \\ -\alpha_m & \Phi\left(\frac{n}{\delta_n} + \frac{\sigma_8}{\mu_8}\right) - \theta_1 \end{pmatrix}.$$

Since V is a non-singular matrix, we therefore obtain its inverse to be,

$$V^{-1} = \begin{pmatrix} \frac{1}{\delta_2} & 0 \\ \frac{\alpha_m}{\left(\Phi\left(\frac{n}{\delta_n} + \frac{\sigma_8}{\mu_8}\right) - \theta_1\right)\delta_2} & \frac{1}{\Phi\left(\frac{n}{\delta_n} + \frac{\sigma_8}{\mu_8}\right) - \theta_1} \end{pmatrix}.$$

Hence, the next generation matrix is given by

$$FV^{-1} = \begin{pmatrix} \frac{\alpha_2 \alpha_m m}{\left(\Phi\left(\frac{n}{\delta_n} + \frac{\sigma_8}{\mu_8}\right) - \theta_1\right)\delta_0 \delta_2} & \frac{\alpha_2 m}{\left(\Phi\left(\frac{n}{\delta_n} + \frac{\sigma_8}{\mu_8}\right) - \theta_1\right)\delta_0} \\ 0 & 0 \end{pmatrix}. \tag{3.3.2}$$

Thus the eigenvalues for the above matrix in Equation (3.3.2) are

$$\lambda_1 = \frac{\alpha_2 \alpha_m m}{\left(\Phi\left(\frac{n}{\delta_n} + \frac{\sigma_8}{\mu_8}\right) - \theta_1\right)\delta_0 \delta_2}, \quad \lambda_2 = 0$$

Therefore the basic reproductive number is,

$$\mathcal{R}_0 = \frac{\alpha_2 \alpha_m m}{\left(\Phi\left(\frac{n}{\delta_n} + \frac{\sigma_8}{\mu_8}\right) - \theta_1\right)\delta_0 \delta_2}, \tag{3.3.3}$$

with $\Phi\left(\frac{n}{\delta_n} + \frac{\sigma_8}{\mu_8}\right) > \theta_1$.

3.3.2 Stability Analysis of the Equilibrium Points

3.3.2.1 Local Stability of the tumor free Equilibrium

Theorem 3.3.5 (Geshgorin's Theorem). *Let $B = (b_{ij})_{1\leq i,j\leq n}$ be an $n \times n$ matrix and D_i be the disk in the complex plane with center at b_{ii} and radius $r_i = \sum_{j=1, j\neq i}^{n} |b_{ij}|$, then all eigenvalues of the matrix B lie in the union of the disk D_i. In particular, if λ is an eigenvalue of B, then for some $i = 1, 2, \ldots, n$, $|\lambda - b_{ii}| \leq r_i$ [1].*

Corollary 3.3.6. *Let $B = (b_{ij})_{1\leq i,j\leq n}$ be an $n \times n$ matrix with real entries. If the diagonal elements of B satisfies $b_{ii} < -r_i$ where $r_i = \sum_{j=1, j\neq i}^{n} |b_{ij}|$ for $i = 1, 2, \ldots, n$, then the eigenvalues of B are negative. i.e. the matrix has negative real parts [1].*

Theorem 3.3.7. *The tumor free equilibrium E_0 of our model (3.2.1) is locally asymptotically stable if $\mathcal{R}_0 < 1$. [110].*

Proof. The Jacobian matrix evaluated at the tumor free equilibrium E_0 is given below as

$$J(E_0) = \begin{pmatrix}
-\delta_0 & 0 & 0 & 0 & 0 & 0 & -\frac{\kappa m}{\delta_0} & 0 & 0 & 0 & -\frac{\alpha_2 m}{\delta_0} \\
0 & -\delta_1 & 0 & 0 & 0 & 0 & \frac{\kappa m}{\delta_0} & 0 & 0 & 0 & 0 \\
0 & 0 & -\delta_2 & 0 & 0 & 0 & 0 & 0 & 0 & 0 & \frac{\alpha_2 m}{\delta_0} \\
0 & 0 & 0 & -\delta_n & 0 & 0 & 0 & 0 & 0 & 0 & B \\
0 & 0 & 0 & 0 & -\delta_d & 0 & 0 & 0 & 0 & 0 & \frac{\rho_d d}{\eta \delta_d} \\
0 & E & -\frac{\zeta_2 \sigma_0}{\mu_0} & 0 & 0 & -\mu_0 & 0 & 0 & 0 & 0 & -\frac{\varphi_2 \sigma_0}{\mu_0} \\
0 & \frac{\xi_d \sigma_0}{\mu_0} & 0 & 0 & 0 & 0 & -\mu_1 & 0 & 0 & 0 & 0 \\
0 & 0 & \frac{\zeta_2 \sigma_0}{\mu_0} & 0 & 0 & 0 & 0 & -\mu_2 & 0 & 0 & 0 \\
0 & 0 & 0 & 0 & 0 & 0 & 0 & 0 & -\mu_{17} & 0 & \frac{\varphi_2 \sigma_0}{\mu_0} \\
0 & \frac{\omega d}{\delta_d} & 0 & 0 & 0 & 0 & 0 & 0 & 0 & -\mu_8 & M \\
0 & 0 & \alpha_m & 0 & 0 & 0 & 0 & 0 & 0 & 0 & -N
\end{pmatrix} \tag{3.3.4}$$

where,

$$B = \frac{n}{\delta_n}\left(\frac{\rho_n}{\eta} - \beta_n\right),\ E = \frac{\omega d}{\delta_d} - \frac{\xi_d \sigma_0}{\mu_0},\ M = \frac{\sigma_8}{\mu_8}\left(\frac{\rho_t}{\eta} - \beta_8\right),\ N = \Phi\left(\frac{n}{\delta_n} + \frac{\sigma_8}{\mu_8}\right) - \theta_1.$$

Since our Jacobian matrix has real entries, it follows from Corollary 3.3.6, that the eigenvalues of Jacobian matrix (3.3.4) has negative real part under the conditions:

$$\begin{cases} \delta_0 > \frac{m}{\delta_0}(\kappa + \alpha_2), \\ \delta_1 > \frac{\kappa m}{\delta_0}, \\ \boxed{\delta_2 > \frac{\alpha_2 m}{\delta_0}}, \\ \delta_n > \frac{n}{\delta_n}\left(\beta_n - \frac{\rho_n}{\eta}\right), \\ \delta_d > \frac{\rho_d d}{\eta \delta_d}, \\ \mu_0 > \frac{\sigma_0}{\mu_0}(\xi_d + \zeta_2 + \varphi_2) - \frac{\omega d}{\delta_d}, \\ \mu_1 > \frac{\xi_d \sigma_0}{\mu_0}, \\ \mu_2 > \frac{\zeta_2 \sigma_0}{\mu_0}, \\ \mu_{17} > \frac{\varphi_2 \sigma_0}{\mu_0}, \\ \mu_8 > \frac{\omega d}{\delta_d} + \frac{\sigma_8}{\mu_8}\left(\beta_8 - \frac{\rho_t}{\eta}\right), \\ \boxed{\Phi\left(\frac{n}{\delta_n} + \frac{\sigma_8}{\mu_8}\right) - \theta_1 > \alpha_m}. \end{cases}$$

Let us show that at the tumor free equilibrium, $\mathcal{R}_0 < 1$. By multiplying the boxed conditions which corresponds to the disease transmission model, we obtain

$$\left[\Phi\left(\frac{n}{\delta_n} + \frac{\sigma_8}{\mu_8}\right) - \theta_1\right]\delta_2 > \frac{\alpha_2 \alpha_m m}{\delta_0}. \tag{3.3.5}$$

Multiplying Equation (3.3.5) by δ_0, gives

$$\left[\Phi\left(\frac{n}{\delta_n} + \frac{\sigma_8}{\mu_8}\right) - \theta_1\right]\delta_0\delta_2 > \alpha_2 \alpha_m m. \tag{3.3.6}$$

Furthermore, dividing Equation (3.3.6) by its left hand side gives

$$\begin{aligned} 1 &> \frac{\alpha_2 \alpha_m m}{\left[\Phi\left(\frac{n}{\delta_n} + \frac{\sigma_8}{\mu_8}\right) - \theta_1\right]\delta_0\delta_2} = \mathcal{R}_0, \\ \therefore \mathcal{R}_0 &< 1. \end{aligned} \tag{3.3.7}$$

We conclude that the tumor free equilibrium point E_0 is locally asymptotically stable. □

3.3.2.2 Global Stability of the tumor free Equilibrium

In the previous section, we were able to show the local stability of TFE for $\mathcal{R}_0 < 1$. We will now proceed to employ the following theorem used by [19], which guarantees global stability of the tumor free equilibrium point when $\mathcal{R}_0 < 1$.

Theorem 3.3.8. *The disease free equilibrium point E_0 is globally asymptotically stable provided that $\mathcal{R}_0 < 1$ and the following conditions are satisfied. That is,*

If the system is re-written in the form

$$\frac{dX}{dt} = F(X, Y)$$
$$\frac{dY}{dt} = G(X, Y) \ \ with \ \ G(X, 0) = 0,$$

where $X \in \mathbb{R}^n$ components depict the number of uninfected individuals and where $Y \in \mathbb{R}^m$ components depict the number of infected individuals within the system and the following conditions are met:

1. *For $\frac{dX}{dt} = F(X, 0)$, E_0 is globally asymptotically stable, and*
2. *$\hat{G}(X, Y) = AY - G(X, Y) \geqslant 0$ for $(X, Y) \in \Omega$ the feasibility region, where A is the Jacobian matrix formed at the disease free equilibrium [19].*

Therefore, applying Theorem 3.3.8 for global stability, system (3.2.1) can be re-written in the form

$$\frac{dX}{dt} = F(X,0) = \begin{pmatrix} m - \kappa M_0 T_1 - \delta_0 M_0 \\ \kappa M_0 T_1 - \lambda T_2 M_1 - \delta_1 M_1 \\ n - \delta_n N \\ d - \delta_d D \\ \omega M_1 D + \sigma_0 - \xi_d M_1 T_0 - \mu_0 T_0 \\ \xi_d M_1 T_0 - \mu_1 T_1 \\ -\mu_2 T_2 \\ -\mu_{17} T_{17} \\ \omega M_1 D + \sigma_8 - \mu_8 T_8 \end{pmatrix}$$

$$\frac{dY}{dt} = G(X,Y) = \begin{pmatrix} \alpha_2 M_0 C + (\lambda T_2 + \varphi_1 C) M_1 - \xi_t T_1 M_2 - \delta_2 M_2 \\ \theta_1 C(1 - \theta_2 C) + \alpha_m M_2 - \Phi\left(M_1 + N + T_8\right) C - \varepsilon_p T_1 C \end{pmatrix}$$

where $X = [M_0, M_1, N, D, T_0, T_1, T_2, T_{17}, T_8]^T$ and $Y = [M_2, C]^T$.
Therefore,

$$A = \begin{pmatrix} -\delta_2 & \frac{\alpha_2 m}{\delta_0} \\ \alpha_m & \theta_1 - \Phi\left(\frac{n}{\delta_n} + \frac{\sigma_8}{\mu_8}\right) \end{pmatrix},$$

such that

$$AY = \begin{pmatrix} -\delta_2 & \frac{\alpha_2 m}{\delta_0} \\ \alpha_m & \theta_1 - \Phi\left(\frac{n}{\delta_n} + \frac{\sigma_8}{\mu_8}\right) \end{pmatrix} \begin{pmatrix} M_2 \\ C \end{pmatrix}$$
$$= \begin{pmatrix} -\delta_2 M_2 + \frac{\alpha_2 m}{\delta_0} C \\ \alpha_m M_2 + \theta_1 C - \Phi\left(\frac{n}{\delta_n} + \frac{\sigma_8}{\mu_8}\right) C \end{pmatrix}.$$

From condition 2.

$$\begin{aligned} & \hat{G}(X,Y) = AY - G(X,Y) \\ \Rightarrow \quad & \hat{G}(X,Y) = \begin{pmatrix} -(\lambda T_2 + \varphi_1 C)M_1 + \xi_t T_1 M_2 \\ \\ \theta_1\theta_2 C^2 + \Phi M_1 C + \varepsilon_p T_1 C \end{pmatrix} = \begin{pmatrix} \hat{G}_1(X,Y) \\ \\ \hat{G}_2(X,Y) \end{pmatrix} \end{aligned}$$

From the above expression, it is obvious that $\hat{G}_2(X,Y) = \theta_1\theta_2 C^2 + \Phi M_1 C + \varepsilon_p T_1 C \geq 0$ since all parameters used in the model are assumed to be non-negative. However, according to Theorem 3.3.8, for the tumor free equilibrium, E_0, to be globally asymptotically stable, $\hat{G}(X,Y)$ must be greater than or equal zero. It follows that $\hat{G}_1(X,Y)$ must also be greater or equal to zero. Thus, $\hat{G}_1(X,Y) \geq 0$ if and only if $\xi_t T_1 M_2 \geq (\lambda T_2 + \varphi_1 C)M_1$. Therefore the tumor free equilibrium, E_0, will be globally asymptotically stable if the elimination rate of M2 macrophages by Th1 cells is more than the transition of M1 macrophages to M2 macrophages caused by both Th2 cells and tumor cells.

3.4 Numerical Analysis

3.4.1 Parameter Estimation

For system (3.2.1), about 62.2% of the parameters are gotten from literature related to our work, and we use the non-linear least square method, which was proposed by John Nelder and Roger Mead [79], to estimate the unknown parameter values of the model. Graphical representations of the observed data estimates are also depicted.

3.4.1.1 Non-linear Least Square (NLS) Method

Let us consider the following initial value problem

$$\begin{cases} \dfrac{d}{dt}y(t,\theta) = f(t,y,\theta) \\ \quad y(0,\theta) = y_0, \end{cases} \tag{3.4.1}$$

where the function f depends on time t, y is the state variable and the vector of parameters θ is to be estimated. The procedure used by the least square method for estimating parameters is to minimize the sum of the difference between observed data points, $\mathbf{y}(t_i)$, and the solution of the model, $\hat{\mathbf{y}}(t_i,\theta)$, associated with the model parameter θ. Mathematically, given n data points, (t_i, y_i) for $i = 1,\ldots,n$, we seek to minimize the error by

the given function,

$$M(\theta) = \sum_{i=1}^{n} \left[\hat{\mathbf{y}}(t_i, \theta) - \mathbf{y}(t_i)\right]^2. \tag{3.4.2}$$

Therefore, finding the parameters vector $\theta = (\theta_i)_{0 \le i \le m}$ that best fit our model implies solving the following optimization problem

$$\min_{\theta} M(\theta) \text{ subject to } \theta_{min} \le \theta_i \le \theta_{max}, \tag{3.4.3}$$

for $i = 1, \ldots, m$, where m is the number of parameters to be estimated.

3.4.1.2 Estimated Values and Fitted Plot

We implemented our model using the *deSolve* package in R, and fitted the model to real data using *optim* in R. This was done using the non-linear least square (NLS) as explained above. Figure 3.2 shows the suitable curve fitting together with the estimated values to unknown parameters of the model. We fitted our model to observed real data of tumor cells growth used by [26]. The estimated values of the unknown parameters obtained from the non-linear least square method and literature are recorded in Table 3.3. These parameter values will therefore be used for our analysis.

3.4.2 Numerical Simulation

The numerical simulation of our model equation (3.2.1) is done using deSolve package in R software. In these simulations, the initial concentration of the immune system cells used are, resting macrophages, $M_0(0) = 4 \times 10^5$ cells/ml; activated macrophages, $M_1(0) = 8 \times 10^3$ cells/ml [4]; Nk cells, $N(0) = 3.2 \times 10^3$ cells/ml [69]; dendritic cells, $D(0) = 10^3$ cells/ml [41]; $CD8^+$ T cells, $T_8(0) = 7.15 \times 10^3$ cells/ml [27]; naive $CD4^+$ T cells, $T_0(0) = 5 \times 10^3$ cells/ml; the initial concentration of every other cells is zero as explained in equation (3.2.1); and the that of tumor cells, $C(0) = 6.9 \times 10^4$ cells/ml as recorded in [26]. All other parameters used, are stated in Table 3.3.

Figure 3.3 depicts the tumor-immune cell dynamics of our model equation (3.2.1). It suggests that with the parameter estimation and values used in the model, in a biological time frame, our model can produce tumor escape from immunological surveillance in the tumor microenvironment. This shows the capacity of a tumor to escape from immunological surveillance when the immune system cells are depleted at tumor site [69]. This might be because, from our parameter values, the inactivation rate for the two primary immune-effector cells (the NK cells and $CD8^+$ T cells) by tumor cells are assumed to be 1 per cell per day [50, 54]. It follows that there are few cytotoxic immune-effector cells or weak immune system cells at the tumor site.

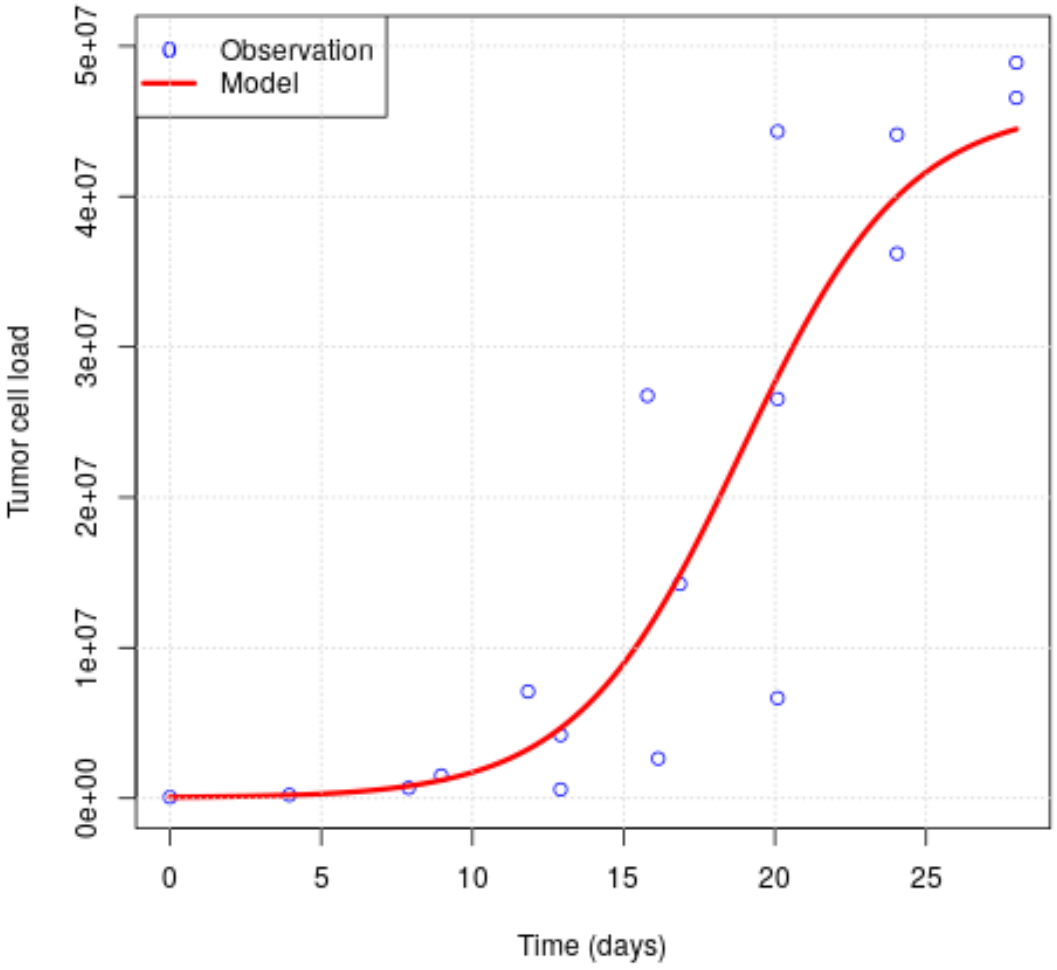

Figure 3.2: Plot showing curve fitting of tumor cell populations of model (3.2.1) to real data of tumor growth.

In order to understand further how the whole immune cells interact in this scenario, let us proceed by taking into consideration related parameter values to the inactivate rate of NK cells and $CD8^+$ T cells due to tumor cells used by [29] and [28], respectively. That is, $\beta_n = 3.5 \times 10^{-6}$ and $\beta_8 = 1 \times 10^{-7}$ in our model which implies that there are more immune-effector cells or strong immune system cells at the tumor site. Thus, it depicts high effectiveness of immunological surveillance mediated by both Nk cells and activated $CD8^+$ T cells as it shows their capability of controlling tumor growth. The

Table 3.3: Description, units and source of parameter values used in the model

Parameter	Description	Value	Units	Source
d	External influx rate of DCs	4.8×10^2	cells/ml/day	[108]
m	External influx rate of macrophages	2.28×10^2	cells/ml/day	[67]
n	External influx rate of NK cells	3.2×10^3	cells/ml/day	[69]
σ_0	Constant supply of Th0 cells upon activation	0.7336828	cells/ml/day	Estimated
σ_8	Constant supply of $CD8^+$ T cells upon activation	1.0×10^2	cells/ml/day	[27]
ρ_1	Proliferation rate of M1 Macrophages	0.995	day^{-1}	Estimated
ρ_3	Proliferation rate of Th1 cell	0.6156879	day^{-1}	Estimated
ρ_4	Proliferation rate of Th2 cell	0.0000001	day^{-1}	Estimated
ρ_5	Proliferation rate of Th17 cell	0.2032233	day^{-1}	Estimated
ρ_n	Proliferation rate of NK cells	0.120393	day^{-1}	Estimated
ρ_d	Proliferation rate of DCs	0.00000029	day^{-1}	Estimated
ρ_t	Proliferation rate of $CD8^+$ T cells	0.4487595	day^{-1}	Estimated
η	Half saturation constant of the immune response	1.0×10^3		[34]
τ	Transition rate from M1 to M2 Macrophages by anti-inflammatory cytokines	0.2	day^{-1}	[67]
β_n	Inactivation rate of NK cells by tumor cells	1	$day^{-1}\ cell^{-1}$	[50],[54]
β_1	Inactivation rate of Th1 cells by tumor cells	0.995	$day^{-1}\ cell^{-1}$	Estimated
β_8	Inactivation rate of $CD8^+$ T cells by tumor cells	1	$day^{-1}\ cell^{-1}$	[50],[54]
θ_1	Intrinsic growth rate of tumor cells	0.3655	day^{-1}	Average([27],[36])
θ_2	Maximum carrying capacity of tumor cells	2.17×10^{-8}	$cell^{-1}$	[27]
α_m	Expansion rate of tumor cells by M2 macrophages	0.0000001	day^{-1}	Estimated
γ_1	Expansion rate of NK and Th1 cells enhanced by IL-2	0.1245	day^{-1}	[36],[54]
γ_2	Expansion rate of dendritic cells enhanced by IL-12 and IL-17	0.8025290	day^{-1}	Estimated
γ_3	Expansion rate of Th2 cells enhanced by IL-4 and IL-10	0.0000001	day^{-1}	Estimated
γ_4	Expansion rate of Th17 cells enhanced by IL-21 and IL-23	0.0000001	day^{-1}	Estimated
γ_5	Expansion rate of $CD8^+$ T cells by enhanced IL-2 and IL-17	0.1245	day^{-1}	[54]
α_1	Polarization of resting macrophages into M1	0.7877726	cells/ml/day	Estimated
α_2	Polarization of resting macrophages into M2	0.4335230	cells/ml/day	Estimated
α_t	Activation rate of T cells	8.0×10^{-3}	cells/ml/day	[34]
$\zeta_i's$	Th0 differentiation into it subsets	5.5×10^{-1}	cells/ml/day	[34]
$\delta_i's$	Apoptosis rate of macrophage phenotypes	2.0×10^{-2}	day^{-1}	[67]
δ_n	Apoptosis rate of NK cells	4.12×10^{-2}	day^{-1}	[27],[69]
δ_d	Apoptosis rate of DCs	2.4×10^{-2}	day^{-1}	[108]
$\mu_i's$	Apoptosis rate of Th0 cell and its subsets	0.05	day^{-1}	[28]
μ_8	Apoptosis rate of $CD8^+$ T cells	2.0×10^{-2}	day^{-1}	[27],[69]
Φ	Elimination rate of tumor cells by immune effector cells	1.0×10^{-5}	day^{-1}	[28]
μ_c	Apoptosis rate of tumor cells by TNF-α	0.2	day^{-1}	[34]
μ_e	Apoptosis rate of M2 macrophages by IFN-γ	0.9398057	day^{-1}	Estimated
h_γ	Inhibition measure by IFN-γ	0.02235745	day^{-1}	Estimated
h_β	Inhibition measure by TGF-β	1.0×10^{-3}	day^{-1}	[50]
h_{10}	Inhibition measure by IL-10	2.0×10^{-7}	day^{-1}	[41]
$\nu_i's$	Production rate of tumor suppressing cytokines by immune cells	3.72×10^{-5}	pg/cell/day	[63]
$\nu_j's$	Production rate of tumor promoting cytokines by immune cells	1.5×10^{-5}	pg/cell/day	[63]
$\nu_k's$	Production rate of tumor promoting cytokines by tumor cells	7.5×10^{-4}	pg/cell/day	[4]
δ_s	Decay rate of tumor suppressing cytokines	10	day^{-1}	[27],[34],[54]
δ_p	Decay rate of tumor promoting cytokines	34	day^{-1}	[34]

results are presented in Figure 3.4, 3.5 and 3.6.

Figure 3.4 and 3.5 give a clear picture of the effects on each of the respective immune cells used in the model in both cases of when there are weak and strong immune effector cells in the tumor microenvironment. Figure 3.4(a) and 3.5(a) is the case where there are weak immune effector cells at the tumor site. It results in tumor promoting immune cells (M2 macrophages, Th2 cells and Th17 cells) evading the system thereby contributing to tumor growth progression as depicted in Figure 3.5(a). On the other hand, the tumor suppressing/cytotoxic immune cells (M1 macrophages, Nk cells, Th1 cells and $CD8^+$ T cells) go into extinction as shown in Figure 3.4(a). Meanwhile, in the case whereby strong immune effector cell is present at the tumor site, as shown in Figure

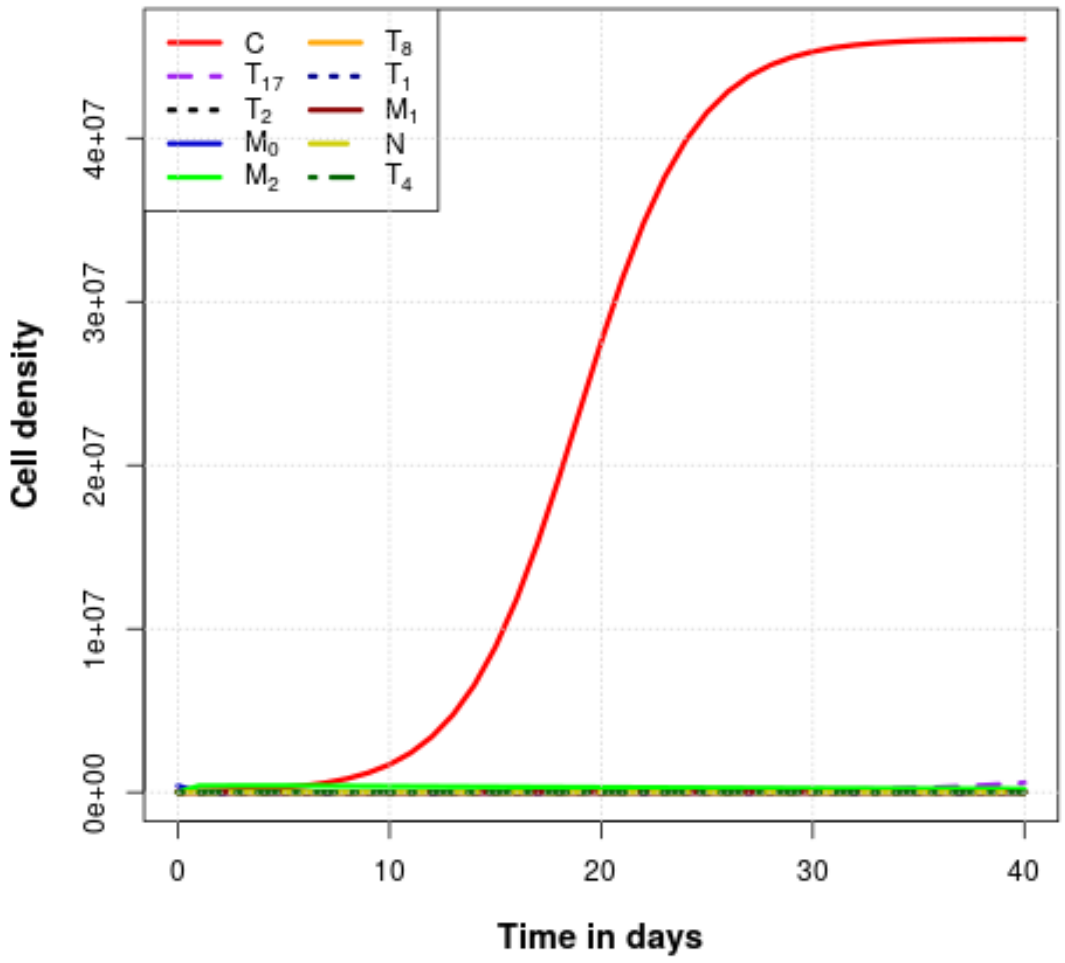

Figure 3.3: Plot showing the growth of tumor and immune cell populations over time. The plot indicates tumor escape of immunological surveillance due to weak immune effector cell.

3.4(b) and 3.5(b), an increase in the the tumor suppressing/cytotoxic immune cell (M1 macrophages, Nk cells and $CD8^+$ T cells) densities lead to the inhibition/decrease of the population of tumor promoting immune cells (M2 macrophages, Th2 cells and Th17 cells) in the system. However M2 macrophages still dominate at some point in time in the system. This is expected to happen because those macrophages that undergo the process of phagocytosis need to be depleted from the system and it will certainly be a

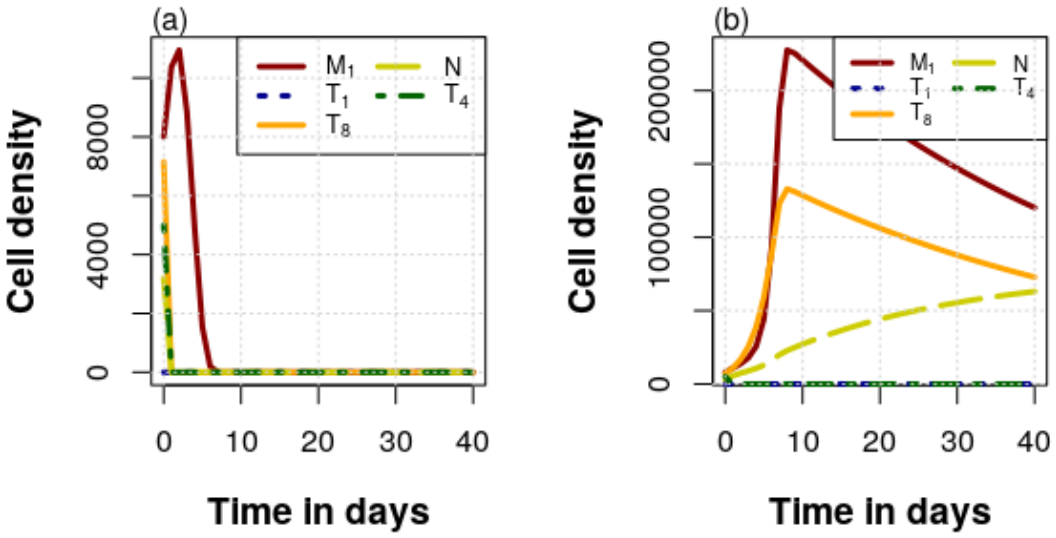

Figure 3.4: Plot shows tumor suppressing immune cell populations over time when: (a) there is a weak immune effector cell at tumor site, and (b) there is a strong immune effector cell at tumor site

gradual process for that to happen.

Figure 3.6 shows the tumor-immune cells dynamics of our model over a period of 40 days to 300 days with $\beta_n = 3.5 \times 10^{-6}$ and $\beta_8 = 1 \times 10^{-7}$. From Figure 3.6 (a), we observed a declined growth of the tumor cells to a dormant stage. However, in Figure 3.6 (b) our model predicts the total extinction of the tumor cells in the system. In the long run (starting roughly from a period of 200 days onward) the immune system will be in place leaving out the innate immune system to perform its first line of defence.

3.4.3 Sensitivity Analysis

It is expected that assumptions made on our model and estimated parameter values might be subject to slight changes or errors. As a result, we proceed by carrying out a sensitivity analysis of the model output to all estimated parameters and key model parameters as presented in Figure 3.7. Using function *sensFun* in *FME* package in R [99], we investigated how alterations in such parameters influence the model output. As

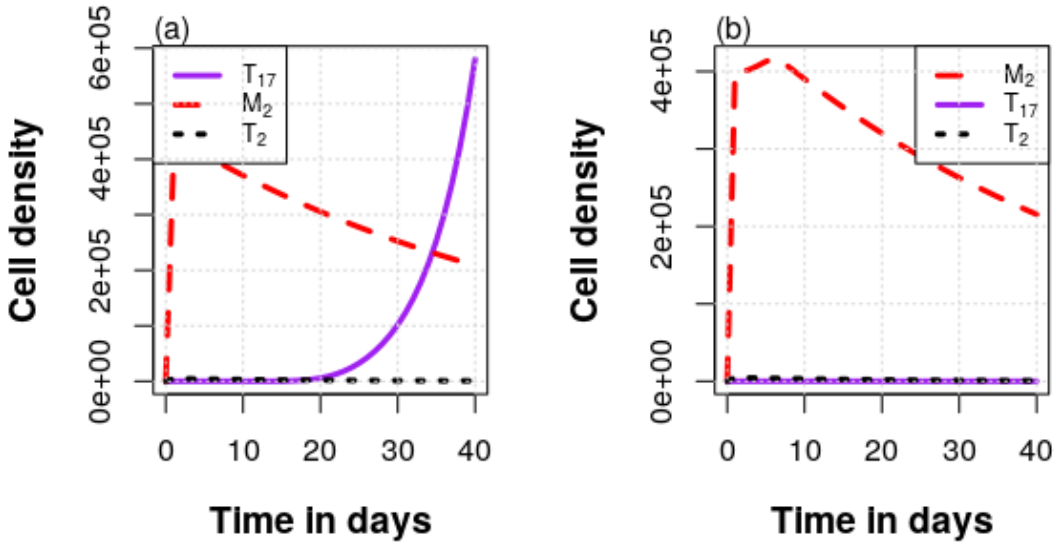

Figure 3.5: Plot shows tumor promoting immune cell populations over time when: (a) there is a weak immune effector cell at tumor site, and (b) there is a strong immune effector cell at tumor site

shown in Figure 3.7, parameters $\gamma_3, \gamma_4, \rho_d, \mu_e, h_\gamma, \rho_3, \rho_4, \mu_1$, and α_m do not have an effect on the number of tumor cell load while parameter Φ has a consistent negative effect on the number of tumor cell load (see Figure 3.7 (e)). This was expected because Φ is the eliminate rate of tumor cells by immune-effector cells while other parameters such as $\sigma_0, n, \alpha_2, \gamma_2, \theta_1, \rho_t, \beta_1, \alpha_1, m, d, \sigma_8, \beta_n, \beta_8, \rho_1, \alpha_t, \delta_0, \delta_2, \rho_n, \delta_n, \mu_0, \mu_2, \mu_8, \mu_{17}, \mu_c$ and τ have an inconsistent effect, either positive or negative, with time. This might be caused by the strength of their respective immune effector cells in that interval of time at the tumor site. To investigate how specific some of these parameters influence our model behaviour, we proceed by performing a local sensitivity analysis on some key parameters of interest.

Figure 3.8 shows the dynamic of the tumor cells with time by varying some key parameters in the model. In Figure 3.8 (a), we varied the intrinsic growth rate, θ_1, of tumor cell. As expected in the numerical solution, an increase in this growth rate leads to a rapid increase in the growth of tumor cell thereby increasing the time evolution of tumor cells in the tumor microenvironment and vice versa. Similarly Figure 3.8 (b) shows effect of varying parameter α_m. It depicts the fact that tumor associated macrophages (TAMs) promote tumor growth and progression before it is eliminated from the system. Also,

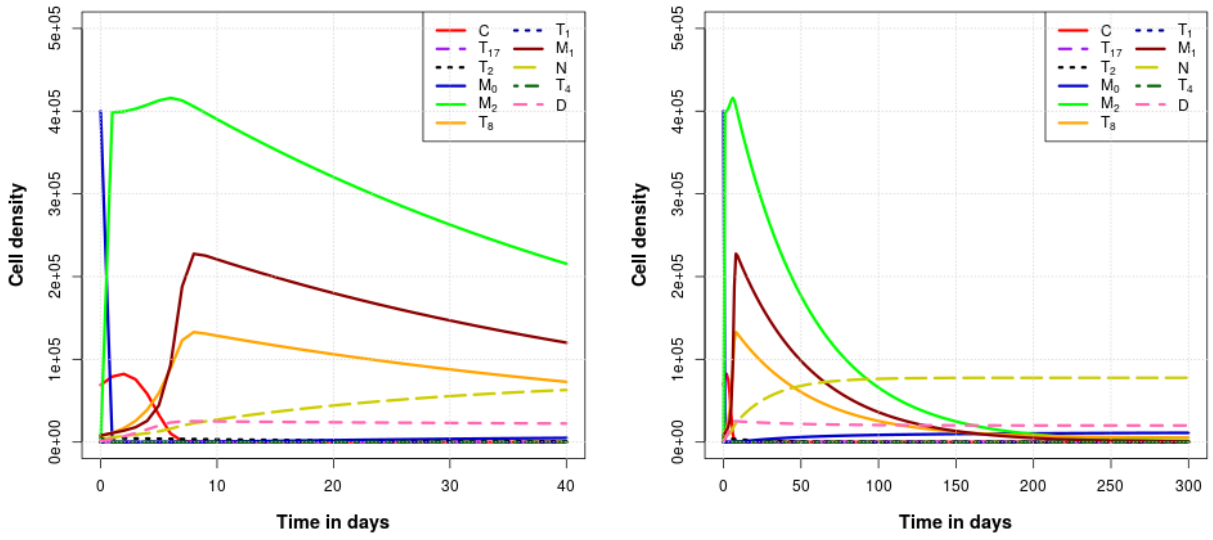

(a) (b)

Figure 3.6: Plot showing the growth of tumor and immune cell populations over time. The plot indicates tumor elimination due to strong immune effector cell at $\beta_n = 3.5 \times 10^{-6}$ and $\beta_8 = 1 \times 10^{-7}$ (a) over a period of 40 days and (b) over a period of 300 days.

it was observed that an increase in the number of α_m contributes towards the growth of tumor cells in the tumor microenvironment. On the other hand, Figure 3.8 (c) and (d) show the effect of varying parameter ρ_1 and Φ, respectively. Figure 3.8 (c) presents the proliferation rate of activated macrophages due to stimulus from tumor cells thereby engulfing and preparing them for death, while Figure 3.8 (d) shows the elimination rate of tumor cells by immune-effector cells. It was observed that an increase in the rate of these parameters does not only reduce the tumor cell populations but also decrease the time evolution of tumor cells in the tumor microenvironment.

Figure 3.8 (e) and (f), depict the effect of varying parameter β_n and β_8, that is, the inactivation rate of NK cell and $CD8^+$ T cells respectively by tumor cells. It was observed that a decrease in the inactivation rate of these cells lead to a decrease in the tumor cell population and delayed tumor growth. In order words, the immune effector cells are more active/stronger in carrying out tumor lysis. Also, we observed from 3.8 (f) that a decrease in β_8 not only leads to the reduction of the tumor cell population but also to a gradual elimination of the tumor cells in the tumor microenvironment.

3.4.4 Effect of Cytokine Concentration in the TME

In the case of our model, the concentrations of both tumor promoting cytokines (IL-4, IL-6, IL-10, IL-13, IL-23, and TGF-β) and tumor suppressing cytokines (IL-12, IL-17, IL-21, TNF-α, and IFN-γ) with respect to time are shown in Figure 3.9 and Figure 3.10. Figure 3.9 is the case where we have weak immune effector cells as explained above. We see that the tumor promoting cytokines start manifesting roughly from Day 10 which correlate to when there is an increase in tumor growth population as shown in Figure 3.3. Also, we observed a continuous increment in the concentration of these cytokines. At Day 40, in Figure 3.9(b), we observed that the concentration of cytokine IL-23 is higher compared to other tumor promoting cytokines in the TME. This may be the reason why the innate immune system are being stopped by IL-23 produced by the tumor cell in the tumor micro-environment [105], and also leads to it inducing immunosuppression through down-regulation of $CD4^+$ and $CD8^+$ T cells infiltrating in tumor tissues as reported by [80] thereby leading to tumor progression. However, the depletion of the tumor suppressing cytokines leads to a decrease in the population, efficiency and the cytotoxic effect of the immune effector cells. While in Figure 3.10 we observe that the concentration of IL-23 is minimal when the immune effector cells are strong in the tumor microenvironment which bring about the elimination of the tumor cells. This supports the idea from previous research that tumor promoting cytokine IL-23 plays a significant role in the growth and proliferation of tumor. Its antibody can therefore be used to achieve an increased tumor eradication or a delayed tumor growth.

In conclusion from the simulation of our model, we predicted that few immune-effector cells at the tumor site led to tumor escape while high immune-effector cells at the tumor site led to tumor regression. Among others, cytokine IL-10, IL-23, TNF-α, TGB-β and IFN-γ are also identified to play a significant role in our model based on the observed dynamics in the level of their concentration in the system. We, therefore, conclude that the availability of these cytokines in the system has a great effect on the host immune cells response and hence in the tumor microenvironment. Thus in the next chapter, we shall identify proteins(breast cancer genes) that regulates these key cytokines in our model and possibly suggest essential proteins as a new development for an effective treatment to eliminate breast cancer.

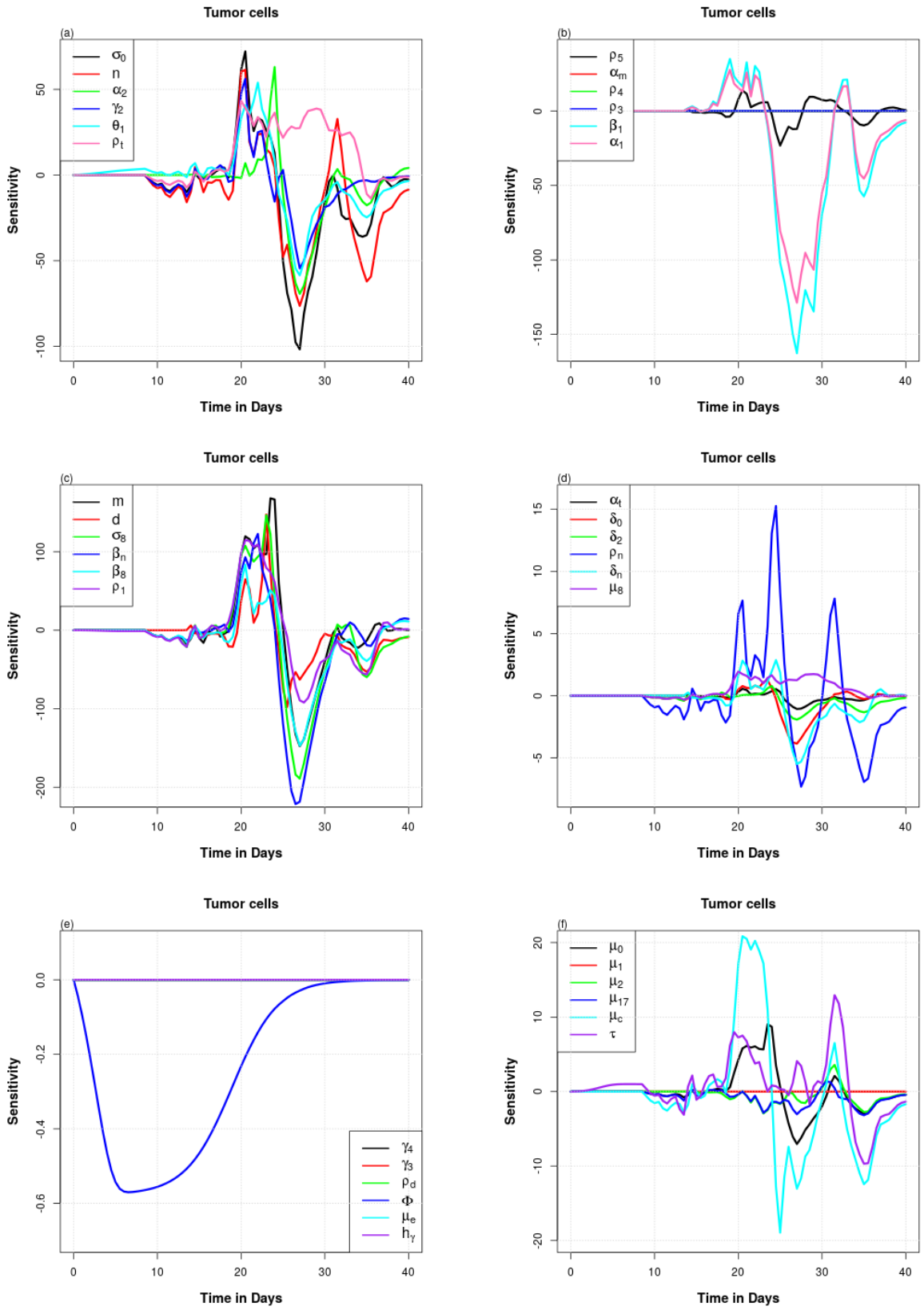

Figure 3.7: Sensitivity functions of model output to parameters.

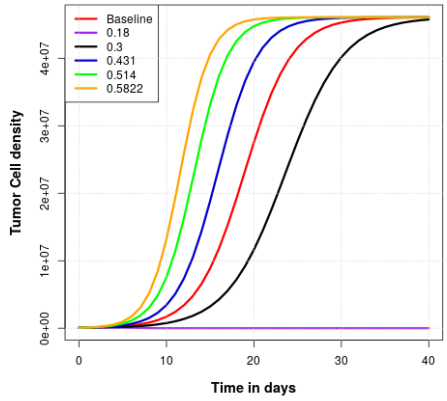

(a) Plot shows the effect of varying the growth rate of tumor cells θ_1 in numerical solution of our model.

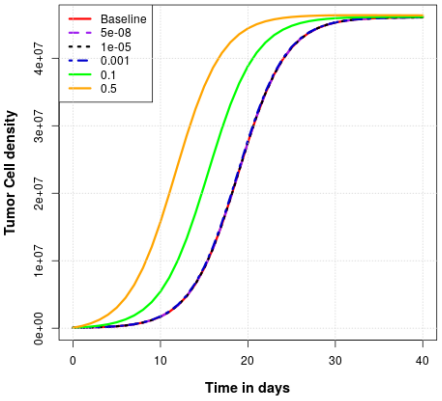

(b) Plot shows the effect of varying the expansion rate of tumor cell by M2 macrophages α_m in numerical solution of our model.

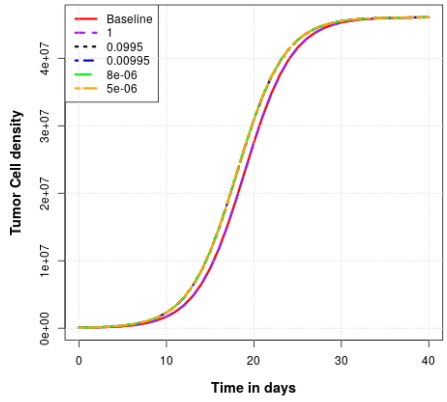

(c) Plot shows the effect of varying the proliferation rate of M1 macrophages ρ_1 in numerical solution of our model.

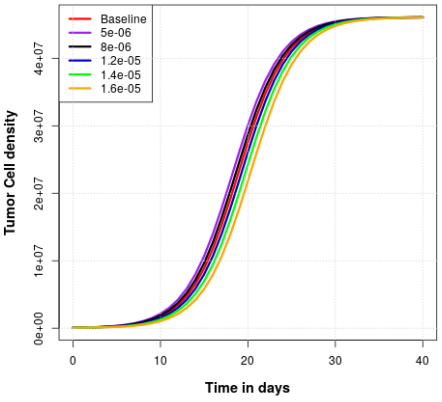

(d) Plot shows the effect of varying the elimination rate of tumor cells by immune effector cells Φ in numerical solution of our model.

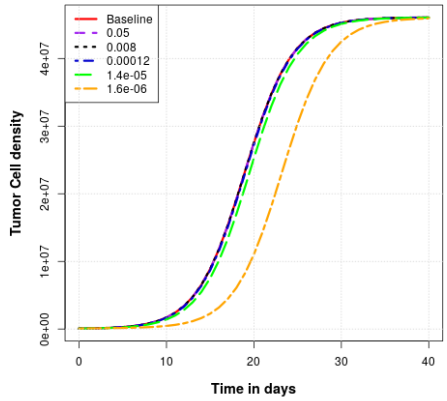

(e) Plot shows the effect of varying the inactivation rate of NK cells caused by tumor cells β_n in numerical solution of our model.

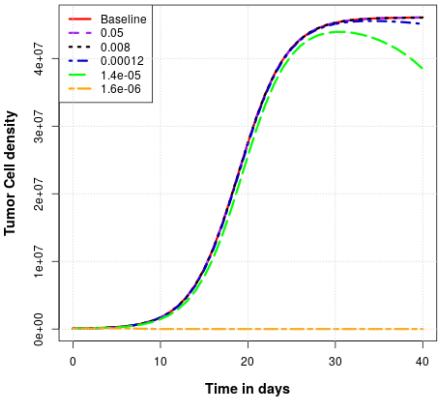

(f) Plot shows the effect of varying the inactivation rate of $CD8^+$ T cells caused by tumor cells β_8 in numerical solution of our model.

Figure 3.8: Plot showing the effect of varying key parameters of interest in numerical solution of our model. Other baseline parameter values used are as stated in Table 3.3.

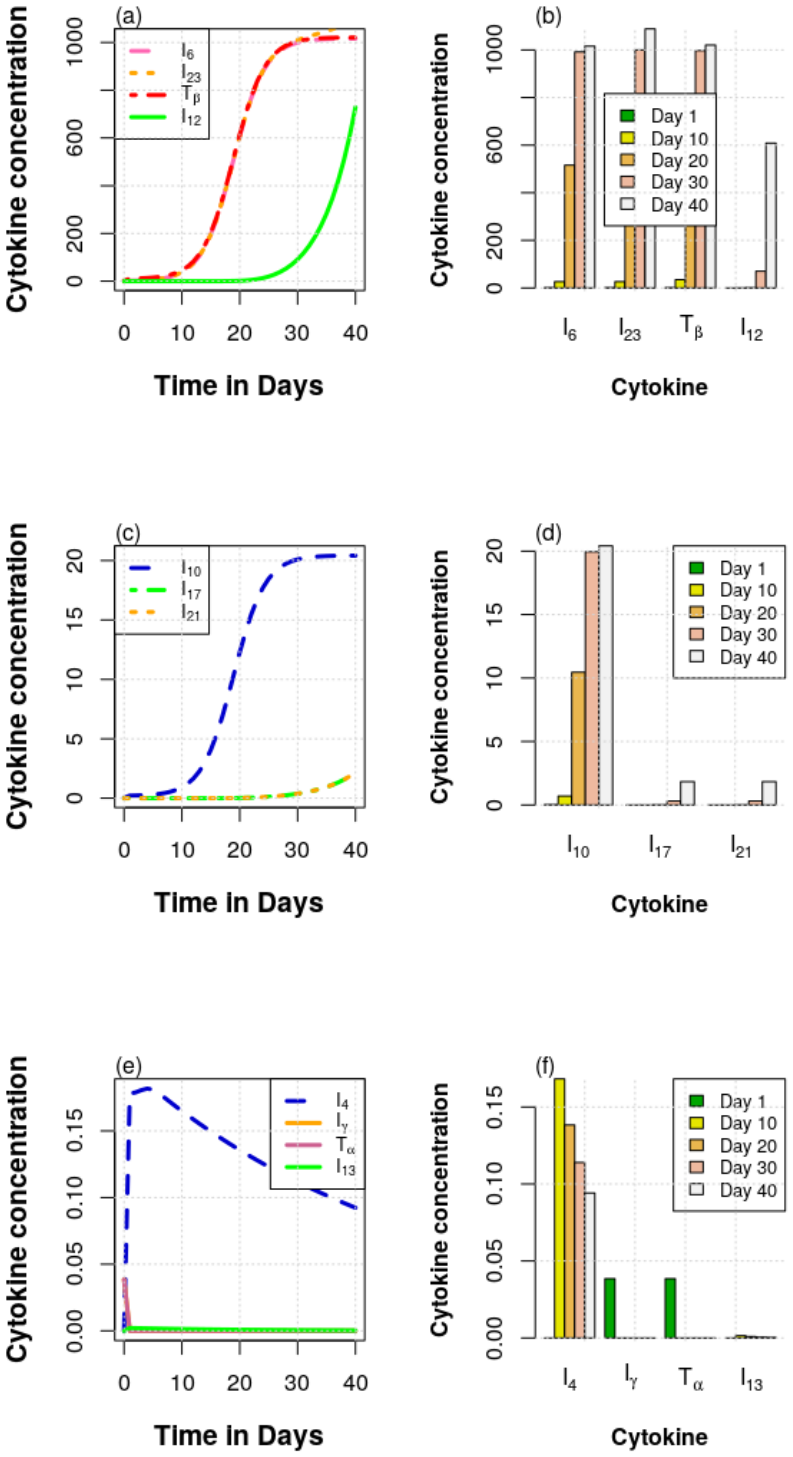

Figure 3.9: Plot indicates the concentration of pro-inflammatory cytokine (IL-12, IL-17, IL-21, TNF-α, and IFN-γ) and anti-inflammatory cytokine (IL-4, IL-6, IL-10, IL-13, IL-23, and TGF-β) when there are weak immune-effector cells at tumor site

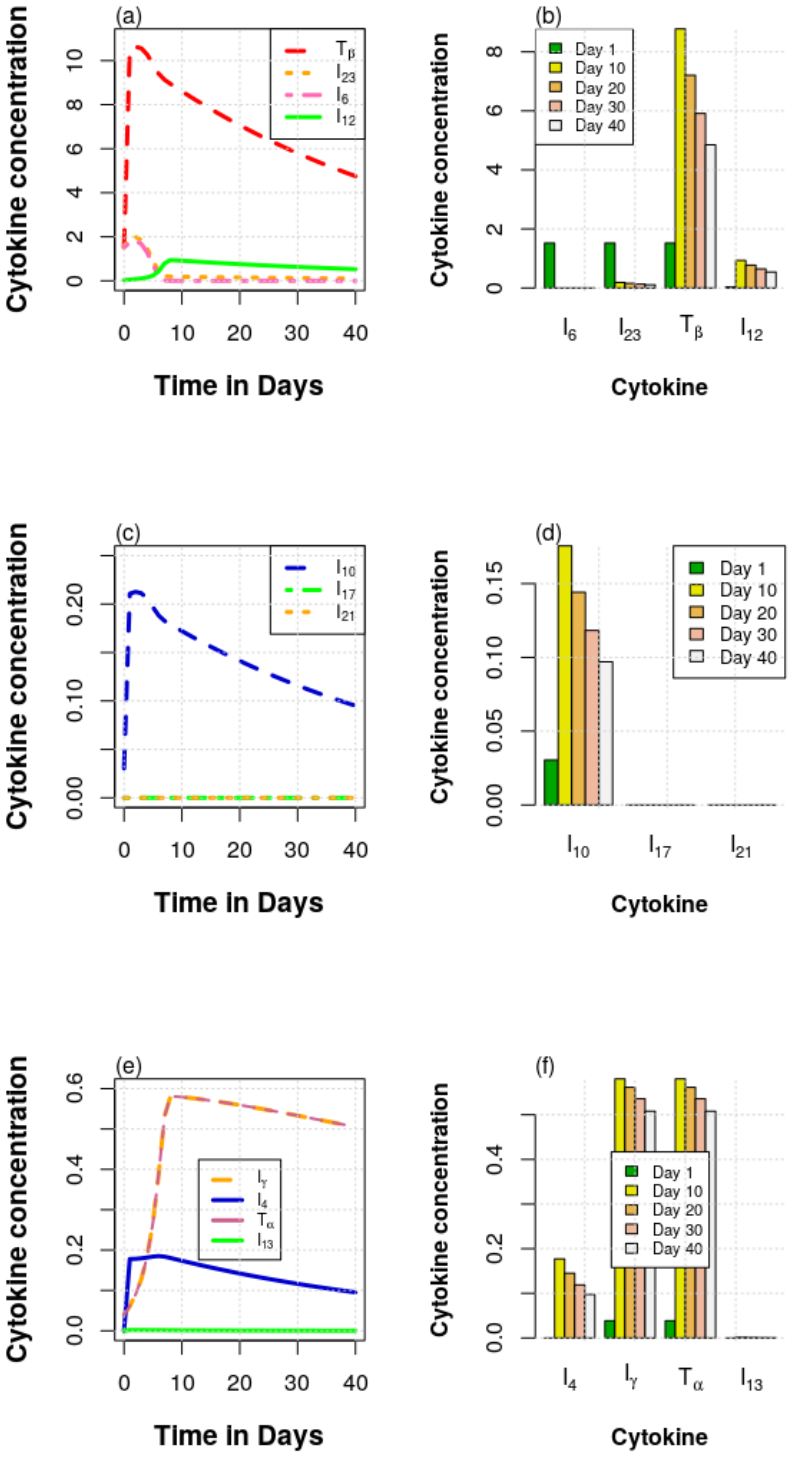

Figure 3.10: Plot indicates the concentration of pro-inflammatory cytokine (IL-12, IL-17, IL-21, TNF-α, and IFN-γ) and anti-inflammatory cytokine (IL-4, IL-6, IL-10, IL-13, IL-23, and TGF-β) when there are strong immune-effector cells at tumor site

Chapter 4

Breast Cancer Drug Target Identification

Breast cancer is a complex disease whereby some cells in the breast grow uncontrollably to form a tumor. Sometimes, breast cancer is caused by abnormal genes passed from parent to child which claimed approximately 5% to 10% of every occurrence of breast cancer. Its prevalence in 2016 has been recorded globally to be the highest among other cancer types [15]. Many research has been carried out on breast cancer [39, 73]. It has been seen to pose a serious public health challenge thereby suggesting that to improve the prevention of breast cancer development; we need to identify the environmental and genetic factors that contribute to the development of breast cancer [39, 73]. This chapter aims to identify breast cancer drug target. We proceed by first generating a unified human functional network using human protein sequences database gotten from different biological data sources. We then characterize its protein-protein interaction networks using network centrality measures. Finally, we identify proteins (breast cancer genes) that triggers key cytokines in our model and suggest essential proteins as a new development for an effective treatment to eliminate breast cancer (see Figure 4.1).

4.1 General View of the Unified Human Protein Functional Network

In order to carry out the analysis of human protein-protein interaction networks, we first generate a unified human protein functional network from different biological data sources: Search Tool for the Retrieval of Interacting Genes/Proteins (STRING) database (https://string-db.org/) and UniProt database (http://www.uniprot.org/). Protein

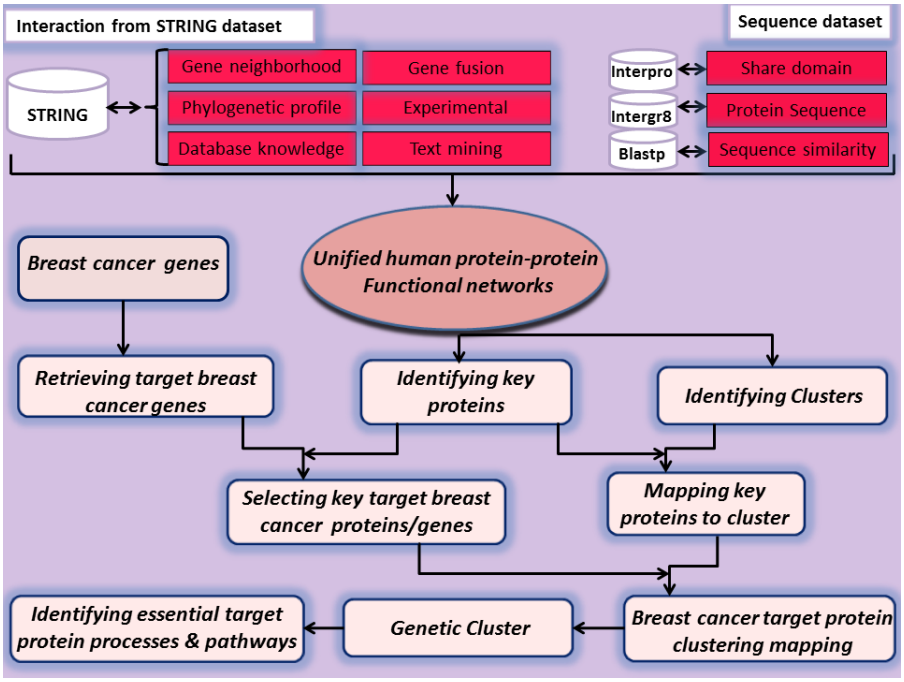

Figure 4.1: Workflow of stepwise process from data integration to extraction of essential drug target pathways for drug discovery in breast cancer.

sequence similarity is extracted by running sequence comparison tool: BLAST (Basic Local Alignment Search Tool) on human protein sequence dataset downloaded from UniProt database in Fasta format. We then proceded by extracting protein signature using InterPro signature data for Human proteins retrieved from the European Bioinformatics Institute (EBI) at http://www.ebi.ac.uk/interpro/. Furthermore, we extracted the interactions of this protein from STRING dataset.

Confidence scores defined by the STRING schemes are used with the functional interaction derived from the STRING database. These confidence scores include conserved genomic neighborhood, gene neighborhood transferred, gene fusion events, gene co-occurrence or phylogenetic profile across multiple genomes, gene co-expression, gene co-expression transferred, experiments, experiments transferred, text mining, text mining transferred, and other databases. Additional interaction data derived from protein sequence similarity and signatures are scored using an information-theoretic based approach which changes the shared biological content between proteins into confidence score. For each evidence source, there are three categories of functional interaction scores between proteins: low, medium and high confidence level. Low confidence interactions level are said to have confidence score strictly less than 0.3, while the medium

confidence level are interactions whose confidence score are between 0.3 and 0.7 inclusively ($0.3 \leq$ score ≤ 0.7) and any interactions whose confidence scores are strictly greater than 0.7 (> 0.7) are categorized as high confidence level. Table 4.1 shows the number of human protein-protein functional interaction in the networks and their confidence scores.

Table 4.1: The number of human protein-protein functional interaction in the networks and their confidence level

Association evidence by type	Low confidence	Medium confidence	High confidence
STRING data	3585678	818652	311597
Sequence data	287997	359519	610485
Combined score	3759260	1159955	911474

For two proteins i and j the combined confidence score as shown in Table 4.1 is computed by combining confidence scores between the proteins from all the datasets for a unified network. Provided that the sources are independent, the combined confidence score is given by

$$C_{ij} = 1 - \prod_{s=1}^{n} \left(1 - c_{ij}^{s}\right), \tag{4.1.1}$$

where c_{ij}^{s} represents the confidence score between protein i and j using the source s in the functional network [75, 76].

In order to minimize the effects of the computational and experimental predictions bias, functional interactions ranging from medium to high confidence levels were considered alongside the functional interactions with low confidence which have been predicted by at least two approaches with a total number of 22,255 interactions. The summary of the general properties of the unified human protein functional interaction network is given in Table 4.2. In the unified human protein functional interaction network, we have in total 19,502 proteins (nodes) with 2,093,684 functional interactions (edges) between proteins. It covers approximately 96% of the human proteome of which 1124 are *structural hubs*. That is proteins that are capable of disconnecting the network and determine the level of integrity in the system. Communication of pairwise protein set over a relative shortest connected path within the system is possible because of the presence of these structural hubs.

Figure 4.2 represents the probability distribution of the shortest path length between pair-wise protein in the unified human protein functional network. The average shortest path length is derived by taking the mean of all shortest path between all pairs of

Table 4.2: General properties of the unified human protein-protein functional network.

Parameters	**Value**
Number of proteins (Nodes)	19502
Number of functional interactions (Edges)	2093684
Average shortest path length	2.63104
Average betweenness	51310.54
Average closeness	0.38008
Average degree	214.715
% of Nodes in largest component	96%
Number of hubs (key proteins)	1124

protein in the network. The biological information communication between a given protein and other proteins within the network is done in just a few steps as the average shortest length achieved is approximately 3. In other words, it shows how fast information can be disseminated in the human protein functional network irrespective of the number of proteins in the system. Another advantage regarding this property is that the system would be able to effectively respond and quickly adjust to any change in the environment [75].

We proceed by performing a degree distribution of the unified human functional network. As illustrated in Figure 4.3, the system shows a scale-free topology, in the sense that, there is an approximate power law $P(k)=k^{-\gamma}$ of degree distribution of proteins with the degree exponent $\gamma \sim 1.32$. This implies that the network has more proteins with few interacting partners (low degree nodes) leaving just a few with many interacting partners (high degree nodes). If the latter is removed from the network, it can disconnect the network thereby affecting functions of the system. They are therefore considered to be responsible for the completeness of the system thus essential for the survival of the organism.

4.2 Genes Associated with Breast Cancer

Gene mutations are associated with most inherited cases of breast cancer. Breast cancer gene one (*BRCA1*) and breast cancer gene two (*BRCA2*) are the two well-known susceptibility genes causing cancer in the human breast. Normally, the functions of these breast cancer genes are to repair DNA damages and to act as tumor suppressors by preventing cells from growing and metastasizing [123]. However, when mutations alter these genes, it results in a higher risk of developing cancer. Depending on the population

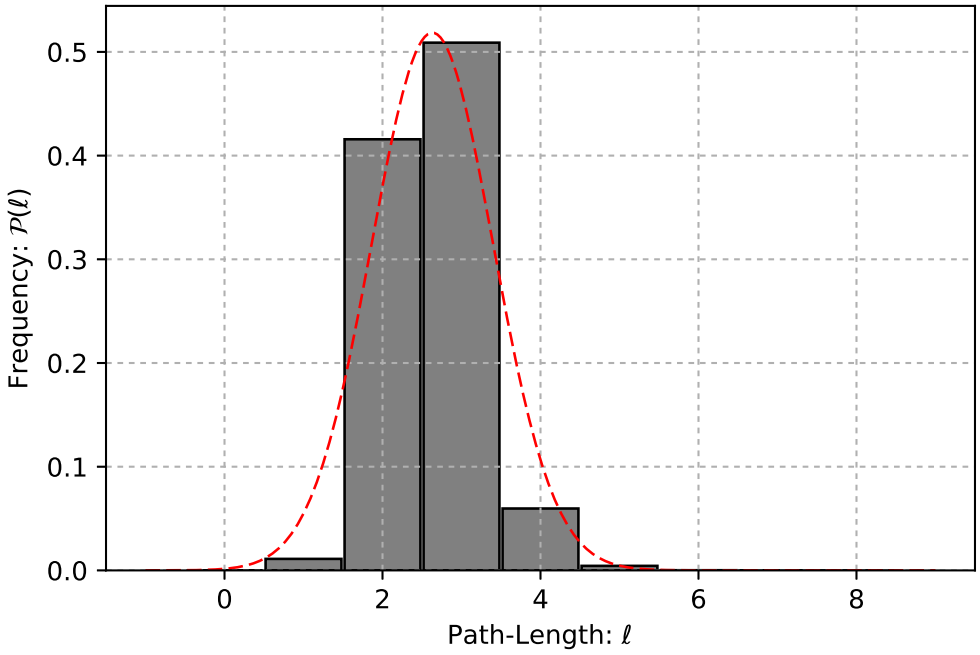

Figure 4.2: Shortest path length probability distribution between pair-wise node in the human protein functional network.

under study, from previous research, a germline mutation in *BRCA1* gene is known to represent a predisposing genetic factor in about 15% to 45% of hereditary breast cancer and at least 80% of breast and/or ovarian cancer. Whereas women with *BRCA1* mutation have about 60% to 80% likelihood of developing breast cancer [39, 73] and about 20% to 40% probability of developing ovarian cancer. Likewise, *BRCA2* mutation carriers have about 60% to 85% likelihood of developing breast cancer and about 10% to 20% probability of developing ovarian cancer [39, 73]. Furthermore, men with *BRCA2* mutation have approximately 6% chance of breast cancer risk while men with BRCA1 mutation have a high risk of having prostate cancer.

The breast cancer genes mentioned above are described as *high penetrance* in the sense that both women and men who have mutations in them are linked with high risk of developing breast cancer and other subtypes of cancer. Meanwhile, there are several other genes associated in one way or the other to developing high risk of breast cancer. Some of them are features of rare genetic syndromes including: *Li-Fraumeni syndrome* often caused by *p53* gene mutations; *Cowden syndrome* usually caused by *PTEN* gene mutations; *Ataxia-telangiectasia* caused by homologous in the *ATM* gene; *hereditary dif-*

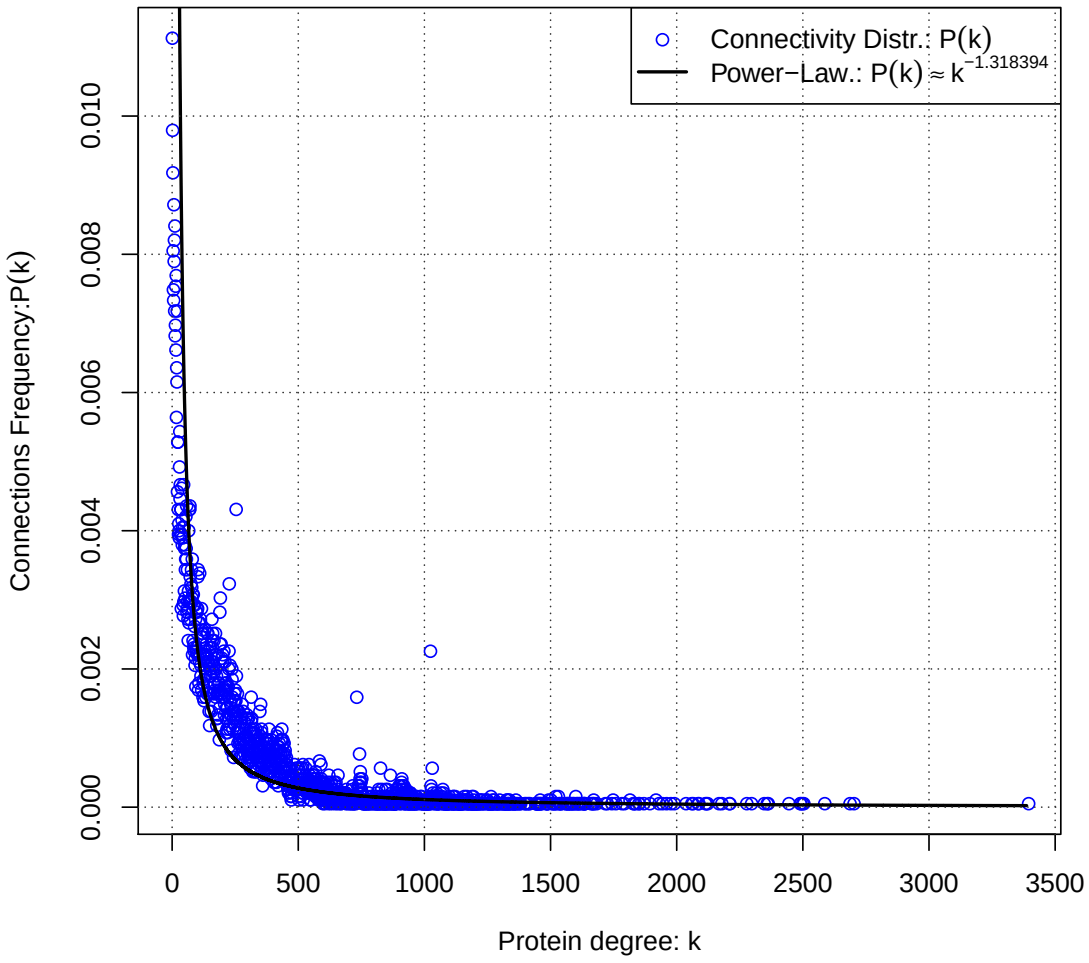

Figure 4.3: Degree distribution of detected k function interactions per protein against the connection frequency P(k).

fuse gastric cancer resulting from *CDH1* gene mutations; *Peutz-Jeghers syndrome* which mainly derives from *STK11* gene mutations; and *Muir-Torre syndrome* typically results from *MSH2* gene mutations [123]. Table 4.3 lists the genes associated with breast cancer with their description obtained from the UniProt knowledge-base database (`http://www.uniprot.org`).

Table 4.3: Description of human target proteins associated with breast cancer.

UniProt-ID	Gene name	Description
P38398	*BRCA1*	Breast cancer type 1 susceptibility protein (EC:2.3.2.27)(RING finger protein 53)
P51587	*BRCA2*	Breast cancer type 2 susceptibility protein (Fanconi anemia group D1 protein)
Q8NBR0	*p53*	Tumor protein p53-inducible protein 13 (Damage-stimulated cytoplasmic protein 1)
P60484	*PTEN*	Phosphatidylinositol 3,4,5-trisphosphate 3-phosphatase and dual-specificity protein phosphatase PTEN (EC:3.1.3.16,EC:3.1.3.48,EC:3.1.3.67) (Mutated in multiple advanced cancers 1)
Q13315	*ATM*	Serine-protein kinase ATM (EC:2.7.11.1)(Ataxia telangiectasia mutated)
P12830	*CDH1*	Cadherin-1(Epithelial cadherin)
Q15831	*STK11*	Serine/threonine-protein kinase STK11(EC:2.7.11.1) (Liver kinase B1(*LKB1*))
P43246	*MSH2*	DNA mismatch repair protein Msh2(MutS protein homolog 2)
I3L2S5	*PALB2*	Partner and localizer of BRCA2
Q99728	*BARD1*	BRCA1-associated RING domain protein 1 (EC:2.3.2.27) (RING-type E3 ubiquitin transferase BARD1)
Q9BX63	*BRIP1*	Fanconi anemia group J protein (EC:3.6.4.13) (BRCA1-interacting protein C-terminal helicase 1)
Q06609	*RAD51*	DNA repair protein RAD51 homolog 1
Q14790	*CASP8*	Caspase-8 (EC:3.4.22.61)(Apoptotic cysteine protease)
P54278	*PMS2*	Mismatch repair endonuclease PMS2 (DNA mismatch repair protein PMS2)
O96017	*CHEK2*	Serine/threonine-protein kinase Chk2 (EC:2.7.11.1) (Checkpoint kinase 2)
P16410	*CTLA4*	Cytotoxic T-lymphocyte-associated antigen 4
Q05D78	*MRE11A*	MRE11A protein
P11511	*CYP19A1*	Aromatase (EC:1.14.14.14) (Cytochrome P450 19A1)
O60934	*NBN*	Nibrin (Cell cycle regulatory protein p95)
P21802	*FGFR2*	Fibroblast growth factor receptor 2 (EC:2.7.10.1) (Keratinocyte growth factor receptor)
P40692	*MLH1*	DNA mismatch repair protein Mlh1 (MutL protein homolog 1)
P33241	*LSP1*	Lymphocyte-specific protein 1
Q92878	*RAD50*	DNA repair protein RAD50
O43502	*RAD51c*	DNA repair protein RAD51 homolog 3
O14746	*TERT*	Telomerase reverse transcriptase (EC:2.7.7.49)(Telomerase-associated protein 2)
O15405	*TOX3*	TOX high mobility group box family member 3
O43543	*XRCC2*	DNA repair protein XRCC2 (X-ray repair cross-complementing protein 2)
O43542	*XRCC3*	DNA repair protein XRCC3 (X-ray repair cross-complementing protein 3)

Mutation in *PALB2*, *BARD1*, *LKB1*, *BRIP1*, *RAD51*, *CASP8*, *PMS2*, *CHEK2*, *CTLA4*, *MRE11A*, *CYP19A1*, *NBN*, *FGFR2*, *MLH1*, *LSP1*, *TERT*, *RAD50*, *TOX3*, *XRCC2*, *RAD51c* and *XRCC3* genes and several other genes according to research are possible risk factors for breast cancer and are described as *low penetrance* because of their little contribution to breast cancer risk. Interactions between proteins produced by these genes and the *BRCA1* or *BRCA2* as been suspected by researchers to have significant impact in carrier risk of developing breast cancer [39, 73, 123]. We shall therefore proceed in the next section to identify proteins (breast cancer genes) that regulates key cytokines in our model.

4.3 Retrieving Potential Breast Cancer Genes

From our model results, we are able to identify five cytokines that play key roles in the dynamics of tumor-immune interactions in the tumor microenvironment, of which are the tumor promoting cytokines: IL-10, IL-23, and TGF-β, and tumor suppressing cytokines: TNF-α and IFN-γ. We peruse several literatures to identify essential proteins from the aforementioned breast cancer genes which somehow regulates the derived key cytokines. According to Wang et al.(2013), the *ATM* pathway regulates IL-23 expression by human dendritic cells [113], while activation of *LSP1* gene results in the downregulation of IL-23 production [23]. Also according to Li et al. (2016), TGF-β1 production and the TGF-β signalling pathway are inhibited by tumor suppressive function of *LKB1* in breast cancer cells [62]. Meanwhile TGF-β was stated to downregulate the expression of *PTEN* [22], *MSH2*, *ATM*, *BRCA1* and *BRCA2* [65] in breast cancer cells. Also TGF-β upregulates *CTLA4* [127], while TGF-β-SNAI 2 signalling was reported by Ding et al. (2013) to suppress *CDH1* [30]. The subsets of TGF-β target genes are differentially regulated by *p53* thereby promoting cancer malignancy [51]. Gene *p53* directly regulates IL-10 localization [85] while IL-10 mediate the regulation of *CASP8* activation [43].

For the case of the tumor suppressing cytokines IFN-γ, tumor suppressor gene *BRCA1* regulates the IFN-γ-mediated apoptotic response [3], while the expression of IFN-γ related genes are regulated by *BRCA2* [118]. *LKB1* which is a central regulator of T cell development, activation and metabolism was reported to elevate IFN-γ production [68]. Also, data from Leong et al.(2015) suggested that *PTEN* might promote IFN-γ production [61] while dos Santos and Isabel (2012) in their work, identified *ATM* as a regulator of IFN-γ response [32]. According to Ruiz-Ruiz et al. (2004), *CASP8* expression are elevated when human breast cancer cells are being treated with IFN-γ [92], while IFN-γ/Interferon regulatory factor-1(IRF-1)-induced p27kip1 down-regulates human telomerase reverse transcriptase(*hTERT*) expression and telomerase activity in human cervical

cancer [59].

Lastly, breast cancer genes such as *PTEN*, *CASP8* and *p53* regulate the tumor suppressing cytokines TNF-α [42, 84, 106] with *ATM* being a key regulator of TNF-α activated ERK/p38 NF-kappaB pathway[119], while an *LKB1* interacting protein negatively regulates TNF-α induced NF-kappaB activation[66]. Moreover, TNF-α serves as a regulator for both *BRCA1* and *BRCA2* expression [11] and downregulates CDH1[121]. Hence, from all the human genes associated with breast cancer that were retrieved as previously elucidated, only those identified to be target genes and are able to regulate our model key cytokines are summarized in Table 4.4 with key cytokines they triggered. We then proceed by mapping these target genes identified onto the unified functional network in order to select those which are key proteins.

Table 4.4: Human target proteins associated with breast cancer with cytokines they trigger.

Gene name	Cytokines
PTEN	TNF-α, TGB-β, IFN-γ
BRCA1	TNF-α, TGB-β, IFN-γ
ATM	IL-23, TNF-α, TGB-β, IFN-γ
CDH1	TNF-α, TGB-β
CASP8	IL-10, TNF-α, IFN-γ
MSH2	TGB-β
TERT	IFN-γ
CTLA4	IL-10, TGB-β, IFN-γ
BRCA2	TNF-α, TGB-β, IFN-γ
LSP1	IL-23
p53	IL-10, TNF-α, TGB-β
LKB1	TNF-α, TGB-β, IFN-γ

4.4 Selecting Essential Breast Cancer Genes

In this section, we identify and elucidate clusters containing key target proteins within the unified functional network. We employ clustering method used by Blondel et al., which has been proven to outperform other methods used in clustering different functional networks [10]. A total of 90 clusters were generated from the unified human protein functional network with the biggest cluster containing 4169 proteins. We identified 858 key proteins in the unified human functional network using the degree and closeness with the degree and betweenness joint threshold values. These threshold val-

ues are approximate as follows, 215 for degree measure, $1/2.631 \approx 0.38$ for closeness measure as defined in (2.4.2) and 51310.54 for the betweenness measure.

Table 4.5: Distribution of human proteins and key proteins in 5 different clusters in terms of number of proteins (#pr), key proteins (#KPr), target proteins (TPr) and key target proteins (KTPr).

Cluster ID	**#Pr**	**#KPr**	**TPr**	**KTPr**
0	3857	140	*p53*	Nil
2	4619	299	*CDH1*, *PTEN*, *TERT*, *CASP8*, and *CTLA4*	*CDH1*, *PTEN*, *TERT*, and *CASP8*
3	2783	164	*ATM*, *BRCA1*, and *BRCA2*	*ATM* and *BRCA1*
7	1274	135	*MSH2*	*MSH2*
8	1200	120	*LSP1*	Nil
Total	13 733	858	11	7

Among the 90 clusters in the unified human functional network, only 11 clusters contains key proteins of which the target proteins are distributed among only 5 clusters as shown in Table 4.5, with 299 key proteins in the biggest cluster. Hence, analysing the target proteins at the system level using the unified human functional network, out of the previously listed target proteins, we identified 7 key target proteins associated with breast cancer, and are given in Table 4.6 with their respective network centrality scores. These human key target proteins are contained in three of the five clusters containing human target proteins, as previously elucidated. They are therefore considered to be breast cancer target proteins and promising target for further research towards the development of new drug and vaccine for breast cancer.

Table 4.6: Human key target proteins associated with breast cancer with their network centrality scores.

Gene name	**Betweenness**	**Closeness**	**Degree**
PTEN	149261.55	0.47858	1047
BRCA1	207445.38	0.47151	1159
ATM	106979.92	0.46922	906
CDH1	235111.26	0.46682	817
CASP8	70405.12	0.45799	550
MSH2	58147.12	0.45653	676
TERT	216312.77	0.45582	439

Furthermore, we perform enrichment and pathway analysis to identify enriched biological processes and pathways in which the human proteins interacting with the breast cancer-associated key proteins are involved. In order to do this, we considered the cluster containing high penetrance genes, *BRCA1* and *BRCA2* (cluster #3) as a breast cancer genetic cluster with a total number of 2783 human proteins. Hence we performed functional analysis on this genetic cluster in the next sections.

4.5 Process and Pathway Enrichment Analysis

To gain insight into the enriched biological processes in which a set of the target protein is involved, we performed process and pathway enrichment analysis using the following annotation databases: Gene Ontology (GO) [24], Gene Ontology Annotation (GOA) [14] and Kyoto Encyclopedia of Genes and Genomes (KEGG) [82]. For the process analysis, GO and the GOA mapping given by the UniProtKB-GOA dataset was used [74, 78]. It contains evidence-based annotations and biological description of individual proteins. The domains of GO include biological processes, molecular function or cellular component [24]. In the course of this study, we only focused on predicting enriched biological processes of the target proteins. For the pathway enrichment analysis, we used KEGG data sets extracted from the KEGG database at (`http://www.genome.jp/kegg/`). KEGG pathway, in this study, is used to map key proteins in the genetic cluster with biological functional information or interacting molecules in cells.

Process and pathway enrichment analysis use different statistical methods to determine the enriched biological process and significant pathway associated with the outcome of a disease [33]. They are Fisher's exact, hypergeometric and χ^2 test. In this study, we used a hypergeometric distribution test, because it appropriately models the probability that a particular annotation term occurs j times in the list of target proteins. The p-value for each process or pathway is the probability of observations made on at least x proteins involved in the process or pathway under consideration and it is calculated using its frequency in the dataset [74, 77]. The formula is given by

$$P[X \geq x] = 1 - \sum_{k=0}^{x-1} \frac{\binom{m}{k}\binom{N-m}{n-k}}{\binom{N}{n}}.$$

where the random variable X is the number of occurrences of the target-associated process or pathway within a given target gene set of size n, knowing that the reference dataset (whole human proteome) contains m such annotated genes out of N genes

[74, 77]. The p-value obtained was adjusted using the Bonferroni multiple testing correction, and we selected GO terms and pathway enriched in our target proteins list by requiring a p-value less than 0.05 [78].

In the following section, a detailed discussion on the identified GO terms and KEGG pathways will be presented.

4.5.1 Enriched biological processes associated with breast cancer

The main GO terms associated with the target protein list in the genetic cluster were identified as a result of performing statistically enriched biological processes on key proteins in the breast cancer genetic cluster. A total of 15 biological processes were found to be significant for breast cancer disease outcome in human (see Table 4.7). The higher the level, the more specific the GO term.

Among the enriched biological processes of human proteins predicted to interact with associated breast cancer proteins, are the activation of different levels of Mitogen-activated protein kinases (MAPKs). They include GO:0000185 (activation of MAPKKK activity), GO:0000187 (activation of MAPK activity) and GO:0000186(activation of MAPKK activity).

Table 4.7: 15 most statistically significant GO biological process terms associated with target proteins in the BRCA genetic cluster.

GO-ID	Biological Process	Level	p-value	Adjusted p-value
GO:0000185	activation of MAPKKK activity	13	1.68×10^{-5}	0.01244
GO:0000187	activation of MAPK activity	13	5.08×10^{-6}	0.00376
GO:0000186	activation of MAPKK activity	13	1.68×10^{-5}	0.01244
GO:0007254	JNK cascade	11	4.28×10^{-5}	0.03166
GO:0000086	G2/M transition of mitotic cell cycle	7	2.05×10^{-6}	0.00152
GO:0006977	DNA damage response, signal transduction by p53 class mediator resulting in cell cycle arrest	13	8.24×10^{-7}	0.00061
GO:0010768	negative regulation of transcription from RNA polymerase II promoter in response to UV-induced DNA damage	13	5.76×10^{-5}	0.04262
GO:0007179	transforming growth factor beta receptor signaling pathway	8	1.70×10^{-5}	0.01261
GO:0008543	fibroblast growth factor receptor signaling pathway	8	4.73×10^{-6}	0.00349
GO:0060070	canonical Wnt signaling pathway	8	1.54×10^{-5}	0.01141
GO:0002755	MyD88-dependent toll-like receptor signaling pathway	12	6.02×10^{-6}	0.00446
GO:0002223	stimulatory C-type lectin receptor signaling pathway	11	2.41×10^{-5}	0.01783
GO:0006879	cellular iron ion homeostasis	10	1.66×10^{-6}	0.00123
GO:0070987	error-free translesion synthesis	10	3.34×10^{-5}	0.02473
GO:0035635	entry of bacterium into host cell	8	6.02×10^{-6}	0.00446

Four classes of MAPK intracellular signalling cascade are involved in breast disease and operate in mammary epithelial cells. They include the extracellular regulated kinases (ERK) 1/2 pathway, the ERK5 pathway, the p38 pathway and the c-Jun N-terminal kinases (JNK pathway) [52, 58]. As indicated in Table 4.7, JNK pathway (GO:0007254) is an essential biological process associated with breast cancer. Furthermore, p38 MAP kinase has been shown to be implicated in complex biological processes including cell differentiation, proliferation, migration, invasion, apoptosis, and responses to environmental stress [58]. Dysregulation of p38 MAPK levels in cancer patient results in advanced stages and short survival of the patient [58]. Moreover, dysregulated ERK1/2 signalling alone is insufficient to cause cancer. However, additional crosstalk with other major signaling networks such as p53 and PTEN, enhances cell proliferation, prevents apoptosis and sometimes induces drug resistance [52]. Yue et al. (2002) reported that MAPK activation also enhances long-term estrogen deprived MCR-7 human breast cancer cells to cause hypersensitivity to the mitogenic effect of estradiol (E(2)) [124].

Enriched biological process GO:0000086 (G2/M transition of mitotic cell cycle) deals with the process of cell division of the mother cell into two daughter cells genetically identical to each other. BRCA1 is known to be required for S and G2/M transition which are involved in the cellular response to DNA damage [111]. Also, they help prevent damaged DNA from entering mitosis due to trigger from ATR (Ataxia Telangiectasia and Rad3-related) and Chk1 (Checkpoint kinase 1) [112]. GO:0006977 (DNA damage response, signal transduction by p53 class mediator resulting in cell cycle arrest), in agreement with DNA damage, can cause *cell cycle arrest* (i.e. when cell has entered a quiescent stage and no longer active in the process of cell division) through induction of the p53 pathway (tumor suppressor) which can lead to initiation of DNA repair of apoptosis [126].

Another enriched biological process, GO:0010768, is related to the negative regulation of transcription from RNA polymerase II promoter in response to UV-induced DNA damage. This is in agreement with the fact that large subunit of RNA polymerase II is ubiquitinated in cells after UV-irradiation treatment which include DNA damage preferentially repaired transcriptional-coupled repair (TCR). Moreover, specific mutation in genes is known to cause a defect in TCR including BRCA1, which is defective in TCR of oxidative DNA damage [44]. Various pathways such as: GO:0007179 (transforming growth factor beta (TGF-β) receptor signaling pathway), GO:0008543 (fibroblast growth factor receptor (FGFR) signaling pathway), GO:0060070 (canonical Wnt signaling pathway), and GO:0002755 (MyD88 (myeloid differentiation primary response gene 88)-dependent toll-like receptor signaling pathway) have been predicted to be identi-

fied in breast cancer. Concerning TGF-β receptor signaling pathway, TGF-β has a dual effect on tumor growth, in the sense that, it switches its role from suppressor of primary tumor initiation to a promoter of the later malignant stages. Improved prognostic information for breast cancer patient might be obtained by assessing interaction among TGF-β signaling biomarkers [25].

Likewise, FGFR signaling is implicated in biological processes, such as cell differentiation, proliferation, survival, migration, and apoptosis. Alteration in these processes can promote the development and progression of a tumor. Due to its role in the activation of critical signaling pathways and contribution towards the pathogenesis in breast cancer, targeting FGFR has been highlighted to provide a new opportunity for breast cancer therapeutic strategies [114]. Canonical Wnt signaling dysfunction, on the other hand, mediates the progression of triple-negative breast cancer [88]. As for MyD88-dependent signaling, it was revealed that it enhances the expression of genes that could promote breast cancer progression and have the ability to suppress the expression of genes capable of inhibiting breast cancer progression [49].

Another enriched biological process identified is GO:0002223 (stimulatory C-type lectin receptor signaling pathway). C-type lectin receptors (CLRs) are primarily expressed on myeloid cells (macrophages and dendritic cells). Similar to Toll-like receptors, CLRs signaling are implicated in different levels of innate immune response initiation and promote the production of soluble factors such as cytokines and interferons [95]. Also, intracellular routing of antigen through CLR enhances the presentation of antigen through MHC class I and II molecules. It thereby induces antigen-specific $CD4^+$ and $CD8^+$ T cell proliferation [103]. Agonist or antagonist of CLRs signaling has been therefore suggested to be a potential therapeutic reagent for cancer immunotherapy [95, 103].

GO:0006879 (cellular iron ion homeostasis) involves upkeep of an internal steady state of iron ions at a cell's level. Several studies have linked iron to carcinogenesis, either by continuous failure in the redox balance or due to its vital role in cellular proliferation. Alteration in the processes cellular iron has been reported to likely contribute to breast cancer behavior, development, and recurrence [72]. Also, GO:0070987 (error-free translesion synthesis) involves DNA polymerase that promotes DNA replication by efficiently neglecting different DNA lesions in a relatively error-free manner [70]. Studies postulated that the increased number of translesion synthesis polymerases developed gradually in a higher organism as a tumor suppressive adaptation [55]. Lastly, the target proteins are also enriched in biological process GO:0035635 (entry of bacterium into host cell), in which recent researches have shown interesting results suggesting the ef-

fectiveness of bacteria as an agent for cancer treatment [101].

We shall proceed to briefly highlight the identified enriched pathway in the next section.

4.5.2 Enriched pathways associated with breast cancer

We identified 21 enriched KEGG pathways (see Table 4.8) in which target proteins in the genetic cluster are implicated. According to several published literature, all of these pathways identified in this study have been confirmed to participate in breast cancer associated biological processes. As we have mentioned earlier, pathways such as Wnt signaling pathway, TGF - β signaling pathway and p53 signaling pathway have been reported to contribute to the growth and progression of human breast cancer. Among other KEGG pathways identified is pathways in cancer. This pathway describes the kernel regulatory factors that contribute to the initiation and progression of pan-cancer [122]. Another subtype of cancer, renal cell carcinoma associated biological process, have also been predicted to be associated with breast cancer [109].

Another enriched pathway identified, Hypoxia-inducible factor 1(HIF-1) signaling pathway, is a transcription factor that acts as a major regulator of oxygen homeostasis within cells. Gilkes and Semenza (2013) reported that breast cancer patients with high HIF expression levels in primary tumor biopsies are at risk of angiogenesis, metastasis, and resistance to apoptosis. In addition to intratumoral hypoxia, alteration in EGFR (Epidermal growth factor receptor), PTEN, Tp53 and HER2 (human epidermal growth factor receptor 2) signaling pathways also regulate the expression of HIF-dependent of target genes [40]. As for RIG-I- like receptor (RLR) signaling pathway, activation of RLR causes immunogenic cell death of virus-infected cells which is followed by increased production of inflammatory cytokine and antigen presentation. In recent studies, a different approach to non-infectious RIG-I activation in cancer is being investigated as a treatment option, with a potentially high cytotoxic function of tumor-infiltrating lymphocytes [35].

Concerning the KEGG pathway MicroRNAs (miRNAs) in cancer, dysregulated miRNAs have been shown to play a crucial role in almost all cancer subtypes including breast cancer [20]. Altered expression of miRNA in breast cancer cell lines is linked with altered cell cycle progression and cell proliferation. Several analyses carried out on miRNA expression suggested oncogenic or tumor suppressive roles of miRNAs [60]. Moreover, KEGG pathway hsa04330 which describes the Notch signaling pathway has been predicted to contribute to breast cancer. As a regulatory mechanism for cell proliferation, differentiation, and survival, increased Notch signaling has agreed with therapy

Table 4.8: Enriched KEGG pathways associated with target proteins in the BRCA genetic cluster.

Pathway-ID	Pathway-Name	p-value	Adjusted p-value
hsa04310	Wnt signaling pathway	1.31×10^{-8}	1.99×10^{-6}
hsa04350	TGF - beta signaling pathway	5.64×10^{-7}	8.57×10^{-5}
hsa04115	p53 signaling pathway	4.36×10^{-5}	0.00662
hsa05200	Pathways in cancer	1.62×10^{-4}	0.02463
hsa05211	Renal cell carcinoma	1.65×10^{-4}	0.02502
hsa04066	HIF - 1 signaling pathway	7.80×10^{-5}	0.01216
hsa04622	RIG - I - like receptor signaling pathway	3.55×10^{-6}	0.00054
hsa05206	MicroRNAs in cancer	4.42×10^{-5}	0.00672
hsa04110	Cell cycle	1.57×10^{-5}	0.00238
hsa04330	Notch signaling pathway	5.24×10^{-6}	0.00079
hsa04120	Ubiquitin mediated proteolysis	5.87×10^{-9}	8.93×10^{-7}
hsa04520	Adherens junction	1.65×10^{-4}	0.02502
hsa04114	Oocyte meiosis	2.04×10^{-4}	0.03106
hsa04710	Circadian rhythm	1.49×10^{-7}	2.27×10^{-5}
hsa04530	Tight junction	1.32×10^{-5}	0.00200
hsa05165	Human papillomavirus infection	3.79×10^{-5}	0.00577
hsa05162	Measles	3.44×10^{-7}	5.23×10^{-5}
hsa05169	Epstein - Barr virus infection	1.39×10^{-5}	0.00211
hsa05016	Huntington's disease	3.27×10^{-4}	0.04965
hsa05166	HTLV - I infection	3.73×10^{-5}	0.00566
hsa05164	Influenza A	1.16×10^{-7}	1.77×10^{-5}

resistance in oestrogen receptor-positive breast cancer. Recent analysis shows the importance of Notch signaling in BRCA progression via triggering epithelial-mesenchymal transition (EMT) [83].

Furthermore, for enriched KEGG pathway Ubiquitin-mediated proteolysis, protein ubiquitination occurs through sequential activation and conjugation of ubiquitin to target proteins by a reaction cascade consisting of three enzymes namely: the ubiquitin-activating enzyme (E_1), the ubiquitin-conjugating enzyme (E_2), and ubiquitin ligase (E_3) [64]. Several studies have indicated that many E_3s in breast cancer function as either oncogenes or tumor suppressor genes. Also, most cancers related E_3s regulate the cell cycle, p53, transcription, DNA repair, cell signaling, and apoptosis [21]. Among other enriched pathways identified, adherens junction is crucial for maintaining tissue architecture, cell polarity and can reduce cell movement and proliferation. Tumor suppressor gene E-cadherin (CDH1) serves as an essential cell adhesion molecule, and any loss of E-cadherin mediated adhesion form the transition from benign lesions to invasive, metastatic cancer. Also, evidence shows that E-cadherin may also play a role in the Wnt

signal transduction pathway [87].

Other results from our KEGG pathway analysis also showed that, pathogenesis of breast cancer is associated with other biological processes such as Oocyte meiosis [117], Circadian rhythm [9] and Tight junction [12]. We also identified several disease-enriched pathways associated with breast cancer. They include: Human papilloma virus infection [5], Measles [5], Epstein-Barr virus infection [5], Huntington's disease [102], human T-lymphotropic virus type 1(HTLV-I) infection [96] and Influenza A [48]. Infection of such viruses has been confirmed to increase risk of breast cancer.

Chapter 5

Conclusion

In this study, we developed a new mathematical model describing the dynamics of tumor growth and the host immune system components in the tumor microenvironment. These components include: resting macrophages, M1 macrophages, M2 macrophages, natural killer (NK) cells, dendritic cells (DCs), helper T cells ($CD4^+$ T cells) and its subsets, effector T cells ($CD8^+$ T cells), tumor cells, pro-inflammatory cytokines (IL-2, IL-12, IL-17, IL-21, TNF-α, and IFN-γ) and anti-inflammatory cytokines (IL-4, IL-5, IL-6, IL-4, IL-10, IL-13, IL-23, and TGF-β). In addition to this, the local and global stability of the tumor-free equilibrium point was established. We found that tumor free equilibrium will be globally asymptotically stable if the elimination rate of M2 macrophages by Th1 cells is more than the transition of M1 macrophages to M2 macrophages caused by both Th2 cells and tumor cells. Sensitivity analysis on estimated parameters was done to show the parameters that play an important role in the dynamics of the tumor.

From the simulation of our model, we predicted that few cytotoxic immune cells (i.e., NK cells and $CD8^+$ T cells) at the tumor site lead to tumor escape from the mechanisms of immunological surveillance (see Figure 3.3). Our model, therefore, supports strengthening the cytotoxic immune cells in the tumor microenvironment which we see as a significant way of contributing to tumor regression (see Figure 3.6). Also, from the analysis of our model, cytokines, such as IL-10, IL-23, TNF-α, TGB-β, and IFN-γ, have been shown to contribute significantly to the dynamics of tumor growth based on the observed dynamics in the level of concentrations in the tumor microenvironment (see Figure 3.9 and 3.10).

In particular, IL-23 concentration compared to others was observed to be strong at the tumor site contributing to termination of the innate immune cells activities. It induces immuno-suppression through down-regulation of $CD4^+$ and $CD8^+$ T cells infil-

trating in tumor tissues as reported in previous research thereby leading to tumor progression. It was further observed that the depletion of the tumor suppressing cytokines lead to a decrease in the population, efficiency and cytotoxic effect of the immune effector cells while when there are high cytotoxic immune cells at tumor site, IL-23 concentration was observed to be minimal in the tumor microenvironment leading to the elimination of the tumor cells. This supports the idea from previous research that tumor promoting cytokine IL-23 plays a significant role in the growth and proliferation of tumor and its antibody can, therefore, be used to achieve an increased tumor eradication or a delayed tumor growth. All these cytokines are therefore considered to be key cytokines and were used for further analysis in this research.

Finally, switching of an immune (effector) cell from resting to active states, is triggered by some proteins working in a complex protein-protein interaction (PPI) network. We presented a unified human functional protein-protein interaction network using human protein sequences database gotten from different biological data sources. We used text mining technique to identify proteins (breast cancer genes) that regulate key cytokines in our model. Furthermore, with the aid of network centrality measures, we identified proteins which are essential to the functioning of the system. We proceeded by classifying essential proteins in human functional networks and elucidated clusters containing key target proteins in the network. We considered the cluster containing high penetrance genes, *BRCA1* and *BRCA2*, as a breast cancer genetic cluster and performed functional analysis on this genetic cluster.

For the process analysis, GO and GOA mapping given by the UniProtKB-GOA dataset were used while for the enrichment pathway analysis, KEGG data sets extracted from the KEGG database at (http://www.genome.jp/kegg/) were considered. A hypergeometric test was employed to predict enriched biological processes and significant pathways of target proteins associated with breast cancer. From the results of the analysis, a total of 15 biological processes and 21 enriched KEGG pathways were found to be essential for breast cancer disease outcome. Most of the enriched processes and pathways are related to the immune system signaling pathways, thereby enabling the host to detect the cancer cells and respond. We also observed several disease-enriched pathways including Human papillomavirus infection, Measles, Epstein-Barr virus infection, Huntington's disease, human T-lymphotropic virus type 1(HTLV-I) infection and Influenza A are associated with breast cancer. These biological processes, pathways and essential proteins identified can, therefore, be further assessed to check for their suitability as targets for the breast cancer disease for the development of effective therapeutic strategies.

List of references

[1] Linda J.S. Allen. *Introduction to mathematical biology*. Pearson/Prentice Hall, 2007.

[2] H.A. Alshaker and K.Z. Matalka. Ifn-γ, il-17 and tgf-β involvement in shaping the tumor microenvironment: The significance of modulating such cytokines in treating malignant solid tumors. *Cancer cell international*, 11(1):33, 2011.

[3] H.N. Andrews, P.B. Mullan, S. McWilliams, S. Sebelova, J.E. Quinn, P.M. Gilmore, N. McCabe, A. Pace, B. Koller, P.G. Johnston, et al. Brca1 regulates the interferon γ-mediated apoptotic response. *Journal of Biological Chemistry*, 277(29):26225–26232, 2002.

[4] R.A. Aogo. *Modelling the role of HIV and its treatment in non-Hodgkin lymphoma growth dynamics*. PhD thesis, Stellenbosch: Stellenbosch University, 2015.

[5] S. Ariad, N. Milk, A. Bolotin, J. Gopas, N. Sion-Vardy, and D. Benharoch. Measles virus antigens in breast cancer. *Anticancer research*, 31(3):913–920, 2011.

[6] N.A. Awang and N. Maan. Analysis of tumor populations and immune system interaction model. In *AIP Conference Proceedings*, volume 1750, page 030049. AIP Publishing, 2016.

[7] J. Baginska, E. Viry, J. Paggetti, S. Medves, G. Berchem, E. Moussay, and B. Janji. The critical role of the tumor microenvironment in shaping natural killer cell-mediated anti-tumor immunity. *Frontiers in immunology*, 4, 2013.

[8] J. Baloni and R. Us. Mathematical modelling of strategic treatments on tumor growth. *J Appl Comp Math*, 2(4), 2013.

[9] V. Blakeman, J.L. Williams, Q. Meng, and C.H. Streuli. Circadian clocks and breast cancer. *Breast Cancer Research*, 18(1):89, 2016.

[10] V.D. Blondel, J. Guillaume, R. Lambiotte, and E. Lefebvre. Fast unfolding of communities in large networks. *Journal of statistical mechanics: theory and experiment*, 10:P10008, 2008.

[11] Brca2 and brca1 have a common regulator tnf-alpha. The EVEX database, http://www.evexdb.org/indirect/egenomes/common-regulators/?keyword=115916,307561&ggp=225665, Accessed May, 2018.

[12] K. Brennan, G. Offiah, E.A. McSherry, and A.M. Hopkins. Tight junctions: a barrier to the initiation and progression of breast cancer? *BioMed Research International*, 2010:460607:16, 2010.

[13] B. Burkholder, R. Huang, R. Burgess, S. Luo, V.S. Jones, W.enji Zhang, Z. Lv, C. Gao, B. Wang, Y. Zhang, et al. Tumor-induced perturbations of cytokines and immune cell networks. *Biochimica et Biophysica Acta (BBA)-Reviews on Cancer*, 1845(2):182–201, 2014.

[14] E. Camon, M. Magrane, D. Barrell, V. Lee, E. Dimmer, J. Maslen, D. Binns, N. Harte, R. Lopez, and R. Apweiler. The gene ontology annotation (goa) database: sharing knowledge in uniprot with gene ontology. *Nucleic acids research*, 32:D262–D266, 2004.

[15] Number of people with cancer. Our World in Data, https://ourworldindata.org/cancer, Accessed July, 2018.

[16] Cancer. American Cancer Society, Cancer Facts & Figures 2017, 2017.

[17] C. Cantoni, L. Huergo-Zapico, M. Parodi, M. Pedrazzi, M.C. Mingari, A. Moretta, B. Sparatore, S. Gonzalez, D. Olive, C. Bottino, et al. Nk cells, tumor cell transition, and tumor progression in solid malignancies: New hints for nk-based immunotherapy? *Journal of immunology research*, 2016.

[18] M. Casás-Selves and J. DeGregori. How cancer shapes evolution and how evolution shapes cancer. *Evolution: Education and outreach*, 4(4):624–634, 2011.

[19] C. Castillo-Chavez, Z. Feng, and W. Huang. On the computation of r_0 and its role on global stability. *Mathematical approaches for emerging and reemerging infectious diseases: an introduction*, 1:229, 2001.

[20] J. TH Chang, F. Wang, W. Chapin, and R.S. Huang. Identification of micrornas as breast cancer prognosis markers through the cancer genome atlas. *PloS one*, 11(12):e0168284, 2016.

[21] C. Chen, A.K. Seth, and A.E. Aplin. Genetic and expression aberrations of e3 ubiquitin ligases in human breast cancer. *Molecular Cancer Research*, 4(10):695–707, 2006.

[22] J.YC. Chow, M. Ban, H.L. Wu, F. Nguyen, M. Huang, H. Chung, H. Dong, and J.M. Carethers. Tgf-β downregulates pten via activation of nf-κb in pancreatic cancer cells. *American Journal of Physiology-Gastrointestinal and Liver Physiology*, 298(2):G275–G282, 2009.

[23] L. Cipolla. Carbohydrates in drug design and discovery. edited by jesús jiménez-barbero, f. javier cañada and sonsoles martín-santamaría. *ChemMedChem*, 10(9):1585–1586, 2015.

[24] Gene Ontology Consortium. Gene ontology consortium: going forward. *Nucleic acids research*, 43(D1):D1049–D1056, 2014.

[25] E. De Kruijf, TJA Dekker, LJAC Hawinkels, H Putter, VTHBM Smit, JR Kroep, PJK Kuppen, CJH Van de Velde, Peter ten Dijke, RAEM Tollenaar, et al. The prognostic role of tgf-β signaling pathway in breast cancer patients. *Annals of oncology*, 24(2):384–390, 2012.

[26] L. de Pillis and A. Radunskaya. A mathematical model of immune response to tumor invasion. 2003.

[27] L.G. de Pillis, W. Gu, and A.E. Radunskaya. Mixed immunotherapy and chemotherapy of tumors: modeling, applications and biological interpretations. *Journal of theoretical biology*, 238(4):841–862, 2006.

[28] N.Y. den Breems and R. Eftimie. The re-polarisation of m2 and m1 macrophages and its role on cancer outcomes. *Journal of theoretical biology*, 390:23–39, 2016.

[29] A. Diefenbach, E.R. Jensen, A.M. Jamieson, and D.H. Raulet. Rae1 and h60 ligands of the nkg2d receptor stimulate tumour immunity. *Nature*, 413(6852):165, 2001.

[30] X. Ding, S.I. Park, L.K. McCauley, and C. Wang. Signaling between transforming growth factor β (tgf-β) and transcription factor snai2 represses expression of microrna mir-203 to promote epithelial-mesenchymal transition and tumor metastasis. *Journal of Biological Chemistry*, 288(15):10241–10253, 2013.

[31] M.J. Dobrzanski. Expanding roles for cd4 t cells and their subpopulations in tumor immunity and therapy. *Frontiers in oncology*, 3, 2013.

[32] T. dos Santos and C. Isabel. *The Role of ATM in the Regulation of Interferon-gamma Responses*. PhD thesis, Imperial College London, 2012.

[33] E.J. Edelman, J. Guinney, J. Chi, P.G. Febbo, and S. Mukherjee. Modeling cancer progression via pathway dependencies. *PLoS computational biology*, 4(2):e28, 2008.

[34] R. Eftimie, J.L. Bramson, and J.D. Earn. Modeling anti-tumor th1 and th2 immunity in the rejection of melanoma. *Journal of theoretical biology*, 265(3):467–480, 2010.

[35] D.L. Elion and R.S. Cook. Harnessing rig-i and intrinsic immunity in the tumor microenvironment for therapeutic cancer treatment. *Oncotarget*, 9(48):29007, 2018.

[36] M.S. Feizabadi and T.M. Witten. Modeling the effects of a simple immune system and immunodeficiency on the dynamics of conjointly growing tumor and normal cells. *International journal of biological sciences*, 7(6):700, 2011.

[37] O.J. Finn. Immuno-oncology: understanding the function and dysfunction of the immune system in cancer. *Annals of Oncology*, 23(suppl 8):viii6–viii9, 2012.

[38] M. Fukuda, Y. Ohmori, and H. Sakashita. The role of tumor microenvironment in oral cancer. In *Tumor Microenvironment and Myelomonocytic Cells*. InTech, 2012.

[39] Genetics:breast cancer risk factors. breastcancer.org, http://www.breastcancer.org/risk/factors/genetics, Accessed March, 2018.

[40] D.M. Gilkes and G.L. Semenza. Role of hypoxia-inducible factors in breast cancer metastasis. *Future oncology*, 9(11):1623–1636, 2013.

[41] A. Goriely. A mathematical model of tumor-immune interactions. 2010.

[42] C. Günther, E. Martini, N. Wittkopf, K. Amann, B. Weigmann, H. Neumann, M.J. Waldner, S.M. Hedrick, S. Tenzer, M.F. Neurath, et al. Caspase-8 regulates tnf-α-induced epithelial necroptosis and terminal ileitis. *Nature*, 477(7364):335, 2011.

[43] P. Gurung, B. Li, RK.S. Malireddi, M. Lamkanfi, T.L. Geiger, and T.D. Kanneganti. Chronic tlr stimulation controls nlrp3 inflammasome activation through il-10 mediated regulation of nlrp3 expression and caspase-8 activation. *Scientific reports*, 5:14488, 2015.

[44] Á. Gyenis, D. Umlauf, Z. Újfaludi, I. Boros, T. Ye, and L. Tora. Uvb induces a genome-wide acting negative regulatory mechanism that operates at the level of transcription initiation in human cells. *PLoS genetics*, 10(7):e1004483, 2014.

[45] O.A.W. Haabeth, A.A. Tveita, M. Fauskanger, F. Schjesvold, K.B. Lorvik, P.O. Hofgaard, H. Omholt, L.A. Munthe, Z. Dembic, A. Corthay, et al. How do cd4+ t cells detect and eliminate tumor cells that either lack or express mhc class ii molecules? *Frontiers in immunology*, 5, 2014.

[46] S. Hallam, M. Escorcio-Correia, R. Soper, A. Schultheiss, and T. Hagemann. Activated macrophages in the tumour microenvironment dancing to the tune of tlr and nf-κb. *The Journal of pathology*, 219(2):143–152, 2009.

[47] N. Hao, M. Lü, Y. Fan, Y. Cao, Z. Zhang, and S. Yang. Macrophages in tumor microenvironments and the progression of tumors. *Clinical and Developmental Immunology*, 2012.

[48] J. Heo, M. Chun, Young-Taek Oh, O.K. Noh, and L. Kim. Influenza among breast cancer survivors in south korea: A nationwide population-based study. *in vivo*, 31(5):967–972, 2017.

[49] M.J. Higgins, A. Serrano, K.Y. Boateng, V.A. Parsons, T. Phuong, A. Seifert, J.M. Ricca, K.C. Tucker, A.S. Eidelman, M.A. Carey, et al. A multifaceted role for myd88-dependent signaling in progression of murine mammary carcinoma. *Breast cancer: basic and clinical research*, 10:BCBCR–S40075, 2016.

[50] Arciero J.C., Jackson T.L., and Kirschner D.E. A mathematical model of tumor-immune evasion and sirna treatment. *Discrete and Continuous Dynamical Systems Series B*, 4(1):39–58, 2004.

[51] L. Ji, J. Xu, J. Liu, A. Amjad, K. Zhang, Q. Liu, L. Zhou, J. Xiao, and X. Li. Mutant p53 promotes tumor cell malignancy by both positive and negative regulation of the transforming growth factor β (tgf-β) pathway. *Journal of Biological Chemistry*, 290(18):11729–11740, 2015.

[52] Milde-Langosch K., Bamberger A.M., Rieck G., Grund D., Hemminger G., Müller V., and Löning T. Expression and prognostic relevance of activated extracellular-regulated kinases (erk1/2) in breast cancer. *British journal of cancer*, 92(12):2206, 2005.

[53] G.E. Kaiko, J.C. Horvat, K.W. Beagley, and P.M. Hansbro. Immunological decision-making: how does the immune system decide to mount a helper t-cell response? *Immunology*, 123(3):326–338, 2008.

[54] D. Kirschner and J.C. Panetta. Modeling immunotherapy of the tumor–immune interaction. *Journal of mathematical biology*, 37(3):235–252, 1998.

[55] P.A. Knobel and T.M. Marti. Translesion dna synthesis in the context of cancer research. *Cancer cell international*, 11(1):39, 2011.

[56] H. Korkaya, S. Liu, and M.S. Wicha. Breast cancer stem cells, cytokine networks, and the tumor microenvironment. *The Journal of clinical investigation*, 121(10):3804–3809, 2011.

[57] D. Koschützki and F. Schreiber. Centrality analysis methods for biological networks and their application to gene regulatory networks. *Gene regulation and systems biology*, 2:GRSB–S702, 2008.

[58] H.K. Koul, M. Pal, and S. Koul. Role of p38 map kinase signal transduction in solid tumors. *Genes & cancer*, 4(9-10):342–359, 2013.

[59] S. Lee, J. Kim, S. Oh, Y. Kim, S. Rho, K. Park, K. Park, and J. Lee. Corrigendum to:"ifn-γ/irf-1-induced p27 kip1 down-regulates telomerase activity and human telomerase reverse transcriptase expression in human cervical cancer (febs 29236)"[febs letters 579 (2005) 1027–1033]. *FEBS Letters*, 579(27):6288–6288, 2005.

[60] Y.S. Lee and A. Dutta. Microrna s in cancer. *Annual Review of Pathological Mechanical Disease*, 4:199–227, 2009.

[61] J.W. Leong, S.E. Schneider, R.P. Sullivan, B.A. Parikh, B.A. Anthony, A. Singh, B.A. Jewell, T. Schappe, J.A. Wagner, D.C. Link, et al. Pten regulates natural killer cell trafficking in vivo. *Proceedings of the National Academy of Sciences*, 112(7):E700–E709, 2015.

[62] N. Li, J. Zou, H. Lin, R. Ke, X. He, L. Xiao, D. Huang, L. Luo, N. Lv, and Z. Luo. Lkb1/ampk inhibits tgf-β1 production and the tgf-β signaling pathway in breast cancer cells. *Tumor Biology*, 37(6):8249–8258, 2016.

[63] K. Liao, X. Bai, and A. Friedman. Mathematical modeling of interleukin-27 induction of anti-tumor t cells response. *PLoS One*, 9(3):e91844, 2014.

[64] S. Lipkowitz. The role of the ubiquitination-proteasome pathway in breast cancer: ubiquitin mediated degradation of growth factor receptors in the pathogenesis and treatment of cancer. *Breast Cancer Research*, 5(1):8, 2002.

[65] L. Liu, W. Zhou, C. Cheng, X. Ren, G. Somlo, M.Y. Fong, A.R. Chin, H. Li, Y. Yu, Y. Xu, et al. Tgfβ induces "brcaness" and sensitivity to parp inhibition in breast cancer by regulating dna-repair genes. *Molecular Cancer Research*, 12(11):1597–1609, 2014.

[66] W. Liu, C. Chien, C. Chou, and J. Su. An lkb1-interacting protein negatively regulates tnfα-induced nf-κb activation. *Journal of biomedical science*, 10(2):242–252, 2003.

[67] Y. Louzoun, C. Xue, G.B. Lesinski, and A. Friedman. A mathematical model for pancreatic cancer growth and treatments. *Journal of theoretical biology*, 351:74–82, 2014.

[68] N.J. MacIver, J. Blagih, D.C. Saucillo, L. Tonelli, T. Griss, J.C. Rathmell, and R.G. Jones. The liver kinase b1 is a central regulator of t cell development, activation, and metabolism. *The Journal of Immunology*, 187(8):4187–4198, 2011.

[69] K.J. Mahasa, R. Ouifki, A. Eladdadi, and L. de Pillis. Mathematical model of tumor–immune surveillance. *Journal of theoretical biology*, 404:312–330, 2016.

[70] N. Makridakis and J. Reichardt. Translesion dna polymerases and cancer. *Frontiers in genetics*, 3:174, 2012.

[71] A. Marcus, B.G. Gowen, T.W. Thompson, A. Iannello, M. Ardolino, W. Deng, L. Wang, N. Shifrin, and D.H. Raulet. Recognition of tumors by the innate immune system and natural killer cells. *Advances in immunology*, 122:91, 2014.

[72] O. Marques, B.M. da Silva, G. Porto, and C. Lopes. Iron homeostasis in breast cancer. *Cancer letters*, 347(1):1–14, 2014.

[73] A. Martin and B.L. Weber. Genetic and hormonal risk factors in breast cancer. *Journal of the National Cancer Institute*, 92(14):1126–1135, 2000.

[74] G.K. Mazandu, E.R. Chimusa, K. Rutherford, E. Zekeng, Z.Z. Gebremariam, M.Y. Onifade, and N.J. Mulder. Large-scale data-driven integrative framework for extracting essential targets and processes from disease-associated gene data sets. *Briefings in bioinformatics*, 2017.

[75] G.K. Mazandu and N.J. Mulder. Generation and analysis of large-scale data-driven mycobacterium tuberculosis functional networks for drug target identification. *Advances in bioinformatics*, page 14, 2011.

[76] G.K. Mazandu and N.J. Mulder. Scoring protein relationships in functional interaction networks predicted from sequence data. *PLoS One*, 6(4):e18607, 2011.

[77] G.K. Mazandu and N.J. Mulder. Dago-fun: tool for gene ontology-based functional analysis using term information content measures. *BMC bioinformatics*, 14(1):284, 2013.

[78] N. Mulder, G. Mazandu, and H. Rapano. Using host-pathogen functional interactions for filtering potential drug targets in mycobacterium tuberculosis. *Mycobacterial Diseases*, 3:2161–1068, 2013.

[79] J.A. Nelder and R. Mead. A simplex method for function minimization. *The computer journal*, 7(4):308–313, 1965.

[80] W. Nie, T. Yu, Y. Sang, and X. Gao. Tumor-promoting effect of il-23 in mammary cancer mediated by infiltration of m2 macrophages and neutrophils in tumor microenvironment. *Biochemical and biophysical research communications*, 482(4):1400–1406, 2017.

[81] F. Nouroz, F. Bibi, S. Noreen, and N. Masood. Natural killer cells enhance the immune surveillance of cancer. *Egyptian Journal of Medical Human Genetics*, 17(2):149–154, 2016.

[82] H. Ogata, S. Goto, K. Sato, W. Fujibuchi, H. Bono, and M. Kanehisa. Kegg: Kyoto encyclopedia of genes and genomes. *Nucleic acids research*, 27(1):29–34, 1999.

[83] M. Orzechowska, D. Jędroszka, and A.K. Bednarek. Common profiles of notch signaling differentiate disease-free survival in luminal type a and triple negative breast cancer. *Oncotarget*, 8(4):6013, 2017.

[84] Tnf-alpha and irf5 have a common regulator p53. The EVEX database, http://evexdb.org/indirect/homologene/common-regulators/?keyword=496,8088&ggp=460, Accessed May, 2018.

[85] Ifn and p53 co-regulate il-10. The EVEX database, http://www.evexdb.org/indirect/homologene/co-regulation/?keyword=68536,460&ggp=478, Accessed May, 2018.

[86] K. Palucka and J. Banchereau. Cancer immunotherapy via dendritic cells. *Nature Reviews Cancer*, 12(4):265–277, 2012.

[87] N. Pećina-Šlaus. Tumor suppressor gene e-cadherin and its role in normal and malignant cells. *Cancer cell international*, 3(1):17, 2003.

[88] S. Pohl, N. Brook, M. Agostino, F. Arfuso, A.P. Kumar, and A. Dharmarajan. Wnt signaling in triple-negative breast cancer. *Oncogenesis*, 6(4):e310, 2017.

[89] J.W. Pollard. Tumour-educated macrophages promote tumour progression and metastasis. *Nature Reviews Cancer*, 4(1):71–78, 2004.

[90] J. Reiser and A. Banerjee. Effector, memory, and dysfunctional cd8. *Journal of immunology research*, 2016:14, 2016.

[91] M. Robertson-Tessi, A. El-Kareh, and A. Goriely. A mathematical model of tumor–immune interactions. *Journal of Theoretical Biology*, 294:56–73, 2012.

[92] C. Ruiz-Ruiz, C.R. de Almodóvar, A. Rodríguez, G. Ortiz-Ferrón, J.M. Redondo, and A. López-Rivas. The up-regulation of human caspase-8 by interferon-γ in breast tumor cells requires the induction and action of the transcription factor interferon regulatory factor-1. *Journal of Biological Chemistry*, 279(19):19712–19720, 2004.

[93] M.S. Seuneu Tchamga. *Study of Singularly Perturbed Models and its Applications in Ecology and Epidemiology*. PHD thesis, UKZN, 2018.

[94] Share of deaths by cause, world, 2016. Our World in Data, https://ourworldindata.org/causes-of-death#causes-of-death-in-recent-decades, Accessed May, 2018.

[95] T. Shekarian, S. Valsesia-Wittmann, J. Brody, M.C. Michallet, S. Depil, C. Caux, and A. Marabelle. Pattern recognition receptors: immune targets to enhance cancer immunotherapy. *Annals of Oncology*, 28(8):1756–1766, 2017.

[96] M. Shukrun, A. Jabareen, A. Abou-Kandil, R. Chamias, M. Aboud, and M. Huleihel. Htlv-1 tax oncoprotein inhibits the estrogen-induced-er α-mediated brca1 expression by interaction with cbp/p300 cofactors. *PloS one*, 9(2):e89390, 2014.

[97] S. Singh, N. Mehta, J. Lilan, M.B. Budhthoki, F. Chao, and L. Yong. Initiative action of tumor-associated macrophage during tumor metastasis. *Biochimie Open*, 2017.

[98] A. Snijders, P. Kalinski, C.M. Hilkens, and M.L. Kapsenberg. High-level il-12 production by human dendritic cells requires two signals. *International immunology*, 10(11):1593–1598, 1998.

[99] K. Soetaert, T. Petzoldt, et al. Inverse modelling, sensitivity and monte carlo analysis in r using package fme. *Journal of Statistical Software*, 33(3):1–28, 2010.

[100] L.M. Sompayrac. *How the immune system works*. John Wiley & Sons, 2015.

[101] S. Song, M.S. Vuai, and M. Zhong. The role of bacteria in cancer therapy–enemies in the past, but allies at present. *Infectious agents and cancer*, 13(1):9, 2018.

[102] C. M. Sousa, J. R. McGuire, M.S. Thion, D. Gentien, P. De La Grange, S.T. Du Montcel, A. Vincent-Salomon, A. Durr, and S. Humbert. The huntington disease protein accelerates breast tumour development and metastasis through erbb2/her2 signalling. *EMBO molecular medicine*, 5(2):309–325, 2013.

[103] I. Streng-Ouwehand, W.J. Unger, and Y. Van Kooyk. C-type lectin receptors for tumor eradication: future directions. *Cancers*, 3(3):3169–3188, 2011.

[104] M. Strioga, V. Schijns, D.J. Powell Jr, V. Pasukoniene, N. Dobrovolskiene, and J. Michalek. Dendritic cells and their role in tumor immunosurveillance. *Innate immunity*, 19(1):98–111, 2013.

[105] M.W.L. Teng, D.M. Andrews, N. McLaughlin, B. von Scheidt, S. F. Ngiow, A. Möller, G.R. Hill, Y. Iwakura, M. Oft, and M.J. Smyth. Il-23 suppresses innate immune response independently of il-17a during carcinogenesis and metastasis. *Proceedings of the National Academy of Sciences*, 107(18):8328–8333, 2010.

[106] G3bp1 and tnf-alpha have a common regulator pten. The EVEX database, http://www.evexdb.org/indirect/homologene/common-regulators/?keyword=38096,496&ggp=265, Accessed May, 2018.

[107] J.A. Trapani and M.J. Smyth. Functional significance of the perforin/granzyme cell death pathway. *Nature Reviews Immunology*, 2(10):735–747, 2002.

[108] Dann G. Mallet Trisilowati, Scott W. McCue. Numerical solution of an optimal control model of dendritic cell treatment of a growing tumour. *ANZIAM Journal*, *https://doi.org/10.21914/anziamj.v54i0.6654*, 2013.

[109] O. Üreyen, E. Dadalı, F. Akdeniz, T. Şahin, M.T. Tekeli, N. Eliyatkın, H. Postacı, and E. İlhan. Co-existent breast and renal cancer. *Turkish Journal of Surgery/Ulusal cerrahi dergisi*, 31(4):238, 2015.

[110] P. Van den Driessche and J. Watmough. Reproduction numbers and sub-threshold endemic equilibria for compartmental models of disease transmission. *Mathematical biosciences*, 180(1):29–48, 2002.

[111] A.R. Venkitaraman. Cancer susceptibility and the functions of brca1 and brca2. *Cell*, 108(2):171–182, 2002.

[112] R. Visconti, R. Della Monica, and D. Grieco. Cell cycle checkpoint in cancer: a therapeutically targetable double-edged sword. *Journal of Experimental & Clinical Cancer Research*, 35(1):153, 2016.

[113] Q. Wang, H.A. Franks, S.J. Lax, M. El Refaee, A. Malecka, S. Shah, I. Spendlove, M.J. Gough, C. Seedhouse, S. Madhusudan, et al. The ataxia telangiectasia mutated kinase pathway regulates il-23 expression by human dendritic cells. *The Journal of Immunology*, page 1201484, 2013.

[114] S. Wang and Z. Ding. Fibroblast growth factor receptors in breast cancer. *Tumor Biology*, 39(5):1010428317698370, 2017.

[115] Cancer. United Nations,World Cancer Day, http://www.un.org/en/events/cancerday/, Accessed November, 2017.

[116] Cancer. World Health Organisation, http://www.who.int/cancer/en/, Accessed November, 2017.

[117] D. Wu, B. Han, L. Guo, and Z. Fan. Molecular mechanisms associated with breast cancer based on integrated gene expression profiling by bioinformatics analysis. *Journal of Obstetrics and Gynaecology*, 36(5):615–621, 2016.

[118] H. Xu, J. Xian, E. Vire, S. McKinney, V. Wei, J. Wong, R. Tong, T. Kouzarides, C. Caldas, and S. Aparicio. Up-regulation of the interferon-related genes in brca2 knockout epithelial cells. *The Journal of pathology*, 234(3):386–397, 2014.

[119] H.Q. Yan, D. Zhang, Y. Y. Shi, X. You, L. Shi, Q. Li, and F.G. Gao. Ataxia-telangiectasia mutated activation mediates tumor necrosis factor-alpha induced mmp-13 up-regulation and metastasis in lung cancer cells. *Oncotarget*, 7(38):62070, 2016.

[120] A. Yates, C. Bergmann, J.L. Van Hemmen, J. Stark, and R. Callard. Cytokine-modulated regulation of helper t cell populations. *Journal of theoretical biology*, 206(4):539–560, 2000.

[121] J. Y. Yi, Y. Jung, S.S. Choi, and E. Chung. Tnf-alpha downregulates e-cadherin and sensitizes response to γ-irradiation in caco-2 cells. *Cancer research and treatment: official journal of Korean Cancer Association*, 41(3):164, 2009.

[122] H. Yin, S. Wang, Y. Zhang, Y. Cai, and H. Liu. Analysis of important gene ontology terms and biological pathways related to pancreatic cancer. *BioMed research international*, 2016.

[123] Your guide to understanding genetics conditions. U.S. National Library of Medicine, https://ghr.nlm.nih.gov/condition/breast-cancer#genes, Accessed March, 2018.

[124] W. Yue, J. Wang, M. Conaway, S. Masamura, Y. Li, and R.J. Santen. Activation of the mapk pathway enhances sensitivity of mcf-7 breast cancer cells to the mitogenic effect of estradiol. *Endocrinology*, 143(9):3221–3229, 2002.

[125] M. Zanetti. Tapping cd4 t cells for cancer immunotherapy: the choice of personalized genomics. *The Journal of Immunology*, 194(5):2049–2056, 2015.

[126] X. Zhang, F. Liu, and W. Wang. Two-phase dynamics of p53 in the dna damage response. *Proceedings of the National Academy of Sciences*, 108(22):8990–8995, 2011.

[127] S.G. Zheng, J.H. Wang, W. Stohl, K.S. Kim, J.D. Gray, and D.A. Horwitz. Tgf-β requires ctla-4 early after t cell activation to induce foxp3 and generate adaptive cd4+ cd25+ regulatory cells. *The Journal of Immunology*, 176(6):3321–3329, 2006.